

# **Study on Spectrum Efficiency and Energy Efficiency in Cellular Systems**

セルラーシステムにおける周波数利用と  
エネルギー利用効率改善に関する研究

**March 2017**

**Di ZHANG**

# **Study on Spectrum Efficiency and Energy Efficiency in Cellular Systems**

**セルラーシステムにおける周波数利用とエネルギー利用効率改善に関する研究**

**March 2017**

**Graduate School of Global Information and Telecommunication Studies  
Waseda University**

**Wireless Communication System II**

**Di ZHANG**



## Acknowledgements

I want to take this opportunity to thank my supervisor, Prof. Takuro Sato Sensei, very much for his valuable and continual support on my research. He is so kind-hearted and willing to help me not only on the research but also on my living here in Japan. I really appreciate his support a lot and I can never thank him more for the great and continual support. I want to thank Sato Sensei's sharp eyes very much on the research topics. I want to thank his encourage and thoughtful kindness on my research. He gives me some materials and a senior mate's contact information for discussion at the beginning. All of those help me a lot especially at the beginning of my research.

Besides, I really appreciate Tanaka Sensei, Shimamoto Sensei and Liu Jiang Sensei a lot for their great help on my research and living here in Japan. I appreciate Shimamoto Sensei, Tsuda Sensei, Nakajima Sensei very much of their great efforts on reviewing my Thesis and presentation slides, giving help to improve the quality, and endless help on my research. I want to take this opportunity to thank the defense committees and GITS's help and effort as well.

I want to thank the senior mate, Prof. Zhenyu Zhou, North China Electric Power University, China, very much for his effort and endless support on my paper publication. He teaches me a lot on doing research, which will be my great treasure. I want to thank Prof. Muhammad Tariq, FAST National University, Pakistan, senior mate graduated from our lab for his valuable comments and encouragements on my paper publications. I gain a lot from both of them. I also thank my lab mates and other fellows a lot for their help on my research.

I also want to thank Dr. Shahid Mumtaz from Instituto de Telecomunicações, Aveiro, Portugal; Prof. Shi Jin from Southeast University, China; Dr. Yuanwei Liu from King's College of London, London, UK; Prof. Zhiguo Ding from Lancaster University, Lancaster, UK; Dr. Zhengyu Zhu

from Zhengzhou University, China; Dr. Xingwang Li from Beijing University of Posts and Telecommunications (BUPT), China and many other guys a lot for the encouragements, discussions and information sharing on the research. I learn a lot on doing research from all of you.

Finally, I want to thank my family very much for the help, endless support on my life and research. They always try to support me with whatever means they have. The family affection is always my great treasure and I am willing to do whatever I can for my family.

## Abstract

The emerging Spectrum Efficiency (SE) and Energy Efficiency (EE) topics in Fifth Generation (5G) are focused in this dissertation. To increase the SE performance, the Non-Orthogonal Multiple Access massive Multi-Input-Multi-Output millimeter Wave (NOMA -massive-MIMO-mmWave) system is proposed as well as the analysis of its capacity performance. Compared to prior Long Term Evolution (LTE) system, the SE performance is greatly enhanced by this proposal. Additionally, on the study of EE topic, to improve the systems EE performance, a comprehensive system architecture is proposed afterwards. Based on this architecture, the EE analysis is addressed with proposed the Cellular Partition Zooming (CPZ) mechanism and optimization method while taking more elements into consideration. The system EE performance is increased via those methods compared with prior studies. Detail content of each chapter is given as follows:

In chapter 1, titled “Introduction”, the rapid cellular communication evolution and growing massive devices that connected to the internet is reviewed. Recently, as known, the 5G wireless communication is brought up to tumble down the even speedy increasing massive connected devices with the requirements of much larger throughput per cell, and much faster transmission rate per device. Meanwhile, due to the even faster rate, energy consumption becomes another vital issue. In this case, to accomplish the even higher transmission rate and even lower system energy consumption requirements of 5G, the SE and EE are summarized as two critical issues, which is the study focus of this dissertation.

In chapter 2, titled “Capacity Analysis of NOMA-massive-MIMO-mmWave Systems”, the SE issue is focused. As noticed, prior technologies to achieve higher SE performance mainly consist of the massive MIMO and NOMA. Recently, mmWave technology attracts a lot of attentions in literature.

The purpose of mmWave is to allocate more and higher frequency resources to alleviate the bottleneck of spectrum resources shortcoming. Yet it is noticed that less studies have been done on combining the NOMA, mmWave and massive MIMO together for the comprehensive capacity and sum rate analysis. In this dissertation, the combined system is proposed and analyzed of its capacity performance with a proposed mmWave channel model. Due to the complex analysis procedure, the analysis procedure is divided into the low Signal to Noise Ratio (SNR) and high SNR regimes. It is found from the simulation results that the capacity is greatly enhanced with this combined system. Given the even wider bandwidth provided by mmWave, the sum rate can be further increased.

In chapter 3, titled “Integrated Energy Efficiency Architecture and Analysis of 5G”, it is found that in the prior studies of EE performance, most of the work is trying to reduce the system energy consumption, or to integrating optimize the system consumption with more components taking into consideration. Other than those, we first propose a method to re-deign the system of wireless networks for better deployment of select/sleep mechanism with the purpose of better EE performance. Besides, a CPZ mechanism is proposed based the Cloud Radio Access Network (C-RAN) architecture. Compared with prior zooming scheme, this mechanism is capable of saving more energy and of better EE performance. This is especially useful in remote area, late night scenes with fewer users accessing the internet.

In chapter 4, titled “Integrated Energy Efficiency Analysis of Massive MIMO Based C-RAN”, based on the comprehensive system architecture proposed in chapter 3, additionally, a method to further enhance the system EE performance based the convex optimization tool is brought up. In which, more components are taken into consideration. Simulation results demonstrate that this method can satisfy the transmission requirement of each user while further reduce the consumed energy, which in turns, yields better system EE performance.

In chapter 5, titled “Conclusion”, the main discoveries of this dissertation are finally summarized up with regard to both SE and EE topics. The potential mobility environment, Ultra-Reliable Low Latency Communication (URLLC) topics are listed as well for future studies.

To sum up the dissertation, the SE and EE topics in 5G are investigated. It is demonstrated that with the proposed NOMA-mmWave-massive-MIMO system, cellular SE performance is greatly increased compared to prior MIMO systems. In addition, with the proposed comprehensive system model, CPZ mechanism, and optimization method while taking more elements into optimization. The system EE performance is enhanced compared to prior studies in this method. Finally, the potential future research topic is given as well to conclude the dissertation.

# Contents

|          |  |           |
|----------|--|-----------|
| <b>1</b> | <b>Introduction</b>  | <b>1</b>  |
| 1.1      | Summary . . . . .  | 1         |
| 1.2      | SISO to MIMO, and the research topics . . . . .                                | 2         |
| 1.2.1    | The SISO, SIMO, MISO, and MIMO . . . . .                                       | 2         |
| 1.3      | The wireless channel models and their applications . . . . .                   | 4         |
| 1.3.1    | The widely used analytical model, Rayleigh and Rician channel models . . . . . | 4         |
| 1.3.2    | Empirical Models . . . . .   | 6         |
| 1.3.2.1  | Okumura Model . . . . .  | 6         |
| 1.3.2.2  | Hata Model . . . . .   | 6         |
| 1.3.3    | Shadowing Effects . . . . .  | 7         |
| 1.3.4    | Outage probability and cell coverage area . . . . .                            | 8         |
| 1.4      | Capacity and transmission rate analysis . . . . .                              | 9         |
| 1.4.1    | General analysis of the achievable capacity . . . . .                          | 10        |
| 1.4.2    | Capacity analysis of the MIMO system . . . . .                                 | 12        |
| 1.5      | From MIMO to mMIMO . . . . .   | 15        |
| 1.5.1    | Even faster transmission speed . . . . .                                       | 16        |
| 1.5.2    | Energy efficiency . . . . .  | 18        |
| 1.5.3    | Emerging topics in mmWave mMIMO . . . . .                                      | 19        |
| 1.6      | The logical structure of this dissertation and relationship of each chapter    | 20        |
| <b>2</b> | <b>Capacity Analysis of NOMA-massive-MIMO-mmWave Systems</b>                   | <b>22</b> |
| 2.1      | Summary . . . . .  | 22        |
| 2.2      | Introduction . . . . .   | 23        |
| 2.2.1    | Background and motivation . . . . .  | 23        |
| 2.2.2    | Related work . . . . .   | 24        |
| 2.2.3    | Contributions . . . . .  | 25        |
| 2.2.4    | Organizations . . . . .  | 26        |

|          |   |           |
|----------|---|-----------|
| 2.2.5    | Notations . . . . .   | 26        |
| 2.3      | System model . . . . .  | 27        |
| 2.3.1    | The NOMA-mmWave-massive-MIMO system model . . . . .   | 29        |
| 2.3.2    | The proposed mmWave channel assumption . . . . .  | 31        |
| 2.4      | Capacity analysis in the noise-dominated low-SNR regime . . . . .   | 32        |
| 2.5      | Capacity analysis in the interference-dominated high-SNR regime . . . . .                                     | 36        |
| 2.6      | Numerical results . . . . .   | 39        |
| 2.7      | Conclusion . . . . .  | 43        |
| <b>3</b> | <b>Integrated Energy Efficiency Architecture and Analysis of 5G</b>   | <b>50</b> |
| 3.1      | Summary . . . . .   | 50        |
| 3.2      | Introduction . . . . .  | 50        |
| 3.3      | Proposed system model . . . . .   | 53        |
| 3.4      | Energy efficiency analysis . . . . .  | 56        |
| 3.4.1    | The analysis of capacity performance . . . . .  | 56        |
| 3.4.2    | Analysis of propagation model . . . . .   | 57        |
| 3.4.3    | Proposed CPZ scheme . . . . .   | 58        |
| 3.5      | Numerical results . . . . .   | 60        |
| 3.6      | Conclusion . . . . .  | 64        |
| <b>4</b> | <b>Integrated Energy Efficiency Analysis of Massive MIMO Based C-RAN</b>                                      | <b>66</b> |
| 4.1      | Summary . . . . .   | 66        |
| 4.2      | Introduction . . . . .  | 67        |
| 4.3      | Proposed system model and analysis of the transmission rate, energy consumption . . . . .                     | 69        |
| 4.3.1    | The proposed system model . . . . .   | 69        |
| 4.3.2    | The transmission and sum rate analysis . . . . .  | 70        |
| 4.3.3    | The energy consumption analysis . . . . .   | 71        |
| 4.4      | The energy efficiency model and its solution with off-line selection and convex optimization method . . . . . | 73        |
| 4.5      | Numerical analysis and results . . . . .  | 77        |
| 4.6      | Conclusion . . . . .  | 80        |
| <b>5</b> | <b>Conclusion</b>   | <b>84</b> |
| 5.1      | Summary and discussion . . . . .  | 84        |
| 5.2      | Future work . . . . .   | 86        |

# List of Figures

|     |   |    |
|-----|---|----|
| 1.1 | The SISO system. . . . .  | 3  |
| 1.2 | The SIMO system. . . . .  | 3  |
| 1.3 | The MISO system. . . . .  | 4  |
| 1.4 | The MIMO system. . . . .  | 4  |
| 2.1 | The comparison between OFDMA and NOMA. . . . .  | 27 |
| 2.2 | The massive MIMO concept. . . . .   | 28 |
| 2.3 | The conceptual model of the NOMA-mmWave-massive-MIMO system model. . . . .                        | 29 |
| 2.4 | The mmWave frequency used for transmission. . . . .   | 30 |
| 2.5 | Capacity performance of the low-SNR scenario. . . . .   | 40 |
| 2.6 | An analytical comparison of the exact and asymptotic eigenvalue PDFs ( $N = L = K = 6$ ). . . . . | 41 |
| 2.7 | Capacity performance of the high-SNR scenario with the exact eigenvalue PDF ( $N = 10$ ). . . . . | 42 |
| 2.8 | Capacity performance of the high-SNR scenario with the exact eigenvalue PDF ( $N = 20$ ). . . . . | 43 |
| 2.9 | Capacity performance of the high-SNR scenario with the asymptotic eigenvalue PDF. . . . .         | 44 |
| 3.1 | The traditional BS model with variable kinds of users. . . . .                                    | 53 |
| 3.2 | Proposed system model for 5G IoT. . . . .   | 54 |
| 3.3 | System model with different annular regions. . . . .  | 60 |
| 3.4 | One sample division of the coverage area. . . . .   | 63 |
| 3.5 | Power consumption of CPZ and traditional zooming scheme. . . . .                                  | 63 |
| 3.6 | Energy efficiency of CPZ and zooming scheme in [1]. . . . .                                       | 64 |
| 3.7 | Energy consumption of the CPZ and without CPZ. . . . .  | 64 |
| 4.1 | Proposed system model with C-RAN architecture. . . . .  | 70 |
| 4.2 | Component Selection Performance of our scheme, one cellular area. . . . .                         | 79 |

|     |   |    |
|-----|---|----|
| 4.3 | Energy efficiency performance of our scheme, one cellular area. . . . . | 79 |
| 4.4 | Component Selection Performance in the whole system. . . . .            | 81 |
| 4.5 | Energy efficiency performance of the whole system. . . . .              | 81 |

# List of Tables

|     |                                |    |
|-----|--------------------------------|----|
| 3.1 | Simulation elements. . . . .   | 61 |
| 4.1 | Simulation components. . . . . | 78 |

# List of Acronym

|        |  |
|--------|--|
| 3D     | Three Dimensional                                |
| 5G     | Fifth Generation                                 |
| ANC    | Analog Network Coding                            |
| AoA    | Angle of Arrival                                 |
| AoD    | Angle of Departure                               |
| AWGN   | Additive White Gaussian Noise                    |
| BBU    | Baseband Processing Unit                         |
| BS     | Base Station                                     |
| C-RAN  | Cloud Radio Access Network                       |
| CC     | Component Carrier                                |
| CDF    | Cumulative Distribution Function                 |
| CMCC   | China Mobile Communications Corporation          |
| CoMP   | Coordinated Multi-Point                          |
| CPZ    | Cellular Partition Zooming                       |
| CSI    | Channel State Information                        |
| CSIR   | Channel State Information at the Receiver side   |
| D2D    | Device to Device                                 |
| DoF    | Degree of Freedom                                |
| EDF    | Empirical Distribution Function                  |
| EE     | Energy Efficiency                                |
| EH     | Energy Harvesting                                |
| eMBB   | Enhanced Mobile BroadBand                        |
| GPP    | General Purpose Platform                         |
| GSM    | Global System for Mobile communications          |
| HetNet | Heterogeneous Network                            |
| IEEE   | Institute of Electrical and Electronic Engineers |
| IoT    | Internet of Things                               |
| LoS    | Light of Sight                                   |
| LP     | Linear Programming                               |
| LSD    | Limiting Spectrum Distribution                   |
| LTE    | Long Term Evolution                              |
| MEE    | Maximum Energy Efficiency                        |
| MIMO   | Multi-Input-Multi-Output                         |
| MISO   | Multi-Input-Single-Output                        |

|        |   |
|--------|---|
| mMIMO  | massive MIMO                                  |
| mMTC   | Massive Machine Type Communications           |
| mmWave | Millimeter Wave                               |
| NLoS   | Non Light of Sight                            |
| NOMA   | Non-Orthogonal Multiple Access                |
| OFDMA  | Orthogonal Frequency Division Multiple Access |
| OMA    | Orthogonal Multiple Acces                     |
| PA     | Power Amplifier                               |
| PDF    | Probability Distribution Function             |
| PNC    | Physical-layer Network Coding                 |
| PPP    | Poisson Point Process                         |
| RF     | Radio Frequency                               |
| QoS    | Quality of Service                            |
| RMT    | Random Matrix Theory                          |
| SCS    | Structured Compressive Sensing                |
| SE     | Spectrum Efficiency                           |
| SIC    | Successive Interference Cancellation          |
| SIMO   | Single-Input-Multi-Output                     |
| SINR   | Signal to Interference plus Noise Ratio       |
| SIR    | signal to Interference Ratio                  |
| SISO   | Single-Input-Single-Output                    |
| SNR    | Signal to Noise Ratio                         |
| SVD    | Singular Value Decomposition                  |
| UE     | User Equipment                                |
| UR-SP  | Uniform Randon Single Path                    |
| URLLC  | Ultra-Reliable and Low-Latency Communication  |
| VBS    | Virtual Base Station                          |
| ZFBF   | Zero Forced Beam-Forming                      |

# Chapter 1

## Introduction

### 1.1 Summary

In the past decades, wireless communications have witnessed the evolution from analog communications systems (also named as the 1G), Global System for Mobile communications (GSM, also called as the 2G, whereas the internet service was added in), the Third Generation wireless communications (3G), the Fourth Generation (4G, alternatively named as the Long Term Evolution (LTE), and LTE-advanced). Today, we are on the stage of Fifth Generation wireless communications (5G).

For the wireless communication technologies evolution to achieve each goal of different generations, they have experienced the Single-Input Signal-Output (SISO) to Multi-Input Multi-Output (MIMO). Nowadays, we are on the edge of massive MIMO (mMIMO) with 5G. Besides of the increasing number of transmit antenna, the channel modeling, channel coding and channel estimation technologies are intensively addressed with the asymptotic sum rate or ergodic capacity analysis. Due to the bottleneck of frequency limitation, those days the industry and academia are calling for allocating more frequency resources for 5G (e.g., mmWave, un-licensed frequency, etc.). In which, the mmWave frequency attracts more and more attentions. However, mmWave MIMO brings in new challenge to the existing technologies due to the ultra dense cellular. In this regard, some new channel models and channel estimations are needed to cater this potential applications in the near future.

In this beginning chapter, we review the prior studies on SISO and MIMO and finally summarized the emerging technologies in mmWave mMIMO of 5G. As the main technology trends behind the evolution are the methods to boost the transmission rate, capacity with various versatile methods, here in this chapter. The widely used channel model, i.e., Rayleigh and Rician channel models are investigated. In addition, the outage probability analysis for the cellular coverage area is given, as

those are still adopted a lot in 5G studies. The detail studies of this dissertation is given afterwards by the following chapters based on this introduction. <sup>1</sup>.

## 1.2 SISO to MIMO, and the research topics

In this section, the SISO, SIMO, MISO, MIMO concept is investigated beforehand. Afterwards, the focused topics with wireless channel model, outage probability analysis for cellular coverage area is addressed. The emerging topics of 5G will be given by the next section.

### 1.2.1 The SISO, SIMO, MISO, and MIMO

There are a lot of studies on the SISO, MISO, SIMO, and MIMO in prior wireless communication generations, especially in 3G and 4G LTE. The difference between those technologies are due to the required number of antennas and different level of complexity. The simple wireless communications, is the SISO system, as shown by Fig. 1.1. There are one transmit antenna and one receiver antenna at the transmit and receiver sides. Thus no channel diversity and correlation existing no matter from transmitter or receiver sides. The advantage of SISO is obviously that, the system is quite easy to adopt without complex processing methods. Yet it is limited to the channel noise and interference between transmitter to receiver without the diversity effects with multiple antennas. Actually, the majority studies are based on the SISO model with regard to Shannon theory to increase the system capacity and transmission rate by allocating more transmission power and wider bandwidth resources, and by the channel coding methods (for instance, the encoding mechanism with time domain, frequency domain and spreading frequency codes domain).

The SIMO system is given as Fig. 1.2. The SIMO system, also called as the receiver diversity, is to enable the receiver side receive signals from various sources (via its multiple antennas). In this way, the fading effects are greatly reduced of the wireless propagation. Yet it requires greater complexity while decoding at the receiver side. Hence SIMO is widely used for the receiving stations or maritime communications that huge receiving station is possible to install.

The MISO system, on the other hand, can be found as Fig. 1.3. In which multiple transmit antennas transmitting the information for one receiver terminal. The benefit of MISO, compared to the SISO system, is that it can exploit the diversity at the

---

<sup>1</sup>This chapter is based on the work **D. Zhang**, and Shahid Mumtaz "mmWave-Massive MIMO: A Paradigm for 5G, Chapter 2, Elsevier, London, UK, 2017.

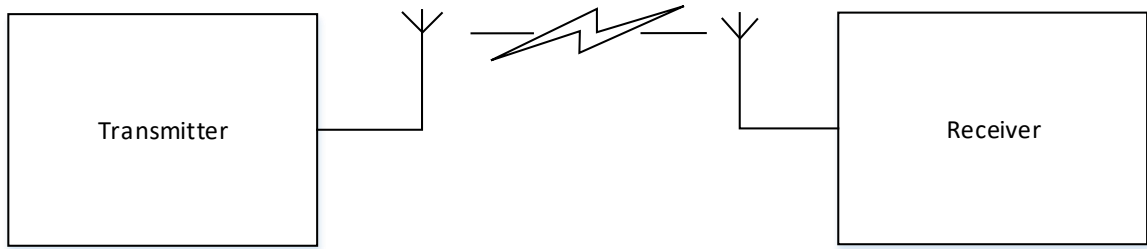


Figure 1.1 The SISO system.

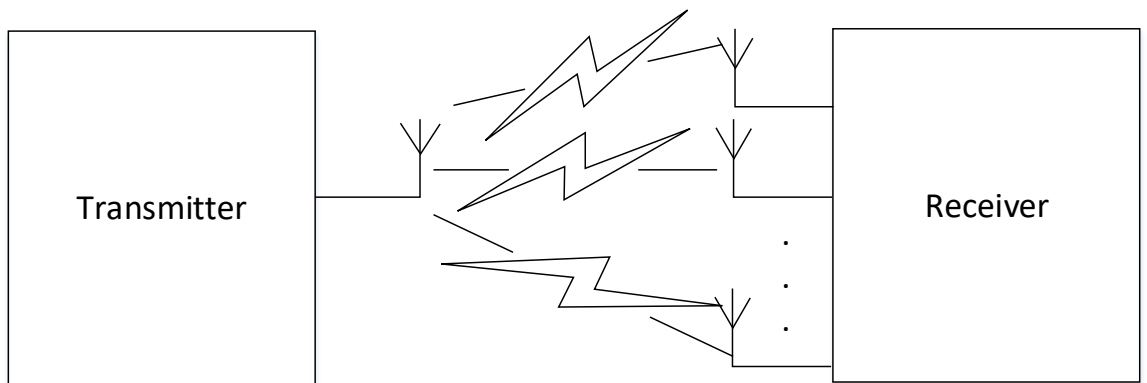


Figure 1.2 The SIMO system.

transmitter side. Thus the receiver is able to receive the optimal signal to extract the required transmitted information. The receiver size can be largely reduced via this method especially transmitting large volume of information, the decoding complexity is reduced as well by the redundancy coding of MISO system.

The MIMO system, as widely used in wireless communications, can be found as Fig. 1.4. The benefit of MIMO is that, it can make use of both SIMO and MISO's merits to enhance the channel robustness and the throughput of the system. In MIMO studies, under ideal and equal channel conditions, MIMO channel can be divided into several SISO channels for calculation compactness. With the raising of MIMO system, the wireless transmission rate is greatly enhanced other than the prior channel coding methods.

We will give the general evolution of the wireless communications from SISO to MIMO. In the introduction, we mostly focus on the cellular coverage area and outage probability analysis, as well as the channel models and therefore capacity and transmission rate analysis based on them.

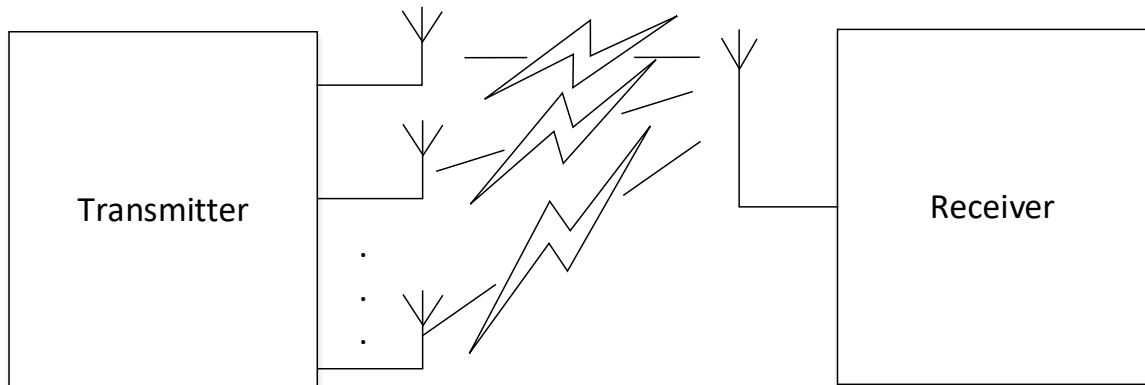


Figure 1.3 The MISO system.

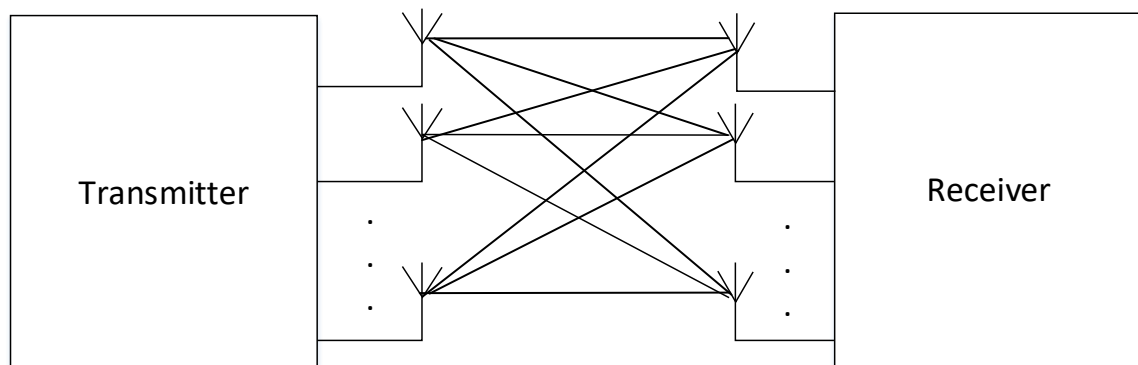


Figure 1.4 The MIMO system.

## 1.3 The wireless channel models and their applications

The wireless channel models will be addressed after the prior review from SISO to MIMO systems. Generally, the wireless channel model is divided into the analytical model and empirical models.

### 1.3.1 The widely used analytical model, Rayleigh and Rician channel models

in literature, the Rayleigh and Rician channel models are widely used for information theory analysis. Generally, Rician channel assumes that the transmission paths from the transmitter to receiver mainly consists of the dominant Light of Sight (LoS) paths and other scattering paths. In contrast, Rayleigh channel relatively consists of scattering channels from the transmitter to receiver, whereas no dominant LoS paths existing.

The Rayleigh channel is introduced here in this section. By assuming the phase on each path  $i$  is  $2\pi ft_i$  modulo  $2\pi$ , where  $ft_i = d_i/\lambda$ , we can have  $d_i \gg \lambda$ . During the path, the phases uniformly vary between 0 to  $2\pi$  whereas different phases are independent. By adding all of the transmission paths together, denoting  $\alpha_i(t), t_i(t)$  as the attenuation and propagation delays on each path  $i$  within a time slot  $t$ , the tap gain can be given as [2]

$$h_l[m] = \alpha_i(m/W)e^{-j2\pi ft_i(m/W)} \sin[l - t_i(m/W)W]. \quad (1.1)$$

This can be used to simulate the widely used *circular symmetric complex random variable*, in which each tap is the sum of a large number of small independent circular symmetric random variables [2]. Mostly, we use the real part of the tap gain to model the zero mean Gaussian random variable. It is worth to note that this circular symmetric complex random variable assumption is used a lot especially in MIMO system. In massive MIMO (mMIMO) system, by assuming that the macro wave is used as the carrier bandwidth, we also adopt this with random matrix theory [3] for large antenna system analysis. In general, with Rayleigh channel assumption, the tap gains are assumed to follow the  $\mathcal{CN}(0, \sigma_l^2)$ . Density of Rayleigh random variable then, can be given as [2]

$$\frac{x}{\sigma_l^2} \exp\left\{-\frac{x^2}{2\sigma_l^2}\right\}, \quad (1.2)$$

and the density of a squared magnitude is  $h_l[m]^2$  [2]

$$\frac{1}{\sigma_l^2} \exp\left\{-\frac{x}{\sigma_l^2}\right\}. \quad (1.3)$$

In contrast, the Rician channel models the channel with a specular path and several scattered paths where the specular path is large and has a know magnitude [2]. Consider two random Gaussian variables  $X, Y$ , where  $X$  has a non-zero mean (say  $m$ ) and  $Y$  has a zero mean, both  $X, Y$  have equal variance as  $\eta^2$ . Then the transformation can be given as

$$Z = \sqrt{X^2 + Y^2} \quad (1.4)$$

where  $Z$  is Rician distributed. The tap gain of Rician channel can be given as [2]

$$h_l[m] = \sqrt{\frac{k}{k+1}}\sigma_l e^{j\theta} + \sqrt{\frac{1}{k+1}}\mathcal{CN}(0, \sigma_l^2), \quad (1.5)$$

where  $k$  (K-factor) denotes the ratio of energy in LoS path and scattered paths, whose expression is

$$k = \frac{m^2}{2\eta^2}. \quad (1.6)$$

Here the first term yields the LoS path with uniform phase  $\theta$ . The second term is the scattering paths which independent of  $\theta$ .

### 1.3.2 Empirical Models

Other than the analytical analysis, in practise, the empirical models have been arose by engineers for estimation usage. The empirical models come from series estimations in the real world while deploying the cellular communications. Some of them are used for general wireless communication model, whereas some of them are obtained according to the estimations in the urban area.

#### 1.3.2.1 Okumura Model

Besides the prior studies, in reality, some engineers propose various radio propagation models within different environments according to their estimation work. The most commonly and still widely adopted model is the Okumura model [4]. This model is obtained with the channel estimation work of Tokyo urban area for several years. It is relatively suit for the urban macro cells' radio propagation with a cellular range  $1 \sim 100$  Km, carrier frequency range  $150 \sim 1500$  MHz, and the transmit Base Station (BS) height around  $30 \sim 100$  M. With these conditions in hand, after transmitting over a distance  $d$ , the path loss power according to Okumura model, can be estimated (in dB) as [4–6],

$$P_l(okumura)\text{dB} = L(f, d) + A_\mu(f, d) - G(h_t) - G(h_r) - G_{AREA}, \quad (1.7)$$

where  $L(f, d)$  represents the free space path loss. Moreover,  $A_\mu(f, d)$ ,  $G(h_t)$ ,  $G(h_r)$  yield the median attenuation at distance  $d$  and frequency  $f$ , BS antenna high gain and receiver antenna height gain factors, respectively. In addition,  $G_{AREA}$  is the gain of the transmission environment.

#### 1.3.2.2 Hata Model

Besides the Okumura model, Hata model [7, 8] is another widely adopted empirical propagation model that valid for the frequency range from 150 to 1500 MHz. It provides a simpler closed-form expression of the urban environment. The expression of path loss with Hata model, is given as (in dB) [6–8]

$$\begin{aligned} P_L(Hata)_{urban}\text{dB} &= 69.55 + 26.16 \lg(f) - 13.82 \lg(h_t) \\ &\quad - \alpha(h_r) + (44.9 - 6.55 \lg(h_t)) \lg(d). \end{aligned} \quad (1.8)$$

Note that here the other parameters are the same as in Okumura propagation model besides the  $\alpha(h_r)$ . Actually,  $\alpha(h_r)$  has different expressions in different environments. For instance, by small to medium sized cities,  $\alpha(h_r)$  can be calculated as (in dB)

$$\alpha(h_r)\text{dB} = 1.1\lg(f) - 0.7h_r - (1.56\lg(f) - 0.8). \quad (1.9)$$

On the other hand, for large cities and frequency larger than 300 MHz, it turns out to be (in dB)

$$\alpha(h_r)\text{dB} = 3.2(\lg(11.75h_r))^2 - 4.97. \quad (1.10)$$

Additionally, for the suburban area, the path loss power with Hata model can be given as (in dB)

$$P_{L,\text{suburban}}(\text{Hata})\text{dB} = P_L(\text{Hata})_{\text{urban}}\text{dB} - 2[\lg(f/28)]^2 - 5.4, \quad (1.11)$$

and in rural environment, path loss power with Hata model denoted by  $P_{L,\text{rural}}(\text{Hata})$  is (in dB)

$$P_{L,\text{rural}}(\text{Hata})\text{dB} = P_L(\text{Hata})_{\text{urban}}\text{dB} - 4.78[\lg(f)]^2 + 18.33\lg(f) - K, \quad (1.12)$$

where the  $K$  varies from 35.94 (countryside) to 40.94 (desert) [6]. Yet it should be pointed out that although those models are relatively useful in prior generations of wireless communication. But within 5G, for the denser cellular deployment and higher carrier frequency band (for instance, mmWave), some new models should be set forth. This is because that, the denser deployment of antenna arrays will results in the channel correlation between each other. On the other hand, with mmWave, the carrier frequency is relatively vulnerable to the wireless propagation. For instance, it is found that the mmWave frequency has really low reflection and refraction effects compared with prior macro Wave frequencies. In this regard, while deploying with mmWave, maybe the straight LoS beamforming is needed from the transmitter to receiver. This will be discussed in the following sections. Furthermore, some other wireless wave propagation models are omitted by this chapter due to the space limitation, such as the moving antenna model either in BS or the user side. Interested readers can refer to alternative literature for this.

### 1.3.3 Shadowing Effects

Besides the prior channel models to estimate the transmission between transceiver, the shadowing effect is another issue affecting the received signal. Generally, shadowing effect is defined as the effects of received signal power fluctuation due to obstructing

between the transmitter and receiver. It is found by prior work with Egli that with transmission distance larger than a few hundred meters, the received power fluctuates with a “log-normal” distribution about the area mean power. With shadowing effect, signal changes of the shadowing mainly come from the reflection and scattering while transmitting. The shadowing effects will also result in the wave lights bending, that is, the transmission is not along the straightforward lines. Apart from *large scale fading*, these effects are mostly summarized as the *small scale fading*. To describe them, some models are needed. One of these is the log-normal shadowing. Which is, while denoting the ratio of transmitting power and receiving power as  $\gamma = P_t/P_r$ , we have [6]

$$P(\gamma) = \frac{\zeta}{\sqrt{2\pi}\sigma_{\gamma_{dB}}\gamma} \exp\left[-\frac{(10\lg\gamma - \mu_{\gamma_{dB}})^2}{2\sigma_{\gamma_{dB}}^2}\right], \quad (1.13)$$

where  $\zeta = 10/\ln 10$ . In addition,  $\sigma_{\gamma_{dB}}$  yields the mean description of  $\gamma_{dB} = 10\lg\gamma$ , mostly obtained by the analytical model or empirical measures. Moreover,  $\sigma_{\gamma_{dB}}$  is the standard deviation of  $\gamma_{dB}$ . In the wireless communication study, shadowing effects can either be incorporated into the path loss lights with LoS or other propagation models, or separately calculated by the shadowing and path loss.

### 1.3.4 Outage probability and cell coverage area

Outage probability is defined as the value lower than a given threshold. In wireless communications, giving the threshold of SNR (or signal to interference plus noise ratio (SINR)), outage probability is the probability that the received signal power lower than the threshold. In this case, no successful transmission can be executed. In this regard, the outage probability is widely adopted to estimate the cellular coverage area. For instance, the outage probability is used for the mmWave assisted 5G systems for the potential coverage area analysis by the study of [9, 10].

As widely known, in wireless communications, ratio of the received power to transmitted power can be estimated as [6]

$$\eta_{\frac{P_r}{P_t}} \text{ dB} = 10\lg K - 10\phi \lg\left(\frac{d}{d_0}\right) - \gamma_{dB}, \quad (1.14)$$

where  $\gamma_{dB}$  yields a Gaussian distributed random variable with mean zero and variance  $\sigma_{\gamma_{dB}}^2$ . In addition,  $\phi$  is the path loss exponent. With this definition in hand, as the prior review of the outage probability definition, a value falling below a given SNR (or SINR) threshold value, the power outage probability in wireless communications

can be given as [6]

$$P_{out}(P_r \leq P_{th}) = 1 - Q\left(\frac{P_{th} - \left(P_t + 10 \lg K + 10\phi \lg\left(\frac{d}{d_0}\right)\right)}{\sigma_{\gamma_{dB}}}\right), \quad (1.15)$$

where  $P_r, P_{th}, Q$  yield the received power, power threshold and Q functions [11], respectively. Note that the conversion between the Q function and complementary error function is given by

$$Q(x) = \frac{1}{2} \operatorname{erfc}\left(\frac{x}{\sqrt{2}}\right). \quad (1.16)$$

whereas the  $\operatorname{erfc}(x)$  function is given as

$$\begin{aligned} \operatorname{erfc}(x) &= 1 - \operatorname{erf}(x) \\ &= \frac{2}{\sqrt{\pi}} \int_x^{+\infty} e^{-y^2} dy. \end{aligned} \quad (1.17)$$

The outage probability can be applied in calculating the coverage area of a cellular BS. This is due to the fact that, as stated before, whenever the received power lower than the received threshold, an outage transmission happens. Because of the shadowing effects, the cellular coverage area is not always a sphere shape; although in theoretical analysis, the sphere shape or even circle area for BS coverage area (while omitting the height of BS for simplicity) is widely adopted. In this regard, by adopting the outage probability definition, cellular coverage area can be estimated as [6]

$$\begin{aligned} C &= \frac{1}{\pi R^2} \int_0^{2\pi} \int_0^R P(P_r \leq P_{th}) r dr d\theta \\ &= \frac{1}{\pi R^2} \int_0^{2\pi} \int_0^R P(1 - P_{out}(P_r \leq P_{th})) r dr d\theta \\ &= \frac{1}{\pi R^2} \int_0^{2\pi} \int_0^R Q\left(\frac{P_{th} - \left(P_t + 10 \lg K + 10\phi \lg\left(\frac{d}{d_0}\right)\right)}{\sigma_{\gamma_{dB}}}\right) r dr d\theta \end{aligned} \quad (1.18)$$

## 1.4 Capacity and transmission rate analysis

Based on the prior discussions, in the following analysis, the capacity and transmission rate of the wireless communications, especially the cellular communications, will be investigated by this section. In this study, the Shannon theory is adopted with entropy analysis from the transmitter to receiver sides while giving the channel noise power value during the transmission. The capacity analysis is addressed beforehand. In this case, once the capacity performance is addressed, by giving the carrier bandwidth value, the sum rate of the system can be obtained according to the Shannon theory.

### 1.4.1 General analysis of the achievable capacity

Information theory roots back to the work of the information entropy invented by Claude Shannon in 1948 titled “A mathematical theory of communication”. Which is used to character the wireless communications of a given channel condition unreliable communications. Shannon theory proves that one can always approach the maximum transmission rate in a given channel while reducing the error rate with sophisticated encoding methods. Whereas the capacity can be derived based on the Shannon theory and Entropy analysis.

By considering a typical communication system, its received signal at the receiver reads

$$y = hx + n, \quad (1.19)$$

where  $h, x, n$  yield the channel matrix, transmit signal matrix, and channel noise matrix, respectively. Typically, the channel noise is assumed to be the Additive White Gaussian Noise (AWGN) that obeys  $\mathcal{CN}(0, \sigma^2)$  with mean zero and variance  $\sigma^2$ . One can obtain the transmitted signal by invoking some decoding mechanisms at the receiver side, such as the Maximum Likelihood Ratio Combining (MLRC). The channel encoding and decoding mechanisms have been investigated a lot in literature. Interested reader can refer those prior work. However, in this introduction, it is focused on the achievable capacity and transmission rate analysis by reviewing the Shannon’s prior study, whereas the encoding and decoding mechanisms are omitted. In SISO scenario, the matrix takes the one-dimensional condition. Accordingly, the capacity performance of SISO system can be given as

$$C = \max_{p(x): EX^2 \leq P} I(X; Y), \quad (1.20)$$

where  $I(X; Y)$  represents the mutual information, which can be obtained by the entropy analysis. For instance, given a  $X$ , the entropy is defined as

$$\begin{aligned} I(x) &= H(x) \\ &= \sum_{i=1}^N p_i \log_2 \left[ \frac{1}{P_i} \right] \\ &= \sum_{x \in X} p(x) \log_2 \left[ \frac{1}{p(x)} \right] \\ &= - \sum_{x \in X} p(x) \log_2 [p(x)], \end{aligned} \quad (1.21)$$

where

$$X = [x_1, \dots, x_i, \dots, x_N], \quad (1.22)$$

is the random variable set. In addition,

$$p(x) = [p_1, \dots, p_i, \dots, p_N], \quad (1.23)$$

is the probability mass function set. The mutual information with  $I(X; Y)$  thus reads [6]

$$\begin{aligned} I(X; Y) &= H(X) - H(X|Y) \\ &= H(Y) - H(hX + N|X) \\ &= H(Y) - H(N). \end{aligned} \quad (1.24)$$

In general, the following equation

$$I(X; Y) = H(Y) - H(N) \quad (1.25)$$

is widely used to calculate the capacity of wireless systems. It gives the differential entropy with

$$H_d(Y) = \log_2(\pi e \sigma_y^2). \quad (1.26)$$

On the other hand, according to [6], the received average power (summarizing the useful received signal power and the channel noise power) at the receiver side is given as

$$\begin{aligned} \sigma_y^2 &= E[Y^2] \\ &= E[(hX + N)(hX + N)^*] \\ &= \sigma_x^2 |h|^2 + \sigma_n^2. \end{aligned} \quad (1.27)$$

With this analysis in hand, according to our prior analysis of the capacity performance with entropy theory, the capacity can be further written as

$$\begin{aligned} C &= \max_{p(x): EX^2 \leq P} I(X; Y) \\ &= H_d(Y) - H_d(N) \\ &= \log_2(\pi e \sigma_y^2) - \log_2(\pi e \sigma_n^2) \\ &= \log_2(\pi e \sigma_x^2 |h|^2 + \sigma_n^2) - \log_2(\pi e \sigma_n^2) \\ &= \log_2 \left( 1 + \frac{\sigma_x^2}{\sigma_n^2} |h|^2 \right) \\ &= \log_2 \left( 1 + \frac{P_t}{\sigma_n^2} |h|^2 \right). \end{aligned} \quad (1.28)$$

This is the widely used capacity performance equation in wireless communications. Moreover, while denoting the SNR as

$$\rho = \frac{P_t}{\sigma_n^2 |h|^2}, \quad (1.29)$$

the capacity performance turns out to be

$$\begin{aligned}
C &= \max_{p(x):EX^2 \leq P} I(X;Y) \\
&= \log_2 \left( 1 + \frac{P_t}{\sigma_n^2} |h|^2 \right) \\
&= \log_2(1 + \rho).
\end{aligned} \tag{1.30}$$

As we can see here, the channel response  $|h|^2$  is assumed to be a fixed scalar value in the SISO system, as well as the channel noise variance and the power value at the transmitter side. In contrast, in MIMO system, those parameters will be given in vectors and matrices form expressions with regards to the associated channel from transmitter to receiver. This will be addressed by the following contents.

### 1.4.2 Capacity analysis of the MIMO system

In MIMO system, although the prior analysis can be adopted with entropy theory, yet the parameters will be vectors and matrices. In addition, due to the extra channel response associating with the channel response matrix, the achievable capacity performance can be further increased. On the other hand, it is known that MIMO system capacity can be boosted without more bandwidth values, and more transmit power values by simply increasing the antenna number at the transmit sides.

By denoting the transmit antenna number  $N$ , and receive antenna number  $M$ , the received signal can be given as

$$\mathbf{y} = \mathbf{H}\mathbf{x} + \mathbf{n}, \tag{1.31}$$

where  $\mathbf{y} \in \mathbb{C}^{M \times 1}$ ,  $\mathbf{H} \in \mathbb{C}^{M \times N}$ ,  $\mathbf{x} \in \mathbb{C}^{N \times 1}$ , and  $\mathbf{n} \in \mathbb{C}^{M \times 1}$ .

As shown, within all channels, transmitted signal  $\mathbf{x}$  and noise  $\mathbf{n}$  are tackled with vectors, which is different with prior SISO system. Taking the average power allocation and equal Rayleigh channel matrix assumption (the different power allocation or optimal power allocation mechanism can be another interesting topic given the channel matrix from transmitter to receiver and the transmission rate requirements. Here we only address the simply case of the achievable capacity performance of MIMO system given the equal power allocation scheme. In addition, it is assumed that the channel noise is equal amongst each channel from the transmitter to receiver),

capacity of the MIMO system can be given as

$$\begin{aligned}
C &= \sum_{i=1}^M B_i \log_2 \left( \det[\mathbf{I}_N + \frac{P_{t_i}}{M\sigma_n^2} \mathbf{H}\mathbf{H}^H] \right) \\
&= \sum_{i=1}^M B_i \log_2 \left( \det[\mathbf{I}_N + \frac{\rho}{M} \mathbf{H}\mathbf{H}^H] \right),
\end{aligned} \tag{1.32}$$

where  $B_i$ ,  $\det, \mathbf{I}_N$  yield the bandwidth allocated to each user, the determinant of a matrix, the  $M \times N$  identify matrix, respectively. Additionally,  $\rho$  here is the average SNR in each channel. Moreover,  $\mathbf{H}^H$  denotes the conjugate transpose of a matrix  $\mathbf{H}$ . In this case, given  $M, N$  as defined as before, the channel matrix can be described with matrix form as

$$\mathbf{H} = \begin{bmatrix} h_{1,1} & h_{1,2} & \dots & h_{1,N} \\ h_{2,1} & h_{2,2} & \dots & h_{2,N} \\ \dots & \dots & \ddots & \dots \\ h_{M,1} & h_{M,2} & \dots & h_{M,N} \end{bmatrix}. \tag{1.33}$$

Each of the entry of  $\mathbf{H}$ , by following the prior defined Rayleigh channel matrix, can be expressed as

$$\begin{aligned}
h_{i,j} &= \alpha + j\beta \\
&= \sqrt{\alpha^2 + \beta^2} e^{j \arctan \frac{\beta}{\alpha}} \\
&= |h_{i,j}| e^{j\phi_{i,j}},
\end{aligned} \tag{1.34}$$

where  $\alpha, \beta$  are random distributed variables, which in turns,  $|h_{i,j}|$  a Rayleigh distributed random variable. While further assuming the Rayleigh channels are i.i.d. complex zero mean and unit entries, expression of  $h_{i,j}$  can be written as

$$h_{i,j} = \text{Normal} \left( 0, \frac{1}{\sqrt{2}} \right) + j \text{Normal} \left( 0, \frac{1}{\sqrt{2}} \right), \tag{1.35}$$

here Normal yields the normal distribution.

To determinate the exact expression of this achievable capacity, the following work is to crack down the matrix expressions with some closed-form expressions. As shown here, the determination expression of  $\mathbf{I}_N + \frac{\rho}{M} \mathbf{H}\mathbf{H}^H$  can be characterized with the eigenvalue. In this case, one can mainly focuses on the eigenvalue of  $\mathbf{H}\mathbf{H}^H$  while calculating the capacity. Thus we have that the eigenvalue (besides 0, because it has no contribution to the MIMO capacity calculation while denoting that the channel is rarely worse for transmission) of  $\mathbf{H}\mathbf{H}^H$  and  $\mathbf{H}^H\mathbf{H}$  with  $\lambda = [\lambda_1, \lambda_2, \dots, \lambda_{\min(N,M)}]$  yielding the nonzero eigenvalues of the  $\mathbf{B}$ . This gives the following equation

$$\mathbf{B} = \begin{cases} \mathbf{H}\mathbf{H}^H, & M < N, \\ \mathbf{H}^H\mathbf{H}, & M > N. \end{cases} \tag{1.36}$$

Let say that the first expression is adopted (it is similar while adopting the second expression), the MIMO capacity will be

$$\begin{aligned}
C &= \sum_{i=1}^M B_i \log_2 \left( \det[\mathbf{I}_N + \frac{\rho}{M} \mathbf{H}\mathbf{H}^H] \right) \\
&= \sum_{i=1}^M B_i \log_2 \left( \prod_{i=1}^{\min(N,M)} \left[ 1 + \frac{\rho}{M} \lambda_i^2 \right] \right).
\end{aligned} \tag{1.37}$$

On the other hand, to pre-code the transmit signal and decode them at the receiver side, the Singular Value Decomposition (SVD) method is used a lot in MIMO system. In SVD, the channel matrix is decomposed by

$$\mathbf{H} = \mathbf{U}\mathbf{D}\mathbf{V}^H, \tag{1.38}$$

where  $\mathbf{D}$  is  $M \times N$  matrix, whose non zero norm by the diagonal entries are the singular values of  $\mathbf{H}$ , and  $\mathbf{U}, \mathbf{V}$  are  $M \times M, N \times N$  unitary matrix, respectively. Substituting those into 1.31 will yield the following equation

$$\mathbf{y} = \mathbf{U}\mathbf{D}\mathbf{V}^H \mathbf{x} + \mathbf{n}. \tag{1.39}$$

While pre-multiplied by  $\mathbf{U}^H$  of both sides to this equation, and with the following definitions

$$\tilde{\mathbf{y}} = \mathbf{U}^H \mathbf{y}, \tag{1.40}$$

$$\tilde{\mathbf{x}} = \mathbf{x}\mathbf{V}^H, \tag{1.41}$$

$$\tilde{\mathbf{n}} = \mathbf{U}^H \mathbf{n}. \tag{1.42}$$

It has

$$\tilde{\mathbf{y}} = \mathbf{D}\tilde{\mathbf{x}} + \tilde{\mathbf{n}}. \tag{1.43}$$

By further adopting  $\lambda_i$  as the eigenvalue of  $i$ th channel matrix, the  $i$ th receiver signal will be

$$\tilde{\mathbf{y}}_i = \lambda_i \tilde{\mathbf{x}}_i + \tilde{\mathbf{n}}_i, \tag{1.44}$$

To address the capacity performance, the covariances and traces of each can be defined as follows

$$R_{\tilde{y}\tilde{y}} = \mathbf{U}^H R_{yy} \mathbf{U}, \tag{1.45}$$

$$R_{\tilde{x}\tilde{x}} = \mathbf{V}^H R_{xx} \mathbf{V},$$

$$tr(R_{\tilde{y}\tilde{y}}) = tr(R_{yy}),$$

$$tr(R_{\tilde{x}\tilde{x}}) = tr(R_{xx}), \tag{1.46}$$

$$tr(R_{\tilde{n}\tilde{n}}) = tr(R_{nn}).$$

With perfect Channel State Information (CSI) and equality power allocation mechanism, one can arrive the expression of 1.37 [12, 13]. As we can see here, the capacity performance of MIMO system mainly determined by the channel matrix with its eigenvalue, the SNR of each i.i.d. channel ( $\rho$ ), and the associating user number  $M$ . By the massive MIMO system that the transmit antenna number is larger than the received user number, it can be shown that the ratio of the number of transmit antenna to received antenna are the determined factor. Interested reader can refer to the work in [14, 15].

## 1.5 From MIMO to mMIMO

The transmission rate balloon is on the way of 5G, where massive MIMO as well as other technologies (for instance, small cell, Heterogeneous Networks (HetNets), mmWave) are believed to be the potential solutions to achieve the 5G requirements with both SE and EE requirements. In massive MIMO, it is proved that with perfect CSI and completely eliminated pilot contamination, with a fixed ratio of transmit to received antenna number, one can always achieve better SNR while simply increasing the transmit antenna number [14, 16].

The side effect brings in by this massive MIMO, however, is the cellular densification, which makes the deployment in large urban area even unacceptable. As known, with the Cooper's law, capacity increase will mostly be due to a denser and denser cell deployment [17]. Besides, the emerging topics in massive MIMO recently, are the EE (how to effectively constraint the energy consumption), low latency backhauls to sustain the even faster transmission speed, etc. This is because of the even greater energy consumption of the massive MIMO system with much faster transmission rate requirement of 5G. With massive user equipments jointing in of 5G era, it is discussed from Institute of Electrical and Electronic Engineers (IEEE) 5G summit in silicon valley in 2016 that re-design the network architecture will be needed. It is also discussed by other scholars in upper layer that the driving forces behind the wireless evolution are changing from the prior "transmission rate centric" to "information-centric". In this case, the study of re-designing the whole network architecture are mostly from the upper layer. Some of the antecedent studies can be listed as follows, the Information Centric Networking (ICN) [18], Software Defined Radio (SDR) [19] (or named Network Functions Virtualization (NFV)), etc. In addition, Devices to Devices (D2D) communications [20], Full Duplex communication

mechanism [21, 22], and collaboration between different users and cellulars [14], are believed to be indispensable elements of 5G.

### 1.5.1 Even faster transmission speed

Other than the prior introduction of capacity analysis of MIMO system, we move ahead to state the mMIMO system capacity analysis in this part. Here for the sake of compactness, we take the assumption that the bandwidth number is 1, and focus the study on the antenna number effects to the achievable transmission rate. Furthermore, the study is limited to one cellular coverage area.

As state aforementioned, in line with the study in [16], the following equations hold

$$\sum_{i=1}^{\min(M,N)} \lambda_i^2 = \begin{cases} tr(\mathbf{H}\mathbf{H}^H), M < N, \\ tr(\mathbf{H}^H\mathbf{H}), M > N. \end{cases} \quad (1.47)$$

Here  $tr$  denotes the trace of a matrix, where the worse case is that all but one of the singular value is equal to zero. Which means only one channel is suitable for transmission. In contrast, the best case is that all of the singular values are not zero and with larger value. This means that each of the user can associate with a suitable channel or multiple channel for its transmission.

In light of this, the capacity upper bound (by assuming the upper value of the achievable capacity) of mMIMO system can be given as [16]

$$\log_2 \left( 1 + \frac{\rho tr(\mathbf{H}\mathbf{H}^H)}{N} \right) \leq C \leq \min(N, M) \times \log_2 \left( 1 + \frac{\rho tr(\mathbf{H}\mathbf{H}^H)}{N \min(N, M)} \right). \quad (1.48)$$

While further assuming the coefficient of the magnitude of propagation is normalized to one, we have  $tr(N, M) = NM$  [16]. Thus the above functions can be re-written as

$$\log_2(1 + \rho M) \leq C \leq \min(N, M) \times \log_2 \left( 1 + \frac{\rho \max(N, M)}{N} \right). \quad (1.49)$$

In addition, on the condition that each channel has a low SNR, simply increase the transmit antenna number has no effect to the capacity performance. This is because of the following approximation

$$C_{\rho \rightarrow 0} \approx \frac{\rho tr(\mathbf{H}\mathbf{H}^H)}{N \ln 2} \approx \frac{\rho M}{\ln 2}. \quad (1.50)$$

It mostly happens at the edge of a cellular coverage area. In this case, some alternative ways to enhance the transmission experience of the cellular edge area are needed. One of the methods is the Non-Orthogonal Multiple Access (NOMA), which pairing two

or more users' transmission located in the center and edge area together within the same channel. On the other hand, the relay assisted system can be invoked to improve the Quality of Service (QoS) at the cellular edge area.

However, with better SNR condition (for cellular center area), as a consequence, we have the following approximation [23]

$$\left(\frac{\mathbf{H}\mathbf{H}^H}{N}\right)_{N \gg M} \approx \mathbf{I}_M, \quad (1.51)$$

where the achievable rate in this case, will turn out to be [16]

$$\begin{aligned} C_{N \gg M} &\approx \log_2 \det(\mathbf{I}_M + \rho \mathbf{I}_M) \\ &= M \log_2(1 + \rho). \end{aligned} \quad (1.52)$$

On the other hand, while keeping the transmit antenna number constant and increasing the receive antenna number, under the column vectors of the propagation matrix are asymptotically orthogonal assumption, we have [16]

$$\left(\frac{\mathbf{H}\mathbf{H}^H}{N}\right)_{M \gg N} \approx \mathbf{I}_N, \quad (1.53)$$

and

$$\det(\mathbf{I} + \mathbf{H}\mathbf{H}^H) = \det(\mathbf{I} + \mathbf{H}^H \mathbf{H}). \quad (1.54)$$

In light of this, the achievable rate is [16]

$$\begin{aligned} C_{M \gg N} &\approx \log_2 \det(\mathbf{I}_N + \frac{\rho}{N} \mathbf{H}^H \mathbf{H}) \\ &\approx N \log_2 \left(1 + \frac{\rho M}{N}\right). \end{aligned} \quad (1.55)$$

Another, in multi-cells condition, with antenna number growing large (with  $\limsup_N K/N < \infty$ .) and all of the impacts adding in, such as the noise, imperfect CSI, interference, pilot contamination, as the study in [15], no matter by what kinds of beamforming techniques, the achievable capacity will approaching to

$$\begin{aligned} R_\infty &= \log_2(1 + \gamma_\infty) \\ &= \log_2 \left(1 + \frac{1}{\alpha(\bar{L} - 1)}\right), \end{aligned} \quad (1.56)$$

where  $\gamma_\infty$  yields the SINR with infinite antenna number,  $\alpha \in (0, 1]$  is the inter-cell interference factor,  $\bar{L} = 1 + (\alpha - 1)$  with  $L$  represents the cell number.

## 1.5.2 Energy efficiency

As higher transmission rate will consume even more power, under 5G background, EE becomes another vital issue that attracts lots of attentions world widely. Nowadays, the studies on enhancing the EE performance can be mainly summarized into the component selection, network coding, and also new network architecture design.

In component selection study, the cellular zooming mechanism based on mMIMO is proposed by [1], where the cellular can be zoomed in to cover more coverage area or zoomed out to save energy. The transmission in low user number areas will be handed over to the neighboring cells with Coordinated Multi-Point transmission/reception (CoMP) technology. Under this, the antenna selection mechanism ([24], et. al.), Radio Frequency (RF) chain selection mechanism([25], et. al.), and the combination of these ([5,26], et. al.) and other components are proposed in mMIMO EE studies with respect to the EE definition. The mostly adopted EE definition is given as the achievable transmission rate divided by the consumed energy to sustain the rate

$$\eta_{EE} = \frac{C}{P}, \quad (1.57)$$

where  $C, P$  yield the achievable capacity (or transmission rate) and consumed power, respectively.

In network coding studies, most of the literatures are based on the two way or multi-way ray network. For instance, the Analog Network Coding (ANC) and Physical-layer Network Coding (PNC) are studied in the two-way wireless relay system for EE issue in [27]; a two-stage Maximum Energy Efficiency (MEE) method is proposed in [28]. Additionally, the joint design of network coding and MIMO package scheduling is studied by [29].

The Cloud Radio Access Network (C-RAN) is becoming a hot network architecture of 5G recently, where as the study from China Mobile (CMCC), with C-RAN's shared machine room, more energy can be saved with less energy consumption from the air conditioner, grids, etc. In this regard, literature based on C-RAN can be found that, for instance, in [30], a simple but efficient pre-coding scheme is proposed to reduce the computation complexity of cooperative transmission, thus lowering the associated power consumption. An energy consumption model for C-RAN is further studied for capturing the energy consumption of centralised BBU resources plus an algorithm that optimises the BBU resource allocation is proposed in [31]. Other literature with network architecture is based on the HetNets, where not only the C-RAN, but also D2D and other deployments are taken into a comprehensive consideration.

### 1.5.3 Emerging topics in mmWave mMIMO

Other than the aforementioned discussions, mmWave is discussed a lot in literature of 5G. This is mainly because of the Shannon theory that with more allocated bandwidth, better transmission rate can be achieved. Mostly, mmWave mMIMO is try to explore new unlicensed frequency resources to boost the 5G transmission rate requirements. As the recommendation, mmWave is defined as the band ranging from 30GHz to 300GHz, both from IEEE and ITU [32]. Most of the recent studies of mmWave mMIMO for 5G are focused on the 28GHz, 38GHz, the 60GHz bands, as well as the E-band (71 ~ 76 GHz and 81 ~ 86 GHz) [32].

However, as the mmWave mMIMO working at even higher frequency, which brings in challenges to the research for both indoor and outdoor environments. For instance, with even higher frequency, much shorter wavelength, mmWave cannot transmit a long distance as prior licensed frequencies. As the much severer conditions that mmWave mMIMO is experiencing for this even higher frequency, new channel model to describe the mmWave transmission will be needed. In addition, due to the short distance of mmWave, denser deployment of the cellular is inevitable. With this regard, small cell with less coverage area range and the D2D proposals are investigated a lot while combining the mmWave.

In mmWave mMIMO channel estimation and modeling work, the New York University together with University of Texas-Austin have done some preliminary studies. For example, as we talked before, in their studies, the stochastic geometry and random geometric graph theory are mostly used in mmWave mMIMO topics for signal to interference ratio (SIR), connectivity, coverage, as well as outage probability and throughput analysis. For the mmWave mMIMO studies, one can find in literature from but not limited to their studies in [9, 33, 34]. With mmWave adding in, the new challenges are waiting to tackle not only the new channel model but also the beamforming techniques, the new system design, channel coding method (such as the NOMA [35–37]), full duplex communications [38] as well as the D2D communications can be good choices.

Other than these technologies that focusing on the Enhanced Mobile Broadband (eMBB) and massive Machine Type Communications (mMTC) scenes, the Ultra-Reliable and Low-Latency Communication (URLLC) is another scene of 5G. In which, the low latency back-hauling and front-hauling links are noticed a lot with the heterogeneous networks that associating macro cell, small cell and D2D communications. On the other hand, the mobility issue is also of vital in vehicular communications

with 5G, especially with a higher moving speed that causing great challenge to the handover between cells.

## **1.6 The logical structure of this dissertation and relationship of each chapter**

As stated by prior sections, various topics are suggested in 5G, which is hard to cover all of them. In this dissertation, it is tried to solve the SE and EE issue of 5G. The logical structure of this dissertation is organized as follows. As state by this introduction chapter, the wireless evolution is reviewed from prior GSM to the latest 5G wireless communications. In which the main technologies in prior generations are briefly introduced. Thus the emerging technologies to achieve the 5G is reviewed, such as the massive MIMO, NOMA, D2D, full duplex.

As 5G is claiming for even higher transmission rate, one of the intuitive methods is to allocate more carrier frequency resources for 5G, such as the mmWave. However, it is not a good choice to allocate frequency resources arbitrarily since the frequency resources are scare. Once allocated, it can not be used for other purpose. The studies both from academia and industry are focusing on some alternative methods to achieve this. In line with prior evolutions especially from 3G to 4G, the driving forces are to increase the SE of the cellular. In light of this, in the chapter 2, the NOMA and massive MIMO are combined together for its capacity performance based on the mmWave channel. In which, the system SE performance is greatly increased with NOMA and massive MIMO. Additionally, giving the even wider bandwidth provided by the mmWave frequencies, much faster transmission rate can be obtained.

As noticed by prior studies, the methods other than the channel coding, will cost much more energy consumptions of the wireless networks. The EE issue, is noticed a lot as an emerging topic in 5G other than prior generations. The concept of EE is to find a trade-off between the increasing transmission rate and the system energy consumption. In light of this, the EE issue is investigated by chapter 3 and chapter 4 besides the SE issue discussed by chapter 2.

The EE issue has been investigated a lot in prior studies. Yet it is noticed that most of the prior studies focused on the links from the transmitter to the receiver, in which, the light of other component that engaging is omitted (such as the machine room, circuit energy consumption). Thus by chapter 2, an integrated system model is proposed by uniformly supplying the power for multiple BS with the same machine room. Moreover, it is assumed that all of the transmission resources as well as the

transmission procedures are processed by the uniformly Base Band Unit (BBU) that sharing amongst multiple BS. In addition, a Cellular Partition Zooming (CPZ) scheme is further provided to further divide the coverage area according to the angle from BS to users. With the integrated system model in hand, chapter 3 further investigates the EE issue while taking more elements into consideration. The system EE performance is further increased with this method by turning off the unwanted elements.

The paper is finally concluded by chapter 5. In which, the main findings of this dissertation are reviewed. In addition, based on the studies by this dissertation, some future work is set forth for further study.

## Chapter 2

# Capacity Analysis of NOMA-massive-MIMO-mmWave Systems

### 2.1 Summary

In prior literature, the Non-Orthogonal Multiple Access (NOMA), millimeter Wave (mmWave), and massive Multiple-Input-Multiple-Output (massive MIMO) have been studied a lot in Fifth Generation (5G), by separately or the combinations of two technologies. However, little light has been casted on the combinations of those three technologies. As studied before, each of them is enable to increase the Spectrum Efficiency (SE) performance. From an intuitive perspective, by combining all of them in a coherent system, even better SE and system capacity performance can be achieved. Yet by what scale the increment can be is still ambiguous. In light of this, this study focuses on the combinations of these three technologies. The ambiguous question with SE enhancement and capacity increment are investigated. That is, based on the prior studies on mmWave with its Uniform Random Single Path (UR-SP) model, a simplified mmWave channel model is introduced beforehand. Afterwards, with all of those three technologies considered in, the system capacity analysis is divided into the noise-dominated low Signal to Noise Ratio (SNR) regime and interference-dominated high SNR regime. In which, the exact achievable capacity expressions are addressed for both regimes. Numerical results is employed to validate the theoretical analysis. It demonstrates that significant capacity improvements can be achieved by the integrated NOMA-mmWave-massive-MIMO systems.<sup>1</sup>

---

<sup>1</sup>This is based on the work of **D. Zhang**, K. Yu, Z. Wen, and T. Sato, "Outage Probability Analysis of NOMA within Massive MIMO Systems," in *IEEE VTC 16' Spring*, pp. 1-5, Nanjing, China, May 2016.

## 2.2 Introduction

### 2.2.1 Background and motivation

The Fifth Generation (5G) wireless communications are calling for even higher transmission rate within each cellular to meet the fast growing high performance smart terminals and emerging new mobile multimedia services [39]. In addition, it is claimed that even massive devices should be connected to the internet via wireless connections in 5G. The full scope of 5G is to connect everything, at every time, from anywhere. Thus some scholars are calling 5G as the IoE era. In which, in line with prior studies, the Spectrum Efficiency (SE) has been studied a lot in 5G. Besides, this transmission rate requirements result in the increasingly prominent contradiction between the exponentially growing data demands and existing spectrum resources. The mmWave then, is proponed to allocated for wireless communication's usage to meet the 5G's demanding SE and Energy Efficiency (EE) requirements [3, 40]. Recently, millimeter Wave (mmWave) [37], Non-Orthogonal Multiple Access (NOMA) [2, 41], and massive Multiple-Input-Multiple-Output (massive MIMO) [14] have been considered as indispensable elements of 5G and have attracted intensive interests from both academy and industry.

Generally, the frequency ranges around  $30 \sim 300$  GHz are referred as the mmWave frequencies. While applying in the wireless communications, the even higher frequency brings in the even shorter propagation distance. Besides, the propagation characteristic implied from the complicated environments is apart from the prior existing frequencies. To this end, the mmWave propagation characteristics and channel models are the focal points in the initial studies of mmWave [37, 42]. Another, the optimal beamforming design attracts lot of interests in mmWave studeis, such as the studies in [43, 44].

Except for allocating more frequencies to wireless communications, the NOMA was proposed to alleviate the bottleneck of spectrum shorting in which multiple users sharing the same frequency bandwidth for the transmission [36]. At the receiver side, the Successive Interference Cancellation (SIC) is employed to remove other users' information associating with higher orders (actually, there are various SIC decoding methods with regards to the Signal to Noise Ratio (SNR), Signal to Interference plus Noise Ratio (SINR), and the user orders with an increasing or decreasing power value. Here in this study, we focus on the last mechanism.). Normally, with NOMA scheme, different transmission rate requirements with users located in the central and edge

sides are needed. Currently, most of the research of NOMA focus on the optimal beamforming design [45], user pairing [46], and power allocation [47].

Furthermore, the massive MIMO aims to tumble the 5G's SE and EE requirement toughies [3]. The benefit of massive MIMO is that, with even more antenna number, thermal noise and fast fading are averaged out. In this case, the system performance mainly depends on the aggregated characteristics rather than the prior propagation conditions or prior channel conditions as in conventional cellular systems [48]. Generally, it would be inefficient to use all of the antennas for transmission especially when the number of users is limited and the total sum power of a large number of Radio Frequency (RF) chains can no longer be ignored [49].

Although various studies have been done of the mmWave, NOMA and massive MIMO, however, little light has been casted on how to combine different technologies into a converged system. In addition, how much performance improvement can be achieved by this combination remains unclear. In this case, in this study, the combinations of all of these three technologies are combined together, and the system capacity performance is investigated.

### 2.2.2 Related work

The related antecedent work can be categorized as follows. The mmWave channel models were investigated in [37, 42, 50] with its propagation characteristics for general model purpose. In addition, the mmWave channel was estimated and the cellular capacity was evaluated in New York City environment [50]. Besides, the Angle of Departure (AoD), Angle of Arrive (AoA), and channel gain characteristics of mmWave propagation were estimated for both Light Of Sight (LOS) and Non Light Of Sight (NLOS) paths in [37]. In [42], a Structured Compressive Sensing (SCS)-based channel estimation scheme was given and the angular sparsity was employed to reduce the required pilot overhead. The simplified Uniform Random Single Path (UR-SP) model was adopted for the optimal beamforming design in [44]. The Kronecker channel model was investigated and a hybrid precoding method was proposed in [51].

Besides the mmWave propagation studies, on the study of integrating NOMA and massive MIMO, a joint antenna selection and user scheduling algorithm was proposed in [52]. Numerical results shown that the proposed algorithm achieved better search efficiency in single-band two-user scenario. A simplified and limited feedback scenario for NOMA-MIMO systems was propounded in [53]. It was proved that the NOMA-MIMO channel can be decomposed into multiple NOMA-SISO channels. In our prior study [54], the outage probability was investigated of NOMA-massive-MIMO. As

we can see, although various work has been done on the combination of MIMO-NOMA, less work has been done for the combination of MIMO-mmWave, and NOMA-mmWave. In addition, even less work has been done on the light of combining the mmWave, NOMA, and massive MIMO.

For the capacity studies and related mathematics tools, conjugate and zero-forcing beamforming techniques were compared by [55] of the massive MIMO system. The convergence probability and transmission capacity were investigated of mmWave Ad-Hoc networks in [10]. The capacity of mmWave-massive-MIMO system was evaluated with the Three-Dimensional (3D) channel model and various beamforming technologies in [56]. In the study of [57], the authors compared the NOMA-MIMO system capacity with prior Orthogonal Multiple Access MIMO (OMA-MIMO) system. It was proved that NOMA-MIMO system achieves better ergodic capacity. As noticed, most prior studies were based on water filling and optimal beamforming design methods [2], which will become un-effective with the number of antennas growing large. In this case, the Random Matrix Theory (RMT) is noticed recently, which provides a powerful and tractable tool to statistically assess the performance of massive MIMO systems. RMT tools have been widely applied in literature to character the ergodic capacity, outage probability, such as the studies in [15, 54, 58–62]. But still, for the more complicated NOMA-mmWave-massive-MIMO system that focused by this study, these methods are of high computational complexity. In this case, low-complexity asymptotic methods are of great importance.

### 2.2.3 Contributions

The aforementioned work plays a vital role and lies solid foundations for the study of mmWave, NOMA and massive MIMO. To step further, the integrated NOMA-mmWave-massive-MIMO system capacity analysis is addressed here. The main contributions can be summarized as follows:

- One integrated NOMA-mmWave-massive-MIMO system is systematically introduced. Afterwards, a simplified mmWave channel model is introduced based on the prior UR-SP model. Based on the proposed simplified channel model, the system capacity is further divided into the low-SNR and high-SNR regimes to simplify the analysis. This is due to the intractable analysis procedure while combining those three to get a comprehensive closed-form expression.
- In the noise-dominated low-SNR regime, the deterministic equivalent method with Stieltjes transform methods are used to surround the capacity expression.

The closed-form expression of the capacity performance is addressed. In addition, the relationship between Stieltjes transform and Shannon transform are proofed.

- In the interference-dominated high-SNR regime, the statistic and eigenvalue distribution tools are employed for the capacity analysis. The exact capacity expression is derived based on the Probability Distribution Function (PDF) of the channel eigenvalues. Yet the exact expression is too complex. In this case, a low complexity approximation expression is further given.
- The derived expressions are verified with the Monte Carlo method. Numerical results further reveal that in the low-SNR regime, SNR and user number have positive correlation with capacity performance. In addition, it is found that that the number of LOS paths has positive but little effect to system capacity increment while growing large.

## 2.2.4 Organizations

The rest of this chapter is organized as follows. The system model and channel model matrix are introduced in section II. Based on the system and channel model matrix, the capacity analysis with low-SNR regime is investigated firstly in section III. Afterwards, section IV provides the capacity analysis for the high-SNR regime. The numerical results are given in section V. The chapter is finally concluded in section VI.

## 2.2.5 Notations

Throughout this chapter, the uppercase boldface letters, lowercase boldface letters, and normal letters denote the matrix, vector, and scalar quantity, respectively. Additionally,  $\mathbb{C}$  and  $\mathbb{R}$  yield the sets of complex and real numbers, respectively, and  $\mathbf{A}^H$ , the Hermitian transposition of a matrix  $\mathbf{A}$ . Furthermore,  $\mathbf{A}_{i,j}$  is the  $(i, j)$ -th entry of a matrix  $\mathbf{A}$  with the  $i$ -th row and the  $j$ -th column,  $tr(\mathbf{A})$ ,  $\det(\mathbf{A})$ , and  $\mathbb{E}(\mathbf{A})$ , the trace, determinant, and expectation of the matrix  $\mathbf{A}$ . On the other hand,  $\mathbf{A}^{-1}$  is the inverse transpose of matrix  $\mathbf{A}$ ,  $\mathbf{A} \otimes \mathbf{B}$ , the Kronecker product of matrix  $\mathbf{A}$  and  $\mathbf{B}$ . In addition,  $N, L, K$  denote the number of transmit antenna, LOS path, and user. Finally, sup and inf respectively denote the supremum and infimum.

## Orthogonal between different users



## Superposition and differential power allocation

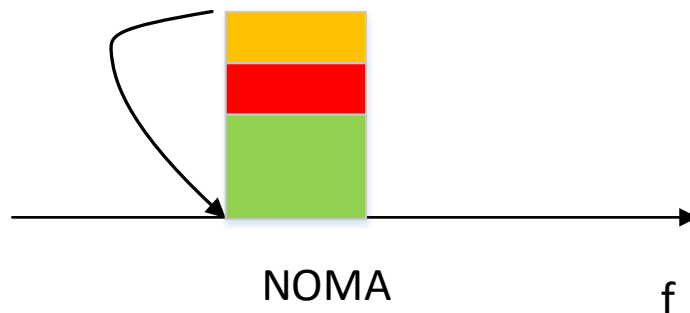


Figure 2.1 The comparison between OFDMA and NOMA.

## 2.3 System model

One exemplary figure to describe the difference between Orthogonal Frequency Division Multiple Access (OFDMA) and NOMA can be found as Fig. 2.1. In which, OFDMA divides the frequency bandwidth for multiple users' transmission, whereas the orthogonal correlation between difference bandwidth is exploited to isolate the interference from neighboring frequencies. As the division of frequencies, better capacity performance can be achieved via this technology.

On the other hand, with NOMA, other than the OFDMA, the superposition encoding scheme is utilized to encode the information amongst multiple users. Which is, within each frequency bandwidth, multiple users are allocated other than the sole user scheme. In addition, differential power values are allocated to differential users

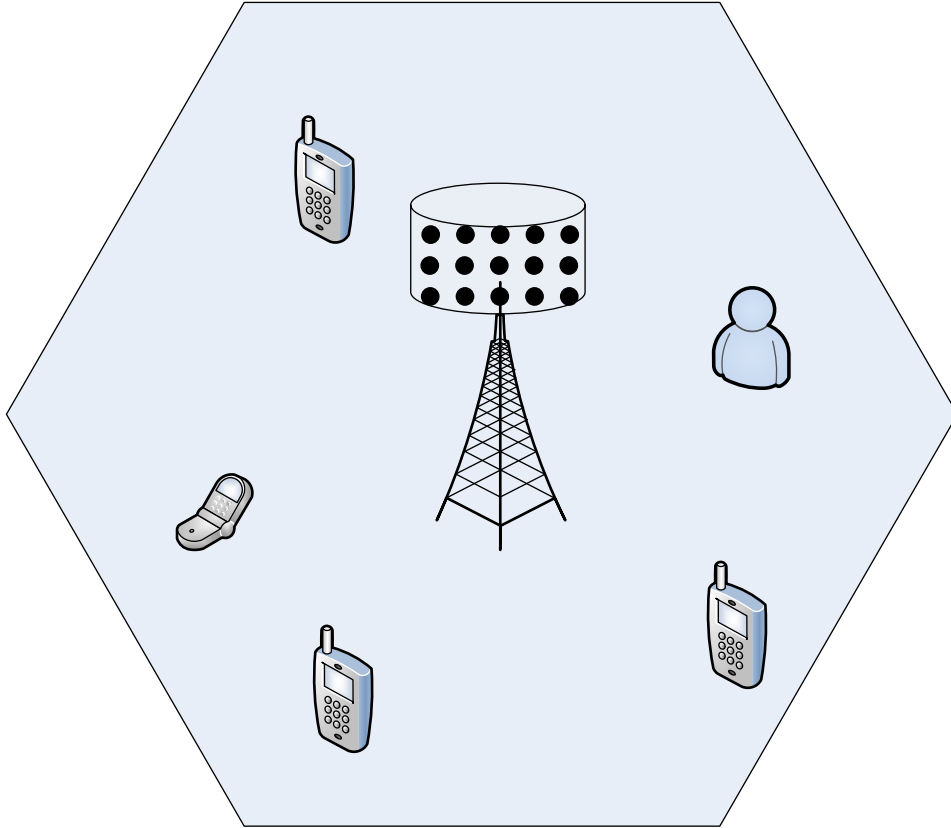


Figure 2.2 The massive MIMO concept.

to distinguish each of them that exploiting the same frequency bandwidth. At the receiver side, the SIC is employed to decode the information. Intuitive observation has that by sharing the same frequency block amongst multiple users, the system SE performance can be enhanced. It was proved that with equal power allocation scheme of two users with NOMA, it can achieve 32% capacity increase compared with OFDMA.

On the other hand, the massive MIMO is trying to use massive transmit antenna serving less user terminals. One exemplary figure to illustrate the concept of massive MIMO can be found as Fig. 2.2. The enhanced degree of freedom brought in via this massive number transmit antenna results in better system capacity performance compared with prior MIMO systems with limited number configuration (for instance,  $4 \times 4$  antennas in LTE system). Prior studies from [3, 63] proved that under ideal channel condition without pilot contamination, arbitrary capacity can be achieved by simply increasing the number. Thus massive MIMO, once propounded, is taken as one of the indispensable elements of 5G.

In addition, although various technologies on the SE issue in 5G have been pro-

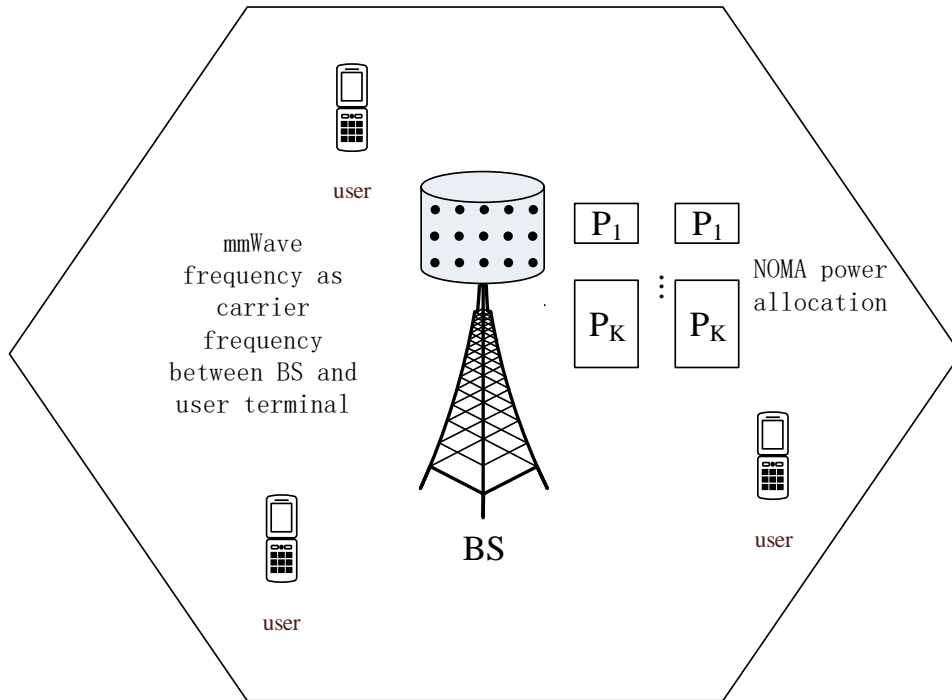


Figure 2.3 The conceptual model of the NOMA-mmWave-massive-MIMO system model.

pounded from different institutions, but still, 5G can not easily be achieved with those. Nowadays, scholars claiming for even higher frequency resources allocated for 5G wireless communications. Thus mmWave was raised up to meet with the even faster transmission rate requirement. As known, according to Shannon theory, faster transmission rate can always be obtained by increasing the carrier bandwidth. With much higher frequencies, wider bandwidth blocks can be easily allocated and discriminated from each other to isolate the inter-channel interferences.

With all of those, system model of NOMA-mmWave-massive-MIMO is elaborated in this section as well as the proposed simplified channel model following by the UR-SP mmWave channel assumption. Detailed information of these two models will be elaborated as follows.

### 2.3.1 The NOMA-mmWave-massive-MIMO system model

The NOMA-mmWave-massive-MIMO system model of this study is shown by Fig. 2.3. As shown here, the system consists of a BS equipped with a massive number of antennas while serving multiple user terminals. The transmission is carried out in the mmWave frequency (note that the specific frequency resources and bandwidth for 5G's

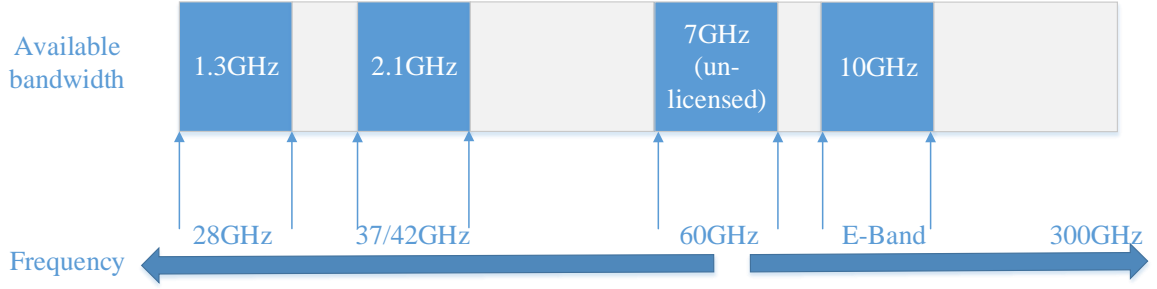


Figure 2.4 The mmWave frequency used for transmission.

usage is still on discussion). The NOMA encoding scheme is utilized for user signal superposition with the same frequency. By employing the NOMA encoding scheme within multiple frequencies, it is assumed that the user within each frequency as the user groups. Thus among different user groups, orthogonal spectrum correlation is assumed to isolate the interference from neighboring frequencies.

In addition, other than the prior wireless communications with macro wave, here the mmWave is invoked to enhance the transmission rate with 5G. The specific division of mmWave frequencies can be found by Fig. 2.4. By compared with macro wave, the benefit of mmWave lies in the fact that, with higher frequency, more bandwidth can be used for the component carrier. Thus in line with Shannon theory, even better transmission can be achieved by simply allocating wider carrier bandwidth. Yet the specific allocation is still waiting for the work from ITU. Thus here the achievable transmission rate analysis is omitted in this study.

With this system model, user terminal can exploit the SIC decoding method [54, 64] to remove the information from users with higher orders. The remaining information from other users with lower orders will be treated as the interference. With perfect orthogonal characteristics among channels, the inter-channel interference can be ignored. Thus the interference mainly comes from co-channel users with a lower order.

Assuming the NOMA power matrix is  $\mathbf{P} = [\mathbf{p}_1, \dots, \mathbf{p}_N]^T \in \mathbb{R}^{N \times K}$  for  $K$  users of the same user group, received signal can be given as

$$\mathbf{y} = \mathbf{P}\mathbf{H}^H \mathbf{x} + \mathbf{n}, \quad (2.1)$$

where  $\mathbf{H} \in \mathbb{C}^{N \times K}$  is the channel model from  $N$  transmit antennas to  $K$  user terminals,  $\mathbf{x} \in \mathbb{C}^{N \times 1}$  is the transmitted signal, and  $\mathbf{n} \in \mathbb{C}^{N \times 1}$  the additive white Gaussian noise (AWGN). Moreover, without loss of generality, it is assumed that  $N \geq K$ . This is due

to the fact that, normally, the transmit antenna number is larger than the receiver antenna number in massive MIMO systems. We further assume that the transmit signal  $\mathbf{x}$  is normalized, which means each column of  $\mathbf{x}$  obeys  $\mathbb{E}[\mathbf{x}_i] = 0$ ,  $\mathbb{E}[\mathbf{x}_i \mathbf{x}_i^H] = 1$ .

With this system model in hand, to determine the capacity performance of NOMA-mmWave-massive-MIMO system, the channel model should be set forth. Given a constant normalized noise value within the channel, capacity performance is largely determined by the allocated power to each user and the channel model [14].

### 2.3.2 The proposed mmWave channel assumption

According to [42, 65], the mmWave channel model consists of the channel gain, AoD and AoA effects. Hence the channel model for mmWave from transmit to receiver ( $k$ th user) can be described as

$$\mathbf{h}_k = \sqrt{N} \left\{ \frac{\beta_k^0 \mathbf{d}(\theta_k^0) \mathbf{a}(\phi_k^0)}{\sqrt{1 + d_k^{\beta_{LOS}}}} + \sum_{i=1}^M \frac{\beta_k^i \mathbf{d}(\theta_k^i) \mathbf{a}(\phi_k^i)}{\sqrt{1 + d_k^{\beta_{NLOS}}}} \right\}. \quad (2.2)$$

Hence the channel matrix will be  $\mathbf{H} = [\mathbf{h}_1, \dots, \mathbf{h}_K]$ . Besides,  $k = 1, \dots, K$  is the user index, and  $i = 1, \dots, M$  is the NLOS path index.  $\beta_k^i$  denotes the channel gain of user  $k$  from the  $i$ -th NLOS path, which can be assumed to obey a complex gaussian distribution, i.e.,  $\beta_k^i \sim \mathcal{CN}(0, 1)$ . Additionally,  $\beta_k^0$  is the channel gain from the LOS path.  $\beta_{LOS}$  and  $\beta_{NLOS}$  represent the LOS and NLOS path losses, respectively.  $M$  is the total number of NLOS paths.  $d_k$  denotes the distance between the transmitter and receiver, and  $\theta_k^i$  represents the normalized AoD of each path (by LOS or NLOS), which follows

$$\mathbf{d}(\theta_k^i) = \frac{1}{\sqrt{N}} [1, e^{-j\pi\theta}, \dots, e^{-j\pi(N-1)\theta}]. \quad (2.3)$$

Similarly, the normalized AoA of each path follows

$$\mathbf{a}(\phi_k^i) = \frac{1}{\sqrt{N}} [1, e^{-j\pi\phi}, \dots, e^{-j\pi(K-1)\phi}]. \quad (2.4)$$

Since LOS paths are the dominant factors in mmWave channel [44], by ignoring the NLOS component, the UR-SP mmWave channel model [44] in (2.2) is rewritten as

$$\begin{aligned} \mathbf{h}_k &= \sqrt{N} \frac{\beta_k^0 \mathbf{d}(\theta_k^0)}{\sqrt{1 + d_k^{\beta_{NLOS}}}} \\ &= \frac{\sqrt{N}}{\sqrt{1 + d_k^{\beta_{NLOS}}}} \mathbf{d}(\theta_k^0) \beta_k^0. \end{aligned} \quad (2.5)$$

Yet in UR-SP channel model, although the array steering vector (AoD vector) is included, the AoA factor is neglected. Thus by following the UR-SP channel model, and further taking the AoA vector into consideration, the extended channel model can be given as

$$\mathbf{h}_k = \frac{\mathbf{d}(\theta_k^0)\beta_k^0\mathbf{a}(\phi_k^0)}{\sqrt{N(1+d_k^{\beta_{NLOS}})}}. \quad (2.6)$$

Additionally, this can be described with matrix

$$\mathbf{H} = \mathbf{D}\mathbf{B}\mathbf{A} \quad (2.7)$$

where  $\mathbf{D} \in \mathbb{C}^{N \times L}$ ,  $\mathbf{B} \in \mathbb{C}^{L \times L}$ ,  $\mathbf{A} \in \mathbb{C}^{L \times K}$  with  $L$ , the number of LoS paths.  $\mathbf{B} = \eta\boldsymbol{\beta}$  with  $\boldsymbol{\beta} = [\beta_1, \beta_2, \dots, \beta_L]$ , and  $\mathbf{D} = [\mathbf{d}(\theta_k^1), \dots, \mathbf{d}(\theta_k^L)]$ ,  $\mathbf{A} = [\mathbf{a}(\theta_k^1), \dots, \mathbf{a}(\theta_k^L)]^T$ . Here  $\eta$  is the coefficient given as

$$\eta = \frac{1}{\sqrt{N(1+d_k^{\beta_{NLOS}})}}. \quad (2.8)$$

This is due to the fact that, the channel gain  $\beta_k$  for all of the receivers from multiple transmitter, can be taken as a matrix consisting of multiple LOS paths with beamforming, in view of the sparse characteristic of multiple LOS paths [42]. Furthermore, the  $\sqrt{N}$  and distance effect  $\sqrt{1+d_k^{\beta_{NLOS}}}$  are the quantity effects of each entry in the channel matrix  $\boldsymbol{\beta}$ . In addition, by assuming that the entries of channel matrix obey random distributions, the distance effect can be absorbed into the channel gain between transmitter and receiver, as a quantity factor. Thus, one can employ a random distributed entry of  $\boldsymbol{\beta}$  to denote both channel gain and distance effect.

## 2.4 Capacity analysis in the noise-dominated low-SNR regime

There exists no tractable method to directly analyze the integrated NOMA-mmWave-massive-MIMO system due to the prohibited complexity. On one hand, SIC is employed by each user to decode its information with NOMA power allocation. On the other hand, the mmWave channel model with multiple paths considered makes the analysis even tough. Thus, we divide the capacity analysis into low-SNR and high-SNR regimes, which can be adapted for various application scenarios such as cell edge, cell center, and etc.

In the low-SNR regime, the impact of the co-channel interference is trivial, and the dominant factor to each user's SINR value is the noise. In comparison, the dominant

factor to SINR in the high-SNR regime is the co-channel interference from other users using the same spectrum resources. In this section, the capacity for the low-SNR regime is analyzed by the deterministic equivalent method with the Stieltjes-Shannon transform [59, 66].

As stated aforementioned, in the low-SNR regime, the interference can be neglected as it is much smaller than the noise power. The dominated factor of the SINR of each user is the channel noise. In this case, the scenario is similar to prior studies in massive MIMO without the NOMA scheme. Taking the power allocation matrix for different users in the NOMA-mmWave-massive-MIMO system as the precoder matrix [59], the Stieltjes transform  $S_{\mathbf{B}_N}(z)$  of matrix  $\mathbf{B}_N$  can be employed (note that here in this study, it is assumed that each user equipped with one receive antenna). In line with prior studies in [59, 66], the Stieltjes transform can be given as

$$\begin{aligned} S_{\mathbf{B}_N}(z) &= \frac{1}{N} \text{tr}(\mathbf{B}_N - z\mathbf{I}_N)^{-1} \\ &= \int \frac{1}{\lambda - z} dF_{\mathbf{B}_N}(\lambda) \\ &\stackrel{a.s.}{\rightarrow} \int \frac{1}{\lambda - z} dF_N(\lambda), \end{aligned} \tag{2.9}$$

where  $z \in \mathbb{C} - \mathbb{R}^+ \equiv \{z \in \mathbb{C}, \Im(z) > 0\}$ ,  $\mathbf{I}_N$  is an identity matrix. In addition,  $F_{\mathbf{B}_N}(\lambda)$  is the Empirical Distribution Function (EDF) of  $\mathbf{B}_N$ , according to the large dimensional random matrix theory. With  $N$  and  $K$  growing large,  $F_{\mathbf{B}_N}(\lambda)$  converges to  $F_N(\lambda)$  (the determinant eigenvalues' CDF of  $\mathbf{B}_N$ ) with probability 1, by employing the Glivenko-Cantelli theorem [67].

The importance of the Stieltjes transform lies in its link to the Shannon transform  $V_{\mathbf{B}_N}(z)$  of  $\mathbf{B}_N$ . In addition, as studied in [59, 66], the Shannon transform is directly linked with the SINR of a wireless communication system. The Shannon transform can be derived from the mutual information analysis in MIMO system, such as the work in [68, 69]. Additionally,  $\mathbf{B}_N$  in this study is defined as

$$\begin{aligned} \mathbf{B}_N &= \mathbf{H}\mathbf{H}^H \\ &= \mathbf{D}\mathbf{B}\mathbf{A}^2\mathbf{B}^H\mathbf{D}^H. \end{aligned} \tag{2.10}$$

**Theorem 2.4.1** *The relationship between Stieltjes transform and Shannon transform*

of a given Hermitian non-negative definite matrix  $\mathbf{B}_N$  can be given as

$$\begin{aligned} V_{\mathbf{B}_N}(z) &= \frac{1}{N} \log \det \left( \mathbf{I}_N + \frac{1}{z} \mathbf{B}_N \right) \\ &= \int_0^{+\infty} \log \left( 1 + \frac{\lambda}{z} \right) dF_N(\lambda) \\ &= \int_z^{+\infty} \left( \frac{1}{w} - S_{\mathbf{B}_N}(-w) \right) dw. \end{aligned} \quad (2.11)$$

Please see Appendix A.

By assuming perfect Channel State Information at the Receiver side (CSIR) and frequency-flat fading channel models, the system mutual information is given by

$$\mathcal{I}_{\mathbf{G}_N}(\sigma^2) = \mathbb{E} \left\{ \log \det \left( \mathbf{I}_N + \frac{1}{\sigma^2} \mathbf{B}_N \right) \right\}. \quad (2.12)$$

In addition, the relationship between the Shannon transform and the ergodic mutual information is

$$\mathcal{I}_{\mathbf{G}_N}(\sigma^2) = NV_{\mathbf{B}_N}(\sigma^2). \quad (2.13)$$

Based on Theorem 2.4.1, the ergodic mutual information can be further determined by the Stieltjes transform on condition that  $F_{\mathbf{B}} \rightarrow F_N(\lambda)$ , which will be discussed in the following analysis. Before delving into details, a lemma and a hypothesis are given to clarify the constraints of this approach.

**Lemma 2.4.2** *The sequences of  $F_{\mathbf{D}}$ ,  $F_{\mathbf{B}}$  and  $F_{\mathbf{A}}$  (EDF of matrix  $\mathbf{D}, \mathbf{B}, \mathbf{A}$ ) are tight, whereas  $\mathbf{D}$  and  $\mathbf{A}$  are the nonnegative Hermitian matrices, and  $\mathbf{B}$  the random matrix with i.i.d. Gaussian entries of zero mean and covariance  $\frac{1}{L}$ .*

The following hypothesis holds as well:

1) Define  $c = \frac{N}{K}$  and assume  $0 < a < b < \infty$ , we have

$$a < \min_M \liminf c < \max_M \limsup c < b. \quad (2.14)$$

This hypothesis is reasonable by assuming that  $c$  is constant within a region  $[0, +\infty]$ . Interested readers can refer to [15, 59] and the references therein.

As a result, the mutual information can be straightforwardly obtained based on the Stieltjes transform of the channel matrix  $\mathbf{B}_N$ . By denoting  $F_{\mathbf{B}_N}(\lambda)$  as the eigenvalues' empirical spectrum distribution function, the Stieltjes transform can be solved with the link of  $F_{\mathbf{B}_N}(\lambda)$  with a Limiting Spectrum Distribution (LSD)  $F_N$  of  $\mathbf{B}_N$ . Thus

the main problem is to find such a  $F_N$ . It is proved by prior studies [59, 66] that the difference between  $F_{\mathbf{B}_N}(\lambda)$  and  $F_N$  converges vaguely to zero, which is equivalent to

$$S_{\mathbf{B}_N}(z) - S_N(z) \xrightarrow{a.s.} 0, \text{ for } z \in \mathbb{C} - \mathbb{R}^+, \quad (2.15)$$

where

$$S_N(z) \equiv \int_{\mathbb{R}^+} \frac{1}{\lambda - z} dF_N \quad (2.16)$$

is the Stieltjes transform of  $F_N$ . The purpose of this approach is to derive a deterministic non-random matrix function  $\Phi(z)$  such that

$$S_{\mathbf{B}_N}(z) - \frac{1}{N} \text{tr}(\Phi(z)) \xrightarrow{a.s.} 0, \text{ for } z \in \mathbb{C} - \mathbb{R}^+. \quad (2.17)$$

Given the channel noise variance  $\sigma^2$  (it is assumed that the channel noise obeys the random Gaussian distribution amongst different channels of this integrated NOMA-mmWave-massive-MIMO system with zero mean and  $\sigma^2$  variance). On the other hand, the matrix of the NOMA power allocation is denoted as  $\mathbf{P}$ . In light of this, the deterministic equivalence of mutual information can be derived by using Lemma 2.4.2 and the hypothesis defined in (2.14) as [59, 61]

$$\mathcal{I}(\sigma^2) = \bigcup_{\substack{\frac{1}{N} \text{tr} \mathbf{P}_k \leq P_k, \\ \mathbf{P}_k \geq 0, \\ k \in \mathcal{S}}} \left\{ R_k : \sum_{k \in \mathcal{S}} R_k \leq \mathbb{E} \{ V_N(\mathbf{P}_k; \sigma^2) \} \right\}, \quad (2.18)$$

here  $\mathcal{S} = \{1, \dots, K\}$ , where the Shannon transform is given by

$$V_N(\mathbf{P}_k; \sigma^2) \stackrel{\text{def.}}{=} \frac{1}{N} \log \det \left( \mathbf{I}_N + \frac{1}{\sigma^2} \sum_{k \in \mathcal{S}} \mathbf{H}_k \mathbf{P}_k \mathbf{H}_k^H \right). \quad (2.19)$$

In this case, by assuming  $\alpha$  as a constant value, i.e.,  $0 < \alpha < \infty$ , the spectral norm satisfies

$$\max\{\|\mathbf{D}\|, \|\mathbf{A}\|, \|\mathbf{H}\mathbf{H}^H\|\} \leq \alpha. \quad (2.20)$$

The deterministic expression of the ergodic capacity in this case, while following the prior studies in [59, 61] can be given as

$$\begin{aligned} R_{sum} &\leq \sum_{k=1}^K \mathbb{E} \{ V_N(\mathbf{P}_k; \sigma^2) \} \xrightarrow{a.s.} \frac{1}{N} \sum_{k=1}^K \log \det(\mathbf{I} + c e_k(-\sigma^2) \mathbf{A}_k \mathbf{P}_k) \\ &+ \frac{1}{N} \log \det(\mathbf{I} + \sum_{k=1}^K f_k(-\sigma^2) \mathbf{D}_k) - \sigma^2 \sum_{k=1}^K f_k(-\sigma^2) e_k(-\sigma^2). \end{aligned} \quad (2.21)$$

where  $e_k(-\sigma^2)$  and  $f_k(-\sigma^2)$  are the unique solutions of the following equations under the symmetric form

$$e_k(-\sigma^2) = \frac{1}{N} \text{tr} \mathbf{D}_k \mathbf{D}_k^H (\sigma^2 [\mathbf{I} + \sum_{k=1}^K f_k(-\sigma^2) \mathbf{D}_k \mathbf{D}_k^H])^{-1}, \quad (2.22)$$

$$f_k(-\sigma^2) = \text{tr} \mathbf{A}_k \mathbf{P}_k \mathbf{A}_k (\sigma^2 [\mathbf{I} + c e_k(-\sigma^2) \mathbf{A}_k \mathbf{P}_k \mathbf{A}_k])^{-1}. \quad (2.23)$$

The sum rate supremum of the NOMA-mmWave-massive-MIMO systems can be addressed by (3.13) with  $e_k(-\sigma^2)$  and  $f_k(-\sigma^2)$  the unique solutions of the equalities given in (2.22) and (2.23), where the iterative algorithm to obtain these solutions have been provided by [61, 70] for reference.

Note that in this work, the power matrix for different users is considered as prior information, other than previous studies which focus on power allocation optimization algorithms (frozen water filling or other algorithms). As discussed before, this equivalence is only valid in the low-SNR scenario. This is because that in the low-SNR regime, interference from the neighboring users within the same frequency is ignored since their value is much smaller compared with the channel noise value. However, in the high-SNR case, the interferences from other users cannot be ignored and will be the dominant factor of the system capacity performance. Thus the analytical procedure will be totally different from the low-SNR regime. The high-SNR capacity analysis will be addressed by the following analysis.

## 2.5 Capacity analysis in the interference-dominated high-SNR regime

The capacity performance within high-SNR regime will be investigated in this section. Firstly, by employing the SIC [71] to perfectly cancel the interference from neighboring users of the same user group with higher orders, SINR for each user  $k$  can be given as

$$\text{SINR}_k = \frac{P_k \mathbf{H} \mathbf{H}^H}{\sum_{k'=1, k' \neq k}^K P_{k'} \mathbf{H} \mathbf{H}^H + \sigma^2} \quad (2.24)$$

$$\stackrel{\text{after}}{\text{SIC}} \frac{P_k \mathbf{H} \mathbf{H}^H}{\sum_{k'=1}^{k-1} P_{k'} \mathbf{H} \mathbf{H}^H + \sigma^2}.$$

As noticed, in high-SNR regime, the interference mostly comes from the NOMA neighboring users within the same frequency. In this case, the channel noise effect can be omitted, whereas only the interference from neighboring users are existing

with regard to the system capacity performance. The intuitionistic ergodic capacity of the NOMA-mmWave-massive-MIMO system in this case, can be approximated as

$$C = \sum_{k'=1}^K \mathbb{E} \left\{ \log \det \left( \mathbf{I}_N + \frac{P_k \mathbf{H}\mathbf{H}^H}{\sum_{k'=1}^{k-1} P'_k \mathbf{H}\mathbf{H}^H + \sigma^2} \right) \right\} \quad (2.25)$$

$$\stackrel{\text{high SNR}}{\approx} \sum_{k'=1}^K \mathbb{E} \left\{ \log \det \left( \mathbf{I}_N + \frac{P_k \mathbf{H}\mathbf{H}^H}{\sum_{k'=1}^{k-1} P'_k \mathbf{H}\mathbf{H}^H} \right) \right\}.$$

As shown by this approximation expression, the capacity expression involving some matrices expressions, which is not a closed-form expression. The next thing needs to do is to crack down this. In light of this discussion, a tractable capacity expression is derived by employing the tools of statistics and eigenvalue distribution methods [62]. First of all, it is noticed that the capacity expression can be divided into the power allocation part and channel characteristic part by the following theorem.

**Theorem 2.5.1** *While ignoring the channel noise effect and focusing on the interference from neighboring users in high-SNR regime, the ergodic capacity of NOMA-mmWave-massive-MIMO system can be given as*

$$C = \frac{1}{\ln 2} \sum_{k'=1}^K \left\{ \ln \left( \frac{\sum_{k'=1}^k P'_k}{\sum_{k'=1}^k P'_k - P_k} \right) + \ln \int_0^{+\infty} \lambda f(\lambda) d\lambda \right\}, \quad (2.26)$$

where  $\lambda$  yields the eigenvalue of  $\mathbf{H}\mathbf{H}^H$ , and  $f(\lambda)$  the PDF function of  $\lambda$ .

See Appendix B.

On one hand, the first part of Theorem 2.5.1 is about the power ratio with NOMA scheme. As shown here, it is already given with the closed-form expression. The only concerned value is the power allocation for each user within the same user group. On the other hand, the second part is about the eigenvalue and its PDF of  $\mathbf{H}\mathbf{H}^H$ . The eigenvalue of the channel matrix with  $\mathbf{H}\mathbf{H}^H$  is easy to obtain according to the eigenvalue decomposition method. Thus the only focus is about the PDF of  $\lambda$ . As stated by the following study, the exact expression of  $f(\lambda)$  can be given by lemma 2.5.2 in the following content. This is obtained by invoking the integral to conditional PDF expressions twice, where the conditional PDF expression can be referred to prior studies with [59, 61, 72].

$$\begin{aligned}
\int_0^{+\infty} \lambda f(\lambda) d\lambda &= \int_0^{+\infty} \frac{\lambda}{\prod_{i=1}^L \Gamma^2(L-i+1) \prod_{i=1}^L \Gamma(N-i+1) L} \\
&\sum_{j=L-K+1}^L \sum_{i=1}^L (-1)^{i+j} \frac{\lambda^{K-L+j-1}}{\Gamma(K-L+j)} \det(\mathbf{M}) N_\lambda(i) d\lambda \\
&= \frac{1}{\prod_{i=1}^L \Gamma^2(L-i+1) \prod_{i=1}^L \Gamma(N-i+1) L} \sum_{j=L-K+1}^L \sum_{i=1}^L (-1)^{i+j} \\
&\int_0^{+\infty} \frac{\det(\mathbf{M}) \lambda^{K-L+j}}{\Gamma(K-L+j)} N_\lambda(i) d\lambda.
\end{aligned} \tag{2.30}$$


---

**Lemma 2.5.2** *By exploring the knowledge of probability analysis, the unconditional PDF of  $\mathbf{H}\mathbf{H}^H$  can be calculated as*

$$\begin{aligned}
f(\lambda) &= \frac{1}{\prod_{i=1}^L \Gamma^2(L-i+1) \prod_{i=1}^L \Gamma(N-i+1) L} \\
&\sum_{j=L-K+1}^L \sum_{i=1}^L (-1)^{i+j} \frac{\lambda^{K-L+j-1}}{\Gamma(K-L+j)} \det(\mathbf{M}) N_\lambda(i).
\end{aligned} \tag{2.27}$$

where  $\mathbf{M}_{i,j}$  is the  $(i,j)$ -th minor of matrix  $\mathbf{M} \in \mathbb{C}^{L \times L}$ , whose entry is given as

$$\mathbf{M}_{i,j} = \Gamma(i+j-1) \Gamma(N-L+j). \tag{2.28}$$

Additionally, the expression of  $N_\lambda(j)$  is

$$N_\lambda(i) = \int_0^\infty 4x^{N+L-2K+i-2} e^{-\frac{\lambda}{x^2}} K_{L-N+i-1}(2x) dx, \tag{2.29}$$

with  $K_m(n)$  is the modified Bessel function of its second kind.

See Appendix C.

The exact capacity expression is acquired by substituting lemma 2.5.2 into (2.26), and  $\int_0^{+\infty} \lambda f(\lambda) d\lambda$  is given as (2.30).

As shown in (2.26) and (2.30), although the exact expression of the capacity is derived, yet the expression is still too complex to obtain a closed-form expression. Fortunately, to obtain the PDF function of eigenvalues of  $\mathbf{H}\mathbf{H}^H$ , the study from [73] gives an asymptotic expression under the similar conditions. By following the deduction procedure, although it is still difficult to obtain the closed-form expression under condition  $N \neq K \neq L$ , yet for a simple case when  $N = L = K$ , the expression is given by [62]

$$f(\lambda) = \frac{1}{\pi} \sqrt{g^2(\lambda) + \frac{1}{4\lambda^2 g(\lambda)}}, \tag{2.31}$$

where  $g^2(\lambda)$  is given as

$$g^2(\lambda) = \frac{\sqrt[3]{64^2\lambda^8}(1 - i\sqrt{3})}{384\lambda^4} \sqrt[3]{\frac{-27 + \sqrt{27^2 - 27\frac{16^2}{\lambda}}}{2}} + \frac{\sqrt[3]{64^2\lambda^8}(1 + i\sqrt{3})}{384\lambda^4} \sqrt[3]{\frac{-27 - \sqrt{27^2 - 27\frac{16^2}{\lambda}}}{2}}. \quad (2.32)$$

This gives the expression of  $f(\lambda)$  as

$$f(\lambda) = \frac{(1 + i\sqrt{3}) \sqrt[3]{\lambda^8} \sqrt[3]{-\sqrt{729 - \frac{6912}{\lambda}} - 27}}{24\sqrt[3]{2}\lambda^4} + \frac{(1 - i\sqrt{3}) \sqrt[3]{\lambda^8} \sqrt[3]{\sqrt{729 - \frac{6912}{\lambda}} - 27}}{24\sqrt[3]{2}\lambda^4}. \quad (2.33)$$

In summary, the exact capacity expression defined in (2.26) is well suited for general cases in NOMA-mmWave-massive-MIMO systems despite its high computation complexity. For the special case that  $N = L = K$ , the asymptotic capacity expression with (2.33) can be employed, which will be verified through numerical results.

## 2.6 Numerical results

The capacity performance of NOMA-mmWave-massive-MIMO systems are evaluated in this section. The AoA, AoD, and power value for each user are randomly generated. Detail results and discussions are given as follows.

The low-SNR regime analysis is evaluated firstly. As shown by Fig. 2.5, the capacity is mainly determined by the SNR when the  $\mathbf{D}$ ,  $\mathbf{B}$ , and  $\mathbf{A}$  are fixed. It is clear that as SNR grows, the achievable capacity also increase monotonically. Moreover, simulation results also demonstrate that the capacity increases dramatically as the number of users increases. The huge capacity improvement is feasible due to the non-orthogonal user multiplexing in the same frequency enabled by NOMA. It is noted that the capacity performance of the NOMA-mmWave-massive-MIMO system significantly outperforms the existing LTE system (0.07 ~ 0.12 Bits/s/Hz of the cell-edge, which yields low-SNR regime) [74]. For instance, by 10 users and  $-10$  dB, the achievable capacity value is almost 10 times compared with prior LTE systems in low-SNR regime. This is mostly due to the NOMA encoding scheme with superposition of multiple users in the same frequency.

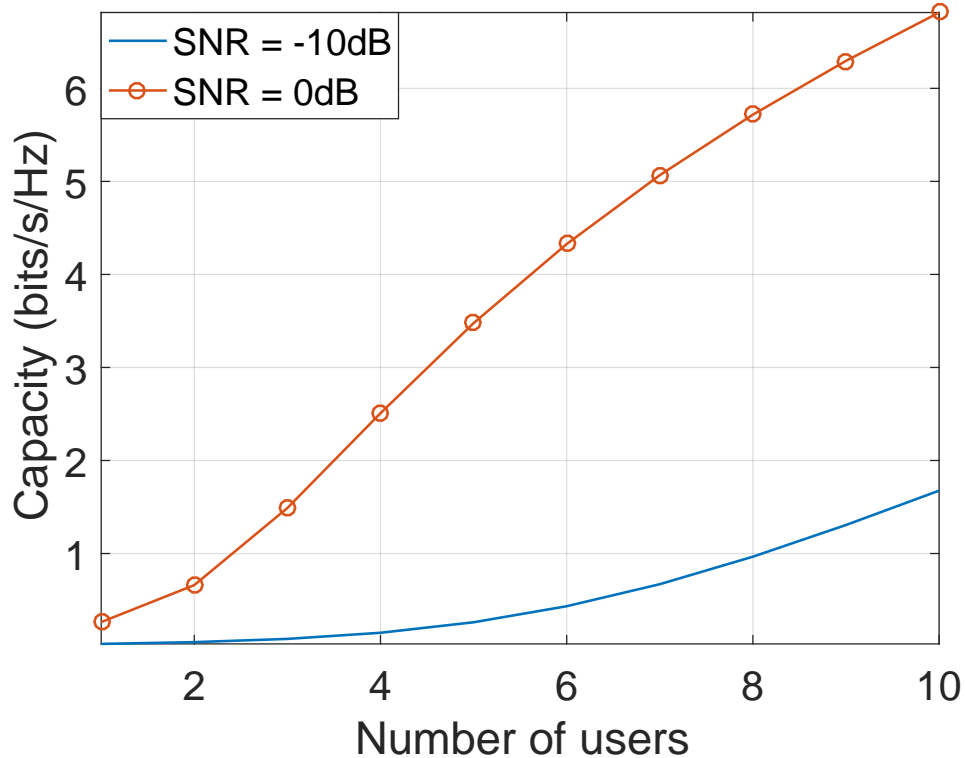


Figure 2.5 Capacity performance of the low-SNR scenario.

In addition, as noticed by this figure that with  $\text{SNR} = -10\text{dB}$ , the capacity performance curve display an exponential tendency increase with number of users increasing. This is due to the face that with user power much lower than the channel noise power, we have

$$\log(1 + x) \approx x. \quad (2.34)$$

Thus the capacity increase with a much cliffy tendency with user number increasing with the sum power of NOMA summing up of each user group. On the other hand, when the power value is comparable with the channel noise power, the  $\log x$  function will display a logarithmic curve. This is the explanatory reason behind these two curves.

To verify the correctness of the PDF deductions, the exact eigenvalue PDF expression defined in (2.27) is compared with the asymptotic PDF expression, i.e., (2.33). One exemplary result of this is shown in Fig. 2.6 with  $N = L = K = 6$ . By observing Fig. 2.6, it is clear that the asymptotic PDF expression is in good agreement with the exact eigenvalue PDF expression in the large and small eigenvalue regions. However, for the eigenvalue regions  $[1, 15]$ , there are difference between the exact and asymptotic PDF expressions. As in prior studies with channel hardening [75], with

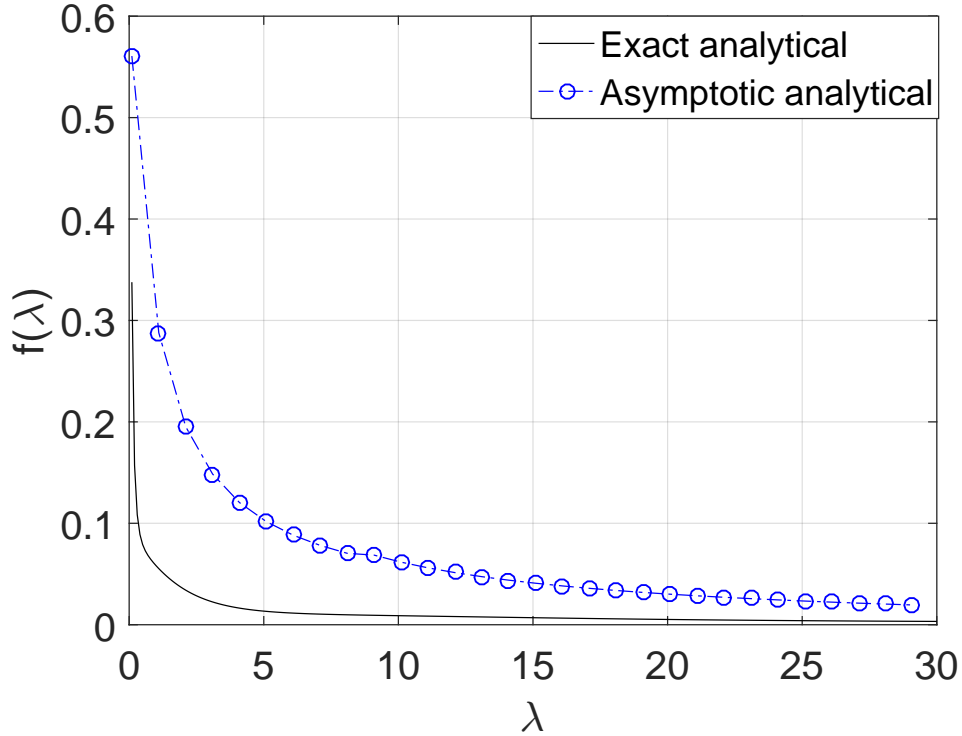


Figure 2.6 An analytical comparison of the exact and asymptotic eigenvalue PDFs ( $N = L = K = 6$ ).

massive MIMO antenna growing large, some of the eigenvalue of channels becoming large while some others becoming to zero. Thus we can say that the asymptotic expression is especially of better agreement with exact expression in massive MIMO system while number growing large. In addition, in smaller eigenvalue region, this disagreement has less effect to the system capacity performance. This can be verified by the capacity equation with Theorem 2.5.2, where little eigenvalue results in a small value of the second part. On the other hand, in the large eigenvalue region, the small performance gap between the asymptotic PDF and the exact eigenvalue PDF leads to a more accurate capacity expression, which is particularly valuable in massive MIMO scenario.

The capacity performances of NOMA-mmWave-massive-MIMO system with the exact PDF expression are shown in Fig. 2.7 and Fig. 2.8 for  $N = 10$  and  $N = 20$ , respectively. The SNR is set to be 30 dB in this simulation. As shown, capacity performance is enhanced with the number of transmit antenna growing (by comparing the Fig. 2.7 and Fig. 2.8). This is because that more transmit antennas brings more degree of freedoms (DoFs) [2] for the transmission. On the other hand, little capacity improvement can be achieved while increasing the LoS paths. Although increasing

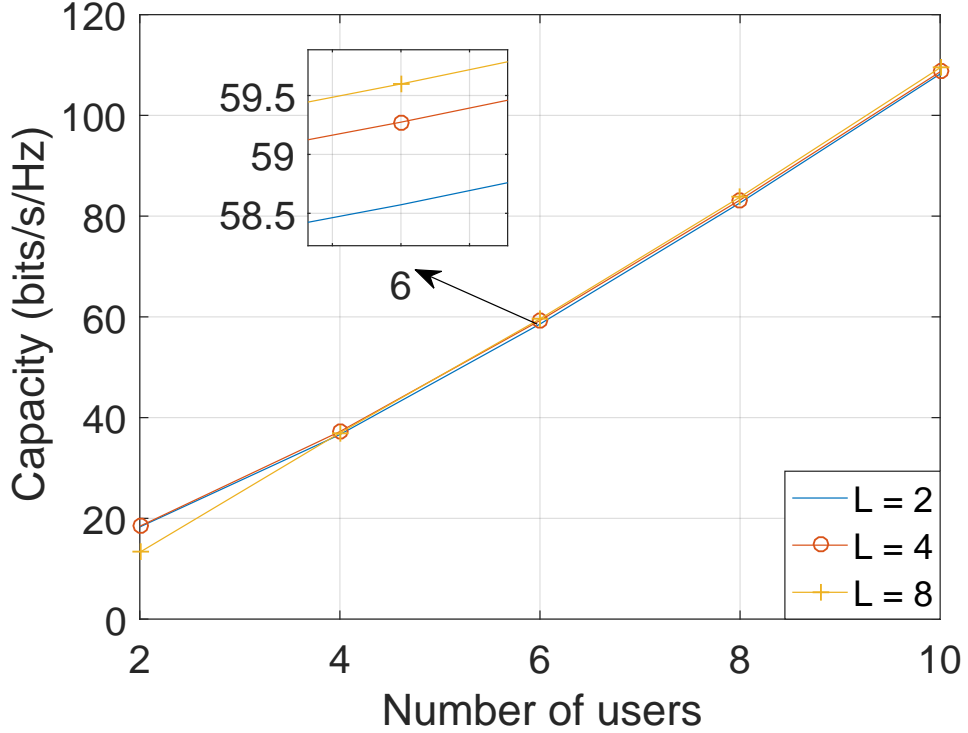


Figure 2.7 Capacity performance of the high-SNR scenario with the exact eigenvalue PDF ( $N = 10$ ).

the number of LOS paths is equivalent to the increasing of the degree of freedom. This is because that the co-channel interference from neighboring users and the correlative effects at transmit and receiver sides are also enhanced while increasing the number of LoS paths.

The relationship between the allocated power value with the capacity increment is further verified, whose results are shown by Fig. 2.9. Note that for the sake of compactness, the allocated power is averaged given a NOMA user group, where the NOMA user group is defined by section II. Average power is calculated by averaging the total allocated power to one user groups, for instance, 10 here in this simulation. Additionally, without loss of generality, it is set with  $N = L = K = 10$ . By comparing the linearly (power increase indicated by the lower arrow text-box) and exponential (power increase indicated by the upper arrow text-box) growing average power effects to the capacity performance, better capacity performance can always obtained just by increasing the average power, although harsh NOMA co-channel interferences induced via this. In addition, by compared with prior studies, it is found that we can achieve the same level SE performance with much less transmit antenna numbers. This is due to the NOMA encoding mechanism with superposition of multiple users within

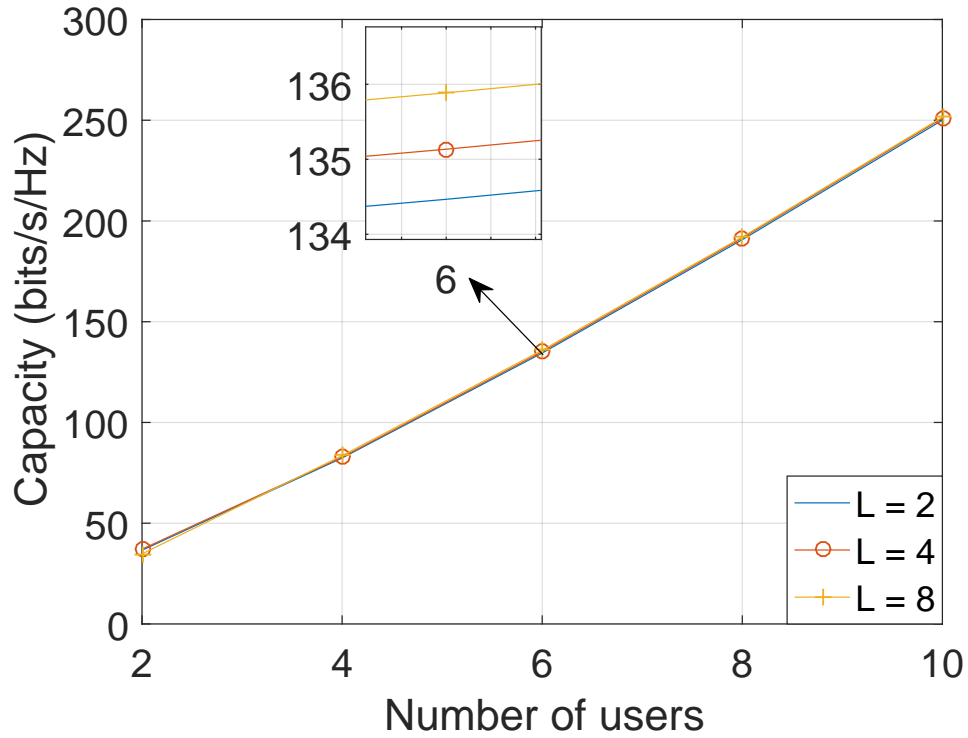


Figure 2.8 Capacity performance of the high-SNR scenario with the exact eigenvalue PDF ( $N = 20$ ).

each user group.

## 2.7 Conclusion

Capacity performance of NOMA-mmWave-massive-MIMO system was investigated in this study. The analysis was divided into low-SNR and high-SNR regimes. The closed-form expression for low SNR regime, as well as the exact and asymptotic capacity expressions for high-SNR regime were addressed with the analysis. Simulation results showed that greater capacity increment via the integrated system model compared with prior LTE systems. Additionally, with mmWave, even greater achievable sum rate can be achieved via the even wider carrier frequencies in 5G. Due to the simple power allocation scheme used in this study, the optimal power allocation with NOMA encoding scheme for different transmission rate requirement of multiple users can be an attractive topic in future.

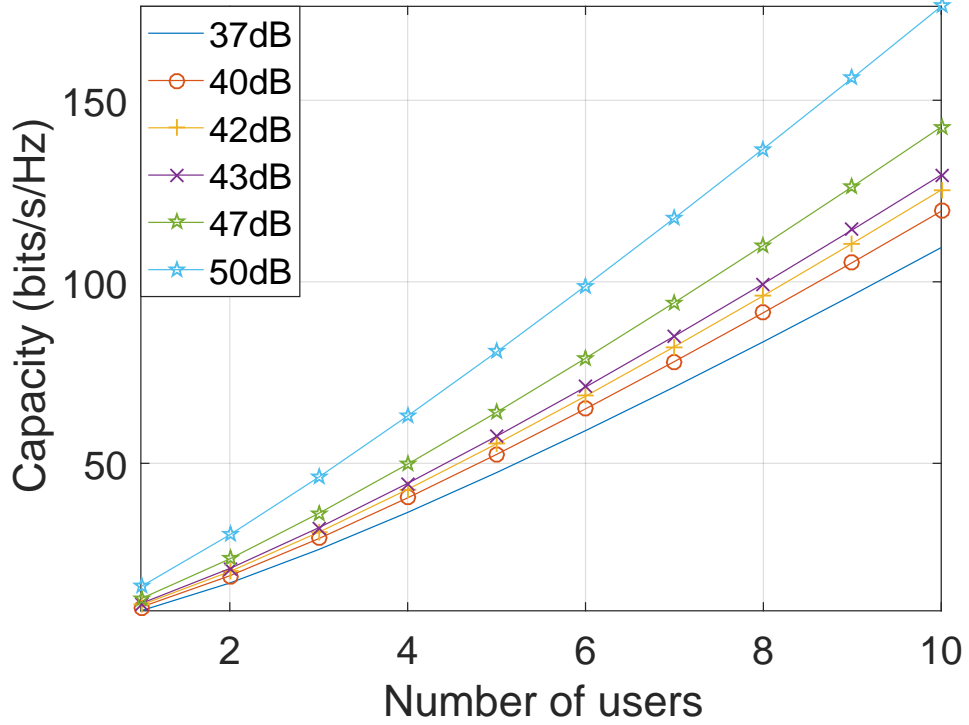


Figure 2.9 Capacity performance of the high-SNR scenario with the asymptotic eigenvalue PDF.

## Appendix A

To prove the relationship between Shannon transform and Stieltjes transform, some notes should be stated beforehand.

*Note 1:* use  $\ln$  for the log base e. For  $b > 0$ , we have

$$\ln(1+b) = \int_0^1 \frac{b}{1+bt} dt. \quad (2.35)$$

*Note 2:* Instead of the distribution function  $dF(x)$ , for convenience, we use  $\rho(x)dx$  as the density. In this case, for  $z \rightarrow \infty$ , say in the upper-half plane, we have

$$\int_0^{+\infty} \rho(\lambda) d\lambda = 1. \quad (2.36)$$

In the following content, we will prove the relationship between the Shannon and Stieltjes transform. Firstly, it is noticed that the Shannon transform is defined as

$$V(x) = \int_0^{+\infty} \log\left(1 + \frac{\lambda}{x}\right) \rho(\lambda) d\lambda. \quad (2.37)$$

In this case, the differential result of this equality will follow

$$\frac{dV(x)}{dx} = -\frac{1}{\log e} \int_0^{+\infty} \frac{\frac{\lambda}{x^2} \rho(\lambda)}{1 + \frac{\lambda}{x}} d\lambda. \quad (2.38)$$

Furthermore, by multiplying  $x$  on both sides, we have

$$\begin{aligned}
x \frac{dV(x)}{dx} &= -\frac{1}{\log e} \int_0^{+\infty} \frac{\lambda \rho(\lambda)}{x + \lambda} d\lambda \\
&= -\frac{1}{\log e} \int_0^{+\infty} \frac{(\lambda + x - x) \rho(\lambda)}{x + \lambda} d\lambda \\
&= -\frac{1}{\log e} \left( 1 - x \int_0^{+\infty} \frac{\rho(\lambda)}{x + \lambda} d\lambda \right).
\end{aligned} \tag{2.39}$$

It is noticed that a Stieltjes transform appeared by the last part of the equality's right side. This result gives

$$x \frac{dV(x)}{dx} = -\frac{1}{\log e} (1 - xS(-x)). \tag{2.40}$$

Which is the link between Shannon transform and Stieltjes transform given by the study of [76]. In addition, it is noticed that in alternative literature, the  $\log e$  factor is omitted to arrive the equivalence given by Theorem 3.1 (for instance, the study in [77]). Thus by omitting the factor and unpacking the log according to (2.35), we have,

$$\begin{aligned}
V(x) &\approx \int_0^{+\infty} \rho(\lambda) \int_0^1 \left( \frac{\frac{\lambda}{x}}{1 + \frac{\lambda}{x}t} dt \right) d\lambda \\
&= \int_0^{+\infty} \rho(\lambda) \left( \int_0^1 \frac{\lambda}{x + \lambda t} dt \right) d\lambda.
\end{aligned} \tag{2.41}$$

Let  $t = \frac{1}{\omega}$ , since  $t \in [0, 1], \omega \in [0, \infty)$ , we see that

$$\begin{aligned}
V(x) &= \int_0^{+\infty} \rho(\lambda) \left( \int_0^1 \frac{\lambda}{x + \lambda \frac{1}{\omega}} d\frac{1}{\omega} \right) d\lambda \\
&= \int_0^{+\infty} \rho(\lambda) \left( \int_1^{\infty} \left( \frac{\lambda}{\omega x + \lambda} \right) \frac{d\omega}{\omega} \right) d\lambda.
\end{aligned} \tag{2.42}$$

By changing the variable with  $\Omega = \omega x$ , whereas  $\omega = \frac{\Omega}{x}, d\omega = \frac{d\Omega}{x}$ , and exchanging the  $\lambda$  and  $\omega$  integration, we have

$$\begin{aligned}
V(x) &= \int_0^{+\infty} \rho(\lambda) \left( \int_1^{\infty} \left( \frac{\lambda}{\omega x + \lambda} \right) \frac{d\omega}{\omega} \right) d\lambda \\
&\stackrel{a}{=} \int_0^{+\infty} \rho(\lambda) \left( \int_x^{\infty} \left( \frac{\lambda}{\Omega + \lambda} \right) \frac{1}{\Omega} d\Omega \right) d\lambda \\
&= \int_0^{+\infty} \frac{1}{\Omega} \rho(\lambda) \left( \int_x^{\infty} \left( \frac{\lambda + \Omega - \Omega}{\Omega + \lambda} \right) d\Omega \right) d\lambda \\
&= \int_0^{\infty} \frac{1}{\Omega} \rho(\lambda) \left( \int_x^{\infty} \left( \frac{\lambda + \Omega - \Omega}{\Omega + \lambda} \right) d\Omega \right) d\lambda \\
&= \int_x^{+\infty} \left( \frac{1}{\Omega} \rho(\lambda) d\lambda - \int_0^{\infty} \left( \frac{\rho(\lambda)}{\Omega + \lambda} \right) d\lambda \right) d\Omega,
\end{aligned} \tag{2.43}$$

where  $a$  denotes the exchange of  $\Omega$  with  $\omega x$ . Thus consequently we have

$$V(x) = \int_x^{+\infty} \left( \frac{1}{\omega} - S(-\omega) \right) d\omega. \quad (2.44)$$

This completes the proof.

## Appendix B

As stated by (2.25), the achievable transmission rate of each user  $k$  can be given as

$$C_k = \mathbb{E} \left\{ \log \det \left( \mathbf{I}_N + \frac{P_k \mathbf{H}\mathbf{H}^H}{\sum_{k'=1}^{k-1} P_{k'} \mathbf{H}\mathbf{H}^H} \right) \right\}. \quad (2.45)$$

While reducing of fractions to a common denominator, we have

$$C_k = \mathbb{E} \left\{ \log \det \left( \frac{\sum_{k'=1}^{k-1} P_{k'} \mathbf{H}\mathbf{H}^H + P_k \mathbf{H}\mathbf{H}^H}{\sum_{k'=1}^{k-1} P_{k'} \mathbf{H}\mathbf{H}^H} \right) \right\}. \quad (2.46)$$

Additionally, this can be further written as

$$\begin{aligned} C_k &= \mathbb{E} \left\{ \log \det \left( \frac{\sum_{k'=1}^k P_{k'} \mathbf{H}\mathbf{H}^H}{\sum_{k'=1}^{k-1} P_{k'} \mathbf{H}\mathbf{H}^H} \right) \right\} \\ &= \mathbb{E} \left\{ \log \det \left( \frac{\sum_{k'=1}^k P_{k'} \mathbf{H}\mathbf{H}^H}{\sum_{k'=1}^k P_{k'} \mathbf{H}\mathbf{H}^H - P_k \mathbf{H}\mathbf{H}^H} \right) \right\} \\ &= \log \left\{ \left( \frac{\sum_{k'=1}^k P_{k'}}{\sum_{k'=1}^k P_{k'} - P_k} \right) \mathbb{E} (\det \mathbf{H}\mathbf{H}^H) \right\}. \end{aligned} \quad (2.47)$$

Exchanging the base of logarithm to the last equality, and following the prior studies by [22, 23, 78] will yield

$$\begin{aligned} C_k &= \log \left\{ \left( \frac{\sum_{k'=1}^k P_{k'}}{\sum_{k'=1}^k P_{k'} - P_k} \right) \mathbb{E} (\det \mathbf{H}\mathbf{H}^H) \right\} \\ &= \frac{1}{\ln 2} \left\{ \ln \left( \frac{\sum_{k'=1}^k P_{k'}}{\sum_{k'=1}^k P_{k'} - P_k} \right) + \ln \int_0^{+\infty} \lambda f(\lambda) \right\}. \end{aligned} \quad (2.48)$$

While summarizing the achievable rate to all  $K$  users, it will be the final result.

## Appendix C

Inspired by the prior studies in [48, 54, 79], the eigenvalue decomposition of  $\mathbf{B}$  can be given as

$$\mathbf{B} = \mathbf{Q}\mathbf{D}_1\mathbf{Q}^H, \quad (2.49)$$

whereas  $\mathbf{Q}$  is the unitary matrix, and  $\mathbf{D}_1$  is the diagonal matrix. With this in hand, for  $\mathbf{BA}$ , the following equality holds

$$\begin{aligned} (\mathbf{BA})(\mathbf{BA})^H &= \mathbf{QD}_1\mathbf{Q}^H\mathbf{A}\mathbf{A}^H\mathbf{QD}_1^H\mathbf{Q}^H \\ &= \mathbf{QD}_1\tilde{\mathbf{A}}\tilde{\mathbf{A}}^H\mathbf{D}_1^H\mathbf{Q}^H \\ &\triangleq \mathbf{QW}_0\mathbf{Q}^H. \end{aligned} \quad (2.50)$$

This gives the matrix  $\mathbf{W}_0$  a central Wishart matrix with  $K$  non-zero eigenvalues defined as  $0 < \chi_1 < \dots < \chi_K < \infty$ . By denoting the eigenvalues of  $\mathbf{BB}^H$  as  $0 < v_1 < \dots < v_L < \infty$ , in line with prior study [79], the CDF of the largest eigenvalue of  $(\mathbf{BA})(\mathbf{BA})^H$  conditioned on  $\mathbf{B}$  can be given as [79, 80]

$$F_{\chi_{max}}(x|\mathbf{B}) = \frac{(-1)^{K(L-K)} \det(\mathbf{\Delta}(x))}{\det(\mathbf{V}) \prod_{i=1}^K \Gamma(K-i+1)}. \quad (2.51)$$

where  $\mathbf{\Delta}(x)$  is an  $L \times L$  matrix with entries

$$\mathbf{\Delta}(x)_{i,j} = \begin{cases} \left(-\frac{1}{v_j}\right)^{L-K-i}, & \text{for } i \leq L-K, \\ v_j^{L-i+1} \gamma(L-i+1, \frac{xL}{v_j}), & \text{for } i > L-K. \end{cases} \quad (2.52)$$

Additionally,  $\mathbf{V}$  is a  $L \times L$  matrix defined as [54]

$$\det(\mathbf{V}) = \left( \prod_{i=1}^L v_i^K \right) \prod_{1 \leq l \leq k \leq L} \left( \frac{1}{v_k} - \frac{1}{v_l} \right). \quad (2.53)$$

By some manipulations with regard to the Vandermonde determinant identity, it can be further written as

$$\begin{aligned} \det(\mathbf{V}) &= \left( \prod_{i=1}^L v_i^K \right) (-1)^{\frac{L(L-1)}{2}} \frac{\prod_{1 \leq i < j \leq L} (v_j - v_i)}{\prod_{i=1}^L v_i^{L-1}} \\ &= \left( \prod_{i=1}^L v_i^{K-L+1} \right) \prod_{1 \leq i < j \leq L} (v_i - v_j) \end{aligned} \quad (2.54)$$

On the other hand, by following the prior studies [79, 80], for the square matrix  $\mathbf{B} \in \mathbb{C}^{L \times L}$  here in this paper, the joint PDF of the eigenvalue  $0 < v_1 < \dots < v_L < \infty$  of the matrix constituted by  $\mathbf{BB}^H$  is given by

$$f_v(\mathbf{D}_1) = \frac{e^{-\sum_{i=1}^L v_i} \prod_{i < j}^L (v_j - v_i)^2}{\prod_{i=1}^L \Gamma(L-i+1)^2}. \quad (2.55)$$

To this end, the unconditional CDF of  $0 < \chi_1 < \dots < \chi_K < \infty$  will be

$$F_{\chi_{max}}(x) = \int_{\mathcal{U}} F_{\chi_{max}}(x|\mathbf{B})f_v(\mathbf{D}_1)dv_1, \dots, dv_L, \quad (2.56)$$

where  $\mathcal{U} \triangleq \{0 < \chi_1 < \dots < \chi_K < \infty\}$ , this gives

$$F_{\chi_{max}}(x) = \frac{(-1)^{K(L-K)} \det(\mathbf{D}(x))}{\prod_{k=1}^K \Gamma(K-k+1) \prod_{i=1}^L \Gamma(L-i+1)^2}, \quad (2.57)$$

where  $\mathbf{D}(x)$  is given as

$$\mathbf{D}(x) = \int_{\mathcal{U}} \det(\mathbf{\Delta}(x)) e^{-\sum_{i=1}^L v_i} \prod_{i=1}^L v_i^{L-K-1} \prod_{i < j} (v_i - v_j) dv_1, \dots, dv_L. \quad (2.58)$$

Observation has that

$$\prod_{i < j} (v_i - v_j) = \det(v_j^{i-1}). \quad (2.59)$$

By following the analysis in [79],  $\mathbf{D}(x)$  is finally given as

$$\mathbf{D}(x)_{i,j} = \begin{cases} (-1)^{L-K-i} \Gamma(i+j-1), & \text{for } i \leq L-K, \\ \int_0^{+\infty} e^{t2L-K-i+j-1} \gamma(L-i+1, \frac{xL}{t}) dt, & \text{for } i > L-K. \end{cases} \quad (2.60)$$

To determine the second expression, it is noticed that  $\gamma(\cdot, \cdot)$  is defined as [54, 79]

$$\begin{aligned} \gamma(a, x) &= \int_0^x t^{a-1} e^{-t} dt \\ &= (a-1)! \left( 1 - e^{-x} \sum_{i=0}^{a-1} \frac{x^i}{i!} \right). \end{aligned} \quad (2.61)$$

Furthermore, observation from [81] has that

$$\int_0^{+\infty} x^{\alpha-1} e^{-\beta x - \frac{\gamma}{x}} dx = 2 \left( \frac{\gamma}{\beta} \right)^{\frac{\alpha}{2}} K_{\alpha}(2\sqrt{\beta\gamma}), \quad (2.62)$$

where  $K_a(b)$  as the modified Bessel function of the first kind. By substituting this (2.62) and (2.61) into (2.60), with tremendous calculation, the determinant expression of its second part can be finally obtained as

$$\begin{aligned} & \int_0^{+\infty} e^{t2L-K-i+j-1} \gamma(L-i+1, \frac{xL}{t}) dt \\ &= (L-i)! \left[ \Gamma(2L-K-i+j) - \sum_i^{L-i} \frac{(xL)^i}{i!} \right. \\ & \left. 2(xL)^{\frac{2L-K-2i+j}{2}} K_{2L-K-2i+j}(2\sqrt{xL}) \right], \text{ for } i > L-K. \end{aligned} \quad (2.63)$$

Thus the PDF of  $0 < \chi_1 < \dots < \chi_K < \infty$  can be obtained as

$$f_\chi(x) = \frac{(-1)^{K(L-K)} \frac{d}{dx} [\det(\mathbf{D}(x))]}{\prod_{k=1}^K \Gamma(K-k+1) \prod_{i=1}^L \Gamma(L-i+1)^2}. \quad (2.64)$$

In line with [25], the unordered PDF of eigenvalues  $\lambda_1, \dots, \lambda_K$  of  $(\mathbf{DBA})(\mathbf{DBA})^H$  conditioned on  $\mathbf{BA}$  is

$$f_\lambda(\lambda|\mathbf{BA}) = \frac{1}{L \prod_{i<j}^K (\chi_j - \chi_i)} \sum_{m=L-K+1}^L \frac{\lambda^{K-L+m-1}}{\Gamma(K-L+m-1)} \det(\mathbf{G}) \quad (2.65)$$

whereas  $\mathbf{G}$  is a  $L \times L$  matrix with entries

$$\mathbf{G}_{i,j} = \begin{cases} \chi_j^{i-1}, & \text{for } i \neq j \\ \chi_j^{L-K-1} e^{-\frac{\lambda}{\chi_j}}, & \text{for } i = j. \end{cases} \quad (2.66)$$

Thus by using  $f(\lambda) = f_\lambda(\lambda|\mathbf{BA})f_\chi(x)$  and integrating it to all  $\chi$ , we can finally obtain the result.

# Chapter 3

## Integrated Energy Efficiency Architecture and Analysis of 5G

### 3.1 Summary

Other than the prior study in chapter 2, in the following chapter 3 and chapter 4, the Energy Efficiency (EE) issue will be focused. Firstly, an integrated system architecture is proposed here in this chapter. The purpose of this study is to enhance the Fifth Generation (5G) Internet of Things (IoT) system's EE performance. We first introduced an integrated system structure. In the integrated system structure, we proposed an unified control center. With the unified control center's help, the select-and-sleep mechanism of different components are easier to executed. Then we further propose one Cellular Partition Zooming (CPZ) mechanism for the wireless transmission section. The proposed integrated system model as well as the CPZ mechanism are verified with the simulation result. From the simulation, it is demonstrated that the proposed schemes display better EE performance. This is due to the face that system power consumption are further reduced compared to the prior work<sup>1</sup>.

### 3.2 Introduction

As known, Fifth Generation (5G) is calling for up to 50 billion devices connection word-widely. The connected devices are not only restricted to the cell-phones. The

---

<sup>1</sup>This is based on the work **D. Zhang**, Z. Zhou, S. Mumtaz, J. Rodriguez, and T. Sato, "One Integrated Energy Efficiency Proposal for 5G IoT Communications", *IEEE IoT Journal*, Vol. PP, Issue. 99, DOI: 10.1109/JIOT.2016.2599852; and **D. Zhang**, K. Yu, Z. Zhou, and T. Sato, "Energy Efficiency Scheme with Cellular Partition Zooming for Massive MIMO Systems", in *IEEE ISADS*, Taichung, 2015, pp. 266-271.

cars, electronic households and other devices are claimed to be connected to the wireless network with 5G, to build a smart society. In this case, 5G is aiming at the Internet of Things (IoT) era to connect everything, at anywhere, in anytime. To this end, in the studies both from academia and industry, the massive connected equipments and even faster rate are the two main targets and aims of 5G [82, 83]. For instance, it is calling for the access data rate up to 10 Gbit/s by 2020 [83]. In literature of 5G IoT, it is known that the spectrum efficiency (SE) issue has been studied a lot. The proposed methods on SE issue so far can be listed but not limited to the massive Multi-Input Multi-Output (MIMO) (also called as the multiuser MIMO, or large MIMO) [14], small cell [84], Devices to Devices (D2D) communications [85], Heterogeneous Networks (HetNets) [86], unlicensed spectrum allocation (as well as the millimeter wave (mmWave)) [87]. Recently, the Non-Orthogonal Multiple Access (NOMA) [54] is proposed to share the same frequency resource block amongst multiple users. This in turns, yields a better system SE performance. The full duplex mechanism (to transmit and receive the information at the same time via the same channel) [88] is emerging as another promising technology to achieve the SE target of 5G.

Besides the SE studies, in 5G, the Energy Efficiency (EE) issue is investigated a lot in literature recently as another vital issue of 5G [89, 90]. This is because, with higher transmission rate, more energy will be consumed. In the studies of EE topic of 5G IoT, the select-and-sleep mechanism is brought up as the initial step. Actually, the select-and-sleep mechanism is tailored for EE issue both in wireless and optical communications [1, 91]. The prior studies on this select-and-sleep mechanism can be found in literature. For instance, the cellular zooming scheme was proposed in [1]. In this study, the cellular coverage area is divided into different ring sections. The division is based on the distance from user terminal to Base Station (BS). Afterwards, the cellular can zoom in to cover more users or zoom out to save energy in case less users existing. Inspired by this idea, the antenna select-and-sleep [92] mechanism was further proposed with massive MIMO architecture. As noticed with massive MIMO architecture, some transmit antennas are not effectively used while communicating. Thus the select-and-sleep mechanism can select the wanted transmit antenna while keeping the other ones into sleep mode. In addition, the Radio Frequency (RF) chain select-and-sleep mechanism was investigated in [25], where the concept is similar to the antenna select-and-sleep mechanism. As investigated heretofore, there are series of studies on the 5G IoT's EE issue. Actually, the EE issue has been studied in physical layer, upper layer and even cross-layer. Yet it is noticed that, most of the

prior studies focus on only part of the components with select-and-sleep mechanism, whereas an integrated scope has never been casted.

Based on all of the aforementioned information, in this chapter, we further propose an integrated system model by uniformly scheduling the resources of multiple cells. The unitive machine room is invoked to supply the power for multiple cells as well. In addition, we further take the machine room element into consideration while optimizing the energy consumption of the whole system with regard to the EE definition. With much less circuits and engaged components by this integrated system model, much less energy will be consumed. In this case, the system model is of better EE performance compared with prior studies. This proposal is also of benefits while uniformly scheduling the resources amongst multiple cellular, which will be stated by the following content.

The contributions of this chapter can be summarized as follows: a) An integrated system model for 5G IoT is proposed in this chapter. The system model is based on the Cloud Radio Access Network (C-RAN) architecture. With this system model, the uniformly resource scheduling can be easier to executed of multiple cells. The system EE performance can be further enhanced with this model while taking more elements into consideration. b) The massive MIMO antenna array is invoked to replace the signal antenna Remote Radio Heads (RRHs) in this C-RAN architecture. With this modification, it will be much easier to cover a larger area in the outdoor environment. It is also an economist way to deploy because we can re-use the existing Long Term Evolution (LTE) BSs by just replacing their single antenna with massive MIMO antenna array. 3) One CPZ mechanism is proposed for wireless cellular section to further enhance the system EE performance with regard to the distance from BS to user terminal, as well as the angles of user locations to BS.

The rest of this chapter is organized as follows: section III is the proposed integrating system. As stated before, the integrated system model is based on the C-RAN architecture while replacing the prior single antenna RRHs into massive MIMO based cells. In addition, the uniform BaseBand Unit (BBU) can scheduling all of the multi cells' resources. based on this system model, the EE performance is discussed in section IV. The CPZ mechanism is proposed to further divide the coverage area with regard to the angle from BS to accessing user. With all of the proposals, numerical results is presented while investigating the EE performance in section V. Finally, the main results obtained in this chapter are summarized by section VI.

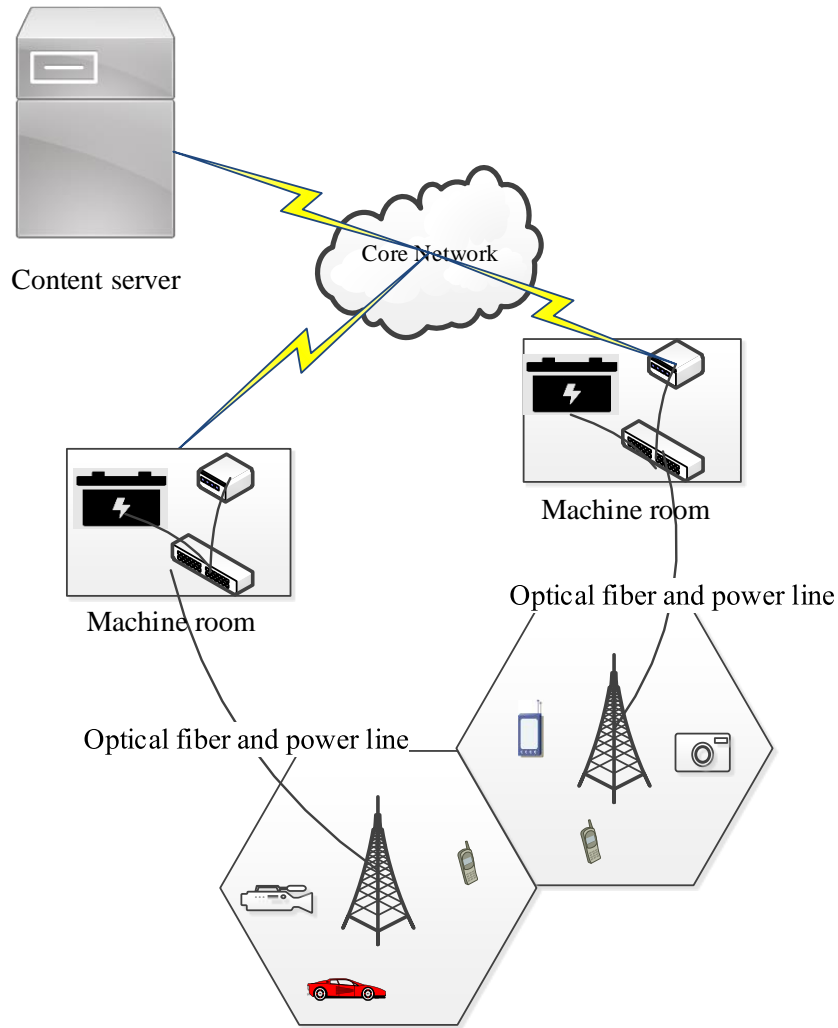


Figure 3.1 The traditional BS model with variable kinds of users.

### 3.3 Proposed system model

The traditional BS model can be depicted by Fig. 3.1. As shown here, each BS is equipped with one control center to exchange the control information, as well as a machine room to supply the power. Additionally, during the transmission procedure, content request of each user will be delivered to the core network to download the required content. In which, a content server is located in the remote area for content acquirement (Note that here in this chapter, we only concern about the streaming data transmission and acquisition with 5G IoT. This is valuable to discuss as it exploiting nearly 83% of the total internet services).

In contrast, C-RAN, generally, consists of a cloud core network, a high-speed switcher, a Gbits/s or even Tbits/s link as the backhaul, and several BSs as its

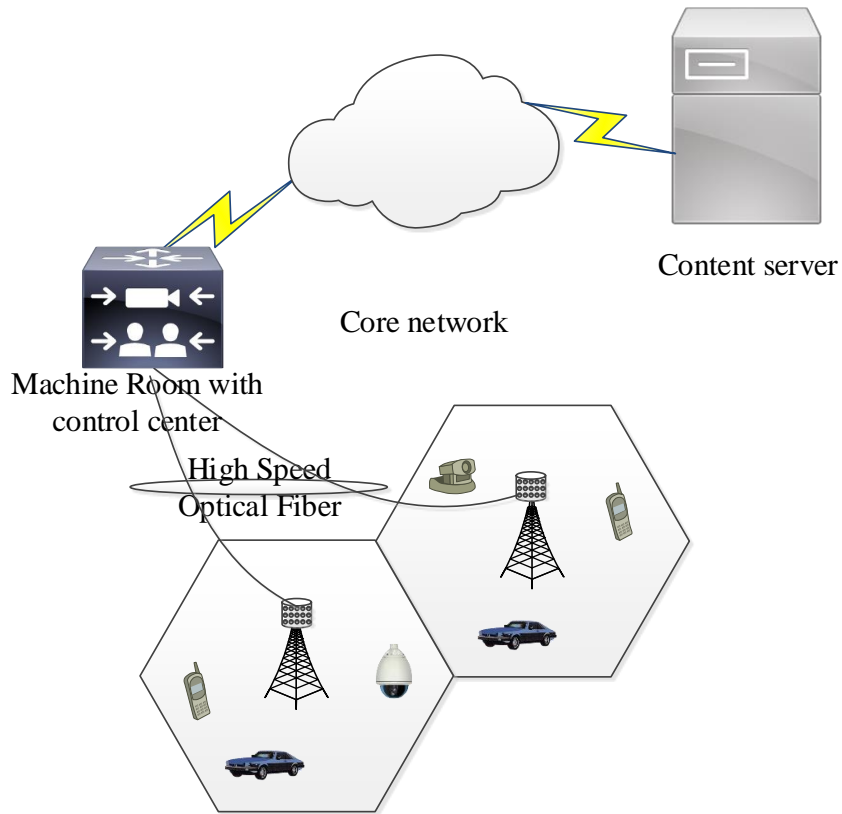


Figure 3.2 Proposed system model for 5G IoT.

RRHs. The function of C-RAN is to schedule the resources uniformly through the Coordinated Multiple Points transmission and reception (CoMP) technology [30,93]. Nevertheless, with large number of the small cell RRHs (one small cell RRH can only cover a limited area compared with prior cellular BS), it can not be an economic choice while deploying in the outdoor environment. Accordingly, to cater to the 5G IoT requirements with even larger coverage to connect everyone and everything, an integrated system architecture based on the C-RAN here is provided, which can be summarized as follows.

As shown by Fig. 3.2, the single antenna RRHs of C-RAN is replaced by the massive MIMO array. This is due to the fact that one single-antenna-RRH can only cover a small area. Thus to cover a huge area in the outdoor environment, large deployment of the single-antenna-RRH is needed, which will result in huge budge load for the operator. On the contrary, as much larger coverage area with massive MIMO BS antenna arrays, lesser deployment number of the RRHs is needed. In addition, one can re-use the existing BS while replacing the existing LTE antenna with massive MIMO array, and plant new ones whenever needed. With this re-used

scenario, the budget can be saved. Afterwards, the proposed integrated model is of better EE performance while uniformly scheduling the resources and sharing the machine room with multiple BSs. This is due to the fact that less energy consumption is needed with this system model. In addition, based on this integrated system model, we further proposed a CPZ mechanism to further enhance the EE performance of the whole system.

The advantages of this integrated model as well as the CPZ mechanism can be summarized by four folds:

- Firstly, the integrated system model is easy to achieve while deploying in the outdoor environment by simply replacing the prior LTE antenna with massive MIMO array. In addition, plant more massive MIMO antenna array enabled BS if needed. As select-and-sleep mechanism calling for on/off control of each antenna, the uniform plant and control center here can control the power supply of each antenna. That is, with CPZ mechanism, it is possible to determine the occasion to turn on or turn off the corresponding antennas by employing the control circuits. In contrast, in previous C-RAN structure, it is impossible to control a specific antenna's behavior. In which, only the BS is capable of turning on or turning off its power supply totally by the machine room.
- Channel State Information (CSI) can be gained from each BS and shared between different BSs within one cluster through backhaul that connecting the uniform control center, where the resources can be uniformly scheduled. While knowing the global CSI information, the control center can decide the required transmission power and frequency resources for the transmission.
- The CPZ mechanism is an economical method to sustain high transmission speed while decreasing the number of needed antenna number. That is because, as the pie-section division of the coverage area, whenever users are in the pie-section, control center can turn on the associating antennas, otherwise, keep it off. On the contrary, in prior zooming mechanism [1], all of the antennas should be kept on. In addition, with this CPZ mechanism by keeping off the un-needed antennas, much more energy can be saved while maintaining the transmission rate. This yields better system EE performance. The specific comparison of EE performance will be addressed by the following numerical results section.

## 3.4 Energy efficiency analysis

Based on the proposed system structure for 5G, we will address its EE analysis by the following section. The EE performance of this proposal is further compared with prior studies in the numerical results section. Intuitively, in line with prior studies, EE can be defined as the capacity (or transmission rate) divided by its consumed energy, i.e., bit/joule [94],

$$\eta = \frac{R}{P}, \quad (3.1)$$

or joule/bit [95],

$$\eta = \frac{P}{R}. \quad (3.2)$$

Here  $R$  is the capacity (or transmission rate) of user terminals while summing together (the system capacity or sum rate). Additionally,  $P$  is the total consumed energy to satisfy such a rate. In the study here of this chapter, the first definition with bit/joule [94] is adopted.

### 3.4.1 The analysis of capacity performance

While replacing the prior LTE antenna with massive MIMO array and planting new BS if needed, as known, there will be hundreds or even thousands of antennas that serving a much less number of users. Take the hypothesis that  $M$  is the number of transmit antennas at the massive MIMO array side, and  $K$  the number of user terminals. In addition,  $\mathbf{B}$  is the beamformer that used to eliminate the co-channel interferences, and  $h_k$ , the channel from BS to user  $k$ . It is assumed that the Zero Forced Beam-Forming (ZFBF) is used to eliminate the interferences (as ZFBF displaying better performance than the low complexity beamforming technologies [96]). With this assumption, ZFBF matrix, according to prior study, can be given as [97]

$$\mathbf{B} = \mathbf{H}^H(\mathbf{H}^H\mathbf{H})^{-1}, \quad (3.3)$$

where  $(\cdot)^H$  and  $(\cdot)^{-1}$  yields the conjugate and inverse transpose of a matrix, respectively. In addition, received signal at the receiver side follows

$$y_k = \mathbf{h}_k \frac{b_k}{\sqrt{\gamma}} x_k + \sum_{i=1, i \neq k}^K \mathbf{H}_{k-1} \frac{b_i}{\sqrt{\gamma}} x_i + n_k, \quad (3.4)$$

where  $x_k$  is the transmit signal of the  $k$ th user. It can be given by  $x_k = \sqrt{P_k} s_k$ , with  $P_k$ ,  $s_k$ , the power consumption and transmitted signal of the  $k$ th user, respectively. Moreover,  $\mathbf{H}_{k-1}$  is the channel matrix without the element  $\mathbf{h}_k$ , where  $b_k$  and  $b_i$ ,

one entry of  $\mathbf{B}$ ,  $n_k$  the noise signal with zero mean  $n_0$  variance  $\mathbf{n} \sim \mathcal{CN}(0, n_0)$ ,  $\gamma$  normalization factor of the  $k$ th user's signal.

Assuming  $B_{sum}$  the total bandwidth, which is equally divided to each user ( $B_{CC_s}$  for each user). Besides,  $\text{SINR}_k$  is the Signal to Interference plus Noise Ratio (SINR) of the  $k$ th user. Then received transmission rate of the  $k$ th user reads

$$C_k = B_{CC_s} \log_2(1 + \text{SINR}_k). \quad (3.5)$$

By further supposing the power consumption of antenna array is  $P_a$ . With equal power allocation scheme, the allocated power for each user is  $\beta = P_a/K$ . Taking  $\rho = \beta/N_0$  as the Signal to Noise Ratio (SNR), and a normalized noise power, SINR of user  $k$  follows

$$\text{SINR}_k = \frac{\rho |h_k b_k|^2}{\rho \sum_{j=1, j \neq k}^{j=K} |h_k b_j|^2 + 1}, \quad (3.6)$$

whereas, achievable transmission rate of the  $k$ th user will be [2]

$$\begin{aligned} C_k &= B_{CC_s} \mathbb{E} \left\{ \log_2 \det \left( \mathbf{I} + \frac{\rho K}{(\mathbf{H}\mathbf{H}^H)^{-1}} \right) \right\} \\ &= B_{CC_s} \left\{ \log_2 \det \left( \mathbf{I} + \frac{\rho K}{\mathbb{E} \{ (\mathbf{H}\mathbf{H}^H)^{-1} \}} \right) \right\}. \end{aligned} \quad (3.7)$$

In addition, with Gaussian i.i.d distribution of each channel gain, channel matrix  $\mathbf{H}\mathbf{H}^H$  will be a non-central Wishart matrix (with eigenvalue larger than zero). This gives

$$\mathbb{E} \{ (\mathbf{H}\mathbf{H}^H)^{-1} \} = \mathbb{E} \{ \|\mathbf{B}\|_F^2 \}. \quad (3.8)$$

As the study of [7], with  $K, M$  growing large,  $\mathbb{E} \{ \|\mathbf{B}\|_F^2 \}$  converges to a fixed deterministic value

$$\mathbb{E} \{ \|\mathbf{B}\|_F^2 \} = \frac{K}{M - K}. \quad (3.9)$$

In this case, max-sum capacity turn out to be [5]

$$C_{sum} = \sum_{k=0}^K B_{CC_s} \log_2 [1 + \rho(M - K)]. \quad (3.10)$$

### 3.4.2 Analysis of propagation model

Observation from prior literature finds that the loss of propagation is neglected for the sake of simplicity although it is unavoidable during transmission. By further

adding this loss into consideration, according to the wireless propagation model, power attenuation will be [6]

$$P_{att} = G \left( \frac{d}{r_0} \right)^{-\alpha} \Psi P_\alpha, \quad (3.11)$$

where  $G$  the path gain,  $d$  the propagation distance,  $r_0$  the omnidirectional antennas power variation (take the value of 1~10m for indoor environment and 10~100m for outdoor environment),  $\alpha$  the path loss exponent,  $\Psi$  the random variable for slow fading effect. With this propagation loss adding, SINR can be rewritten as

$$\text{SINR}_k = \frac{P_\alpha(M-K)}{K + P_{att}}. \quad (3.12)$$

Consequently, achievable sum rate will turn out to be

$$\begin{aligned} R_{sum} &= \sum_{k=0}^K B_{CCs} \log_2(1 + \text{SINR}_k) \\ &\approx \sum_{k=0}^K B_{CCs} \log_2 \left( 1 + \frac{P_\alpha(M-K)}{K + P_{att}} \right) \\ &= \sum_{k=0}^K B_{CCs} \log_2 \left( 1 + \frac{P_\alpha(M-K)}{K + G \left( \frac{d}{r_0} \right)^{-\alpha} \Psi P_\alpha} \right). \end{aligned} \quad (3.13)$$

This is the sum rate expression with regard to the EE definition. In the following content, we will pursue the energy consumption of this integrated system with the proposed CPZ mechanism.

### 3.4.3 Proposed CPZ scheme

According to the aforementioned discussion, by following the definition of EE with bit/joule, we therefore have the EE formula as follows

$$\begin{aligned} &\max_{P_k} \frac{\sum_{k=0}^K B_{CCs} \log_2 \left( 1 + \frac{P_\alpha(M-K)}{K + G \left( \frac{d}{r_0} \right)^{-\alpha} \Psi P_\alpha} \right)}{P_k}, \\ &s.t. \quad \sum_{k=0}^K P_k \leq P_{BS}, \quad P_k \in [0, P_{BS}]. \end{aligned} \quad (3.14)$$

where  $P_{BS}$  is the total power of antenna arrays. Furthermore, the constraint condition here denotes that the total power for information transmission of each user cannot exceed the BS power with massive MIMO antenna array.

In cellular communications, users are randomly distributed in BS coverage area [1,93]. It is found by prior studies that in late night and rural area, much less number are existing within each cellular coverage compared to the urban area. In this regard, the prior study of [1] divides the coverage area into different ring sections with respect to the distance from user to BS for zooming in or out. For instance, if less users are associating for transmission, the BS zooms out to save energy, in contrast, zooms in to cover larger area.

The prior study with cellular zooming inspires us that, if the coverage area is further divided into different pie sections with respect to the angle (take the coverage area as one circle) and distance (from user to the BS), EE performance can be further strengthened. The power allocation scheme is that, allocating power to the area with users, whereas turning off the antenna in the area without users (note that it is assumed that with cylinder massive MIMO antenna array, equal number division of the antenna is adopted with each pie sections). The proposed CPZ scheme can be depicted by Fig. 3. As shown, the number of antenna of each pie section, with a cylindrical massive MIMO antenna array, is counting by the cylindrical column of different pie sections that serving. For instance, if the coverage area is equally divided into different pie sections with an angle  $\theta$ , then one pie area (without considering the distance from user to BS) associating a number of  $M \times \frac{\theta}{2\pi}$  antennas (generally, we allocate the antenna number with an integer value).

While accessing the network, user first reports its location information to the BS. Afterwards, control center will calculate the angle and distance, and compare them with the existing ones, then allocate a minimum required power for the new user's transmission. For instance, consider two users A and B, which is locating on the right side of Fig. 3. Minimum area to cover them will be the pie area with second circle distance counting from the outermost, and the required angle equals to  $\theta$ . While knowing this, BS will allocate the minimum power to this area for their transmission according to their transmission rate. This is achieved by allocating a minimum power value with respect to the achievable rate expression (all of the other parameters are taken as constant). While taking  $A$  as the needed angle,  $d$  distance from user to BS,  $d_{new}^{user}$  distance from new coming user to BS,  $d_{exist}^{user}$  distance from existing user to BS,  $A_{new}^{user}$  required angle of BS to cover the new coming user and  $A_{exist}^{user}$  needed angle of BS to cover the existed users, respectively, detail CPZ mechanism can be given by algorithm 1 in the following page [5].

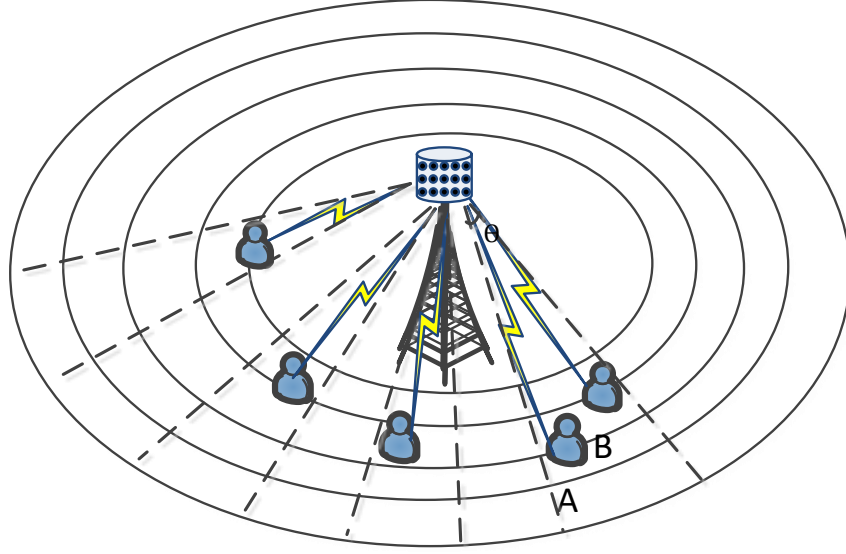


Figure 3.3 System model with different annular regions.

---

**Algorithm 1** CPZ execution algorithm

---

- 1: Initialization: divide the coverage area into several pies with respect to the distance and angle.
  - 2: When new user joins, execute the cell search and initialization, report its location.
  - 3: **if**  $A_{new}^{user} \subseteq \sum\{A_{exist}^{user}\}$  **then**
  - 4:   **if**  $d_{new}^{user} \leq \max d_{exist}^{user}$  **then**
  - 5:      $A = A_{new}^{user}$ ,  $d = \max d_{exist}^{user}$
  - 6:   **else**  $\{d_{new}^{user} > \max\{d_{exist}^{user}\}\}$
  - 7:      $d = d_{new}^{user}$ ; Allocate power with the new elements of  $A$  and  $d$ , and BS goes to sleep mode in other areas.
  - 8:   **end if**
  - 9: **else**  $\{A_{new}^{user} \not\subseteq \sum\{A_{exist}^{user}\}\}$
  - 10:    $A = A_{new}^{user}$ , update  $\{A_{exist}^{user}\}$  with new element  $A_{new}^{user}$ . Allocate power with the new elements of  $A$  and  $d$ , BS goes to sleep in other areas.
  - 11: **end if**
- 

## 3.5 Numerical results

To compare the proposed CPZ scheme with the cellular zooming scheme in [1], we first simulate the active user's location distribution by a random Poisson Point Process (PPP) distribution. The elements and their values used in this simulation is given by Table 1, in line with prior studies of [1, 26, 97–99]. Note that here an configurational example of the modified system structure is used to compare the CPZ with prior zooming scheme for the sake of simplicity, where the coverage area is divided into 20

Table 3.1 Simulation elements.

| Parameters           | Value   | Parameters              | Value  |
|----------------------|---------|-------------------------|--------|
| Bandwidth $B_{CC_s}$ | 5 MHz   | Machine room            | 480 W  |
| Path loss $\alpha$   | 3.7     | Shadow fading $\Psi$    | 8 dB   |
| Omnidirectional r    | 100 m   | Path gain G             | 1      |
| Peak bit rate        | 20 Mb/s | Per antenna Power $P_t$ | 33 dBm |

pies and each pie associating 10 antennas to zoom in or out with the proposed CPZ, as shown in Fig. 4. In addition, it is assumed that there are 10 cells in the system as an example (one C-RAN area can have different number of cells as an configuration). This is due to the fact that various combinations and division methods are existing while adopting the CPZ mechanism.

With this configuration, assuming that user 1 is the existing user, and its corresponding 10 antennas are turned on and zoomed in to the second circle of the pie section for user 1's transmission. Take the hypothesis that in the next step user 2 joins in, zooming to the third circle of this pie area (user 2's location with this CPZ coverage area division) and keeping the antennas in other unrelated areas off. In contrast, if the next user is user 3 but not user 2. As user 3 locating in the area of user 1 (with this CPZ coverage area division), zooming to user 3's location is not necessary. Thus no further pie section is needed to turn on the associating transmit antennas. Yet, on the other hand, on condition that the new coming user is user 4, 10 extra antennas will be turned on and new pie area should be zoomed to the third circle by the neighbouring pie section. Moreover, extra power will be needed as well for the coverage area maintaining and transmission [100].

Additionally, as discussed by Section II, transmission rate has a positive correlation with the consumed power and a negative correlation with the cellular radius. In this regard, one can deduce that once transmission requirement (with respect to the energy consumption for coverage area maintenance) of the marginal user is guaranteed, transmissions of the other users located within the same pie section can be guaranteed. In this case, while setting the maximum transmission rate of each user as 20 Mbit/s, a comparison between the proposed CPZ scheme and the zooming scheme in [1] can be given by the simulation results.

To compare the CPZ mechanism and prior zooming scheme in [1], it is assumed that there are 200 antennas within one massive MIMO antenna array. As an example and performance comparison here, as shown by Fig. 3.5 and Fig. 3.6,  $M = 100$  is used

to denote that one cellular coverage area is divided into two pie sections whereas each of them associating with 100 antennas. Similarity,  $M = 50$  means that the coverage area is divided into 4 pie sections that each of them associating with 50 antennas. Additionally,  $M = 25$  denoting the coverage area is divided into 8 pie sections that each of them associating with 25 antennas.

The power consumption as well as the EE performance comparison of the proposed CPZ and zooming mechanism in [1] are shown by Fig. 3.5 and Fig. 3.6, respectively. Here in Fig. 3.6, the bottom curve denoting the zooming mechanism in [1], and the remaining curves representing the proposed CPZ with different divided pie numbers, as described in the previous section. The effective radius with active UE/m means the turned on CPZ cellular pies with active UEs. Observation from Fig. 3.5 and Fig. 3.6 clearly verifies that the CPZ mechanism is of better performance comparing with prior zooming scheme in [1]. This is due to the fact that, compared with the zooming mechanism in [1], further dividing coverage area of CPZ consumes less energy while keeping other antennas off on condition that no active users in their associating pie sections. Thus with regard to the EE definition, better EE performance can be achieved.

This energy consumption of the CPZ is compared with the without CPZ scheme, which is shown by Fig. 3.7. As shown here, with CPZ's further division method with regard to the angle, the energy consumption can be further reduced. However, with the active user number increasing, the CPZ energy consumption approaches to the without CPZ case. Thus the CPZ mechanism is of effective with remote area or late night that the cellular has less number of users. In urban area with crowded users, the CPZ is of less effect to reduce the energy consumption. It can be deduced that with more active users randomly joining in, both the proposed CPZ mechanism and the zooming mechanism in [1] will approach the conventional without zooming mechanism. Thus one can conclude that the proposed CPZ is effective on off-peak conditions, such as the late night time period [101] and remote area. Yet in the crowd user conditions, such as mass active users under urban environment, both the prior zooming mechanism in [1] and the proposed CPZ here will be of less use. However, as the majority studies on accessing device's performances with EE issue of 5G, such as the Ericsson's white paper on 5G energy performance, "traffic is unevenly distributed, and there are large spatial variations of traffic even within a given area". One can conclude that in real environment, the proposal is always of help with respect to the device's location performance.

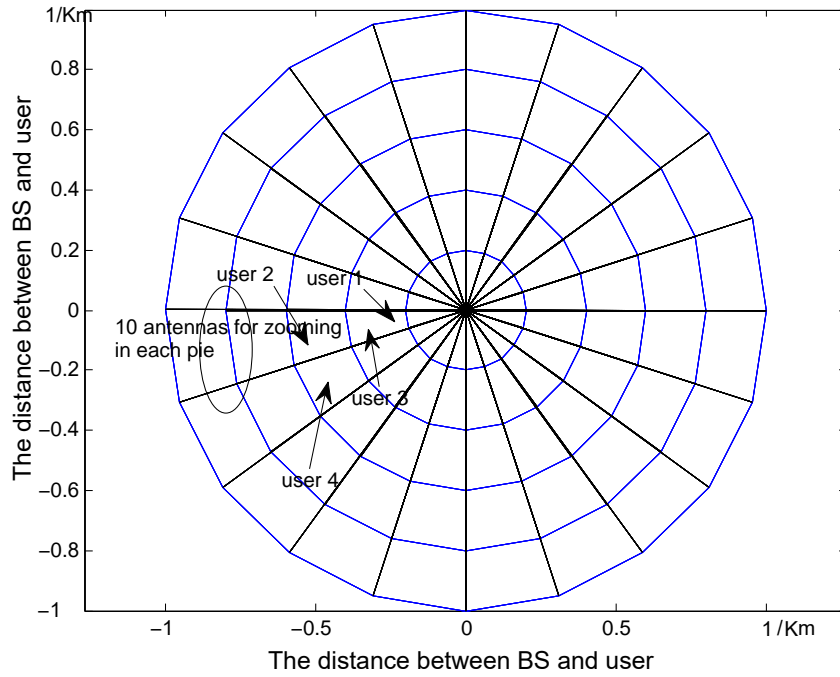


Figure 3.4 One sample division of the coverage area.

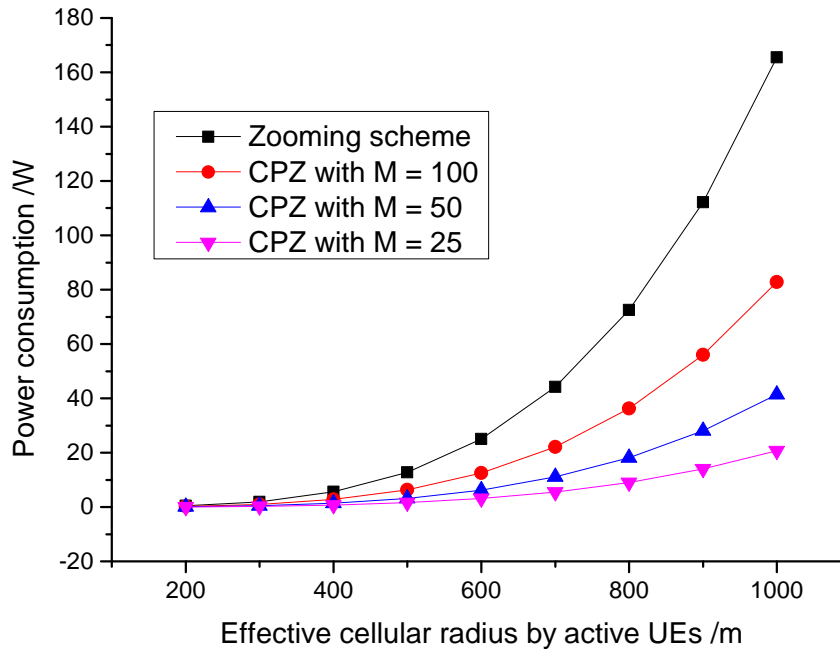


Figure 3.5 Power consumption of CPZ and traditional zooming scheme.

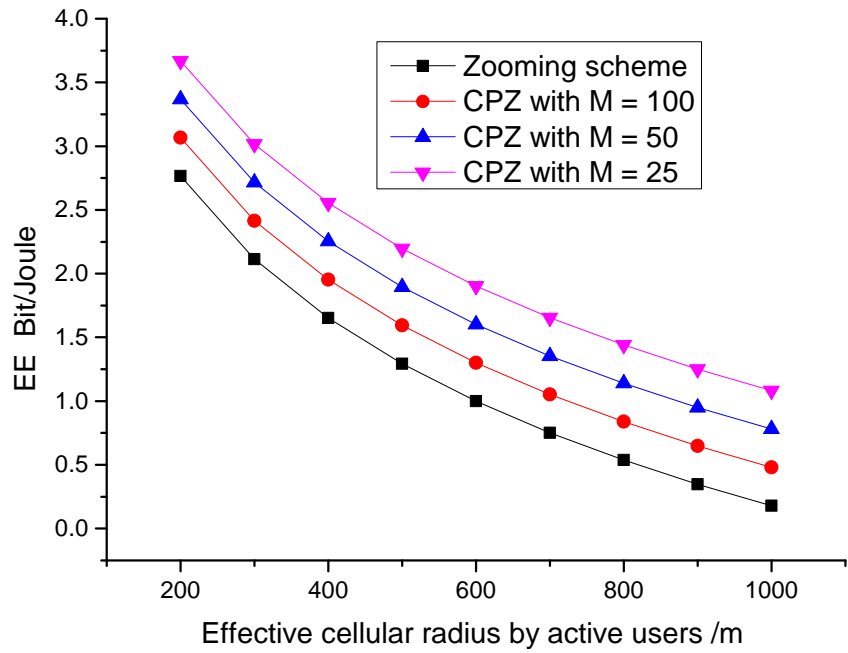


Figure 3.6 Energy efficiency of CPZ and zooming scheme in [1].

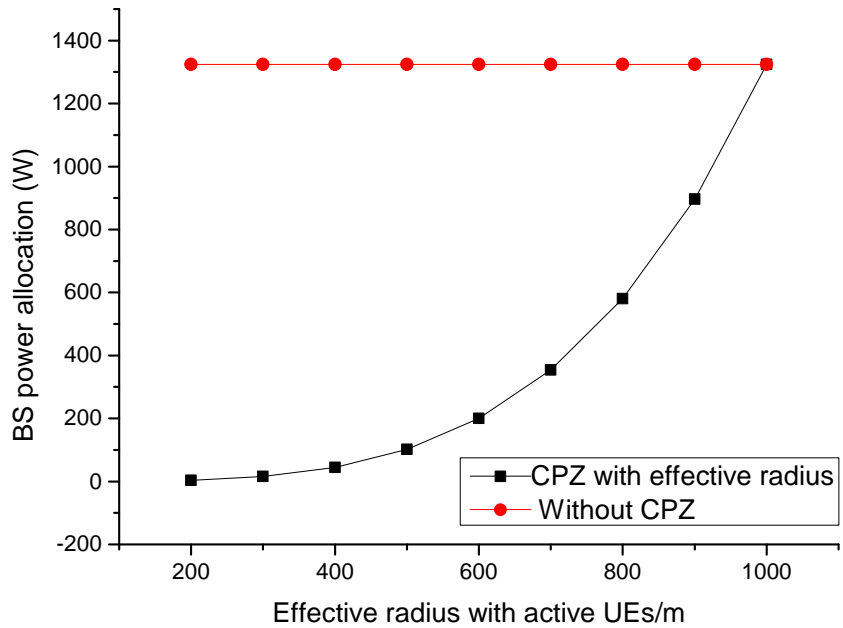


Figure 3.7 Energy consumption of the CPZ and without CPZ.

### 3.6 Conclusion

The EE performance is comprehensively investigated for 5G communications here in this paper. An integrated system structure for the 5G communication systems was

proposed beforehand by this study. Based on this system structure, EE is analyzed as well as an proposed CPZ mechanism with regard to the distance and angle from BS to user terminal. While further dividing the coverage area into pie sections with respect to both distance from BS to user and angle, turning off the unused resources, the total system power consumption is reduced. This in turns, brings better EE performance of the system compared with prior studies.

# Chapter 4

## Integrated Energy Efficiency Analysis of Massive MIMO Based C-RAN

### 4.1 Summary

In Energy Efficiency (EE) studies of wireless communications of its Fifth Generation (5G), most of the prior studies focus on less components for optimization, for instance, the antenna select/sleep mechanism, Radio Frequency (RF) chain select/sleep mechanism. Here in this studies, more engaged components (antenna, RF Chain, circuit, coverage area) are taken into consideration with the EE optimization problem. In addition, the EE optimization problem is based on the integrated system model. That is, we firstly propose one multi-Base Stations (BSs) system model based on the Cloud Radio Access Network (C-RAN) architecture. The benefit of this architecture is that, the resources amongst multiple BSs can be uniformly scheduled. Additionally, the select/sleep mechanism can be easily deployed in this system architecture. Afterwards, we described the optimal system EE with a convex optimization problem while taking varies components engaged in. To solve the optimization problem, we convert the global optimization problem into a convex optimization problem within each time interval of each BS area plus an off-line selection method. Simulation results demonstrate that energy consumption of transmit antenna is the dominant factor of the whole system. In this case, it is also the dominant factor of system EE performance giving the same sum rate<sup>1</sup>.

---

<sup>1</sup>This is based on the work **D. Zhang**, T. Muhammad, S. Mumtaz, J. Rodriguez, and T. Sato, "Integrating Energy Efficiency Analysis of Massive MIMO Based C-RAN", *EURASIP J. Wireless Commun. Networking*, Vol. 2016, No. 1, pp. 277-285, DOI: 10.1186/s13638-016-0778-y.

## 4.2 Introduction

In fifth generation (5G) wireless communication studies, the conventional Spectral Efficiency (SE) is vital to accomplish the higher transmission rate requirement [102, 103]. Another new coming topic is the Energy Efficiency (EE). Because with much higher transmission rate, the consumed energy is extremely high. In EE studies, there are two categories, to reduce the system energy consumption, to effectively re-use the energy. One of the methods to effectively re-use the energy is the Energy Harvesting (EH) [104]. It is proposed and widely studied in literature [104, 105]. The idea of EH is to harvest the energy that not fully used by a neighboring user for the next user's transmission.

On the other hand, to reduce the system energy consumption, the cellular zooming scheme was proposed in [1]. The method of cellular zooming is to further divide the coverage area into multiple circle sections for zooming in or out. The criteria is the distance from the Base Station (BS) to the user terminal. Based on this idea, the massive Multi-Input-Multi-Output (MIMO) antenna select/sleep mechanism is studied a lot in literature, such as the studies in [106, 107]. In which, the idea of transmit antenna select/sleep mechanism is to select the minimum antenna number for associating user's transmission while turning off the unwanted ones. Similarly, the Radio Frequency (RF) chain selecting/sleeping mechanism was investigated a lot as well, such as the study in [25]. The selecting/sleeping mechanism was also introduced in the relay assisted system by [108]. Furthermore, in our prior studies, the cellular partition zooming scheme was further proposed to further enhance the cellular zooming scheme EE performance by [5]. But it is noticed that although various studies have been done, most of them limited to one or two components engaged in. Although it is found that some studies had been done with more components taken into consideration, such as the work in [109]. But in the study there, the study was limited to one BS area scenario.

Moreover, in prior study on EE issue, for instance, the study from [110], it was found that the system EE can be further enhanced while integrated optimizing the whole system. In addition, by previous chapter, it was found that within C-RAN system model of multiple BSs, the selecting/sleeping mechanism can be easily executed by uniformly scheduling all of the resources within such an integrated system. Thus an integrated system model is better than optimizing the EE within each BS area. It is especially better than optimizing the EE within a limited several components

of a sole BS area. But while integrating the multiple BS into an comprehensive architecture, the problem to optimize the integrated system is that, while taking more components into consideration, the problem will become intractable or even impossible to solve. Thus a trade off scope should be kept in this regard. Additionally, by last chapter, while adopting the C-RAN architecture, it is recommended to replace the signal BS antenna Remote Radio Heads (RRHs) with massive MIMO antenna array in the outdoor environment.

As the review, in this chapter, to optimize the system EE performance within 5G, the system is based on the C-RAN. The massive MIMO antenna array is used to replace the C-RAN's signal antenna within each RRH. The benefit of this has been clarified by last chapter. Here in this study, other than the BS antenna, or BS antenna and RF chain for selecting/sleeping, the energy consumption of machine room, circuits are also taken into consideration. We formulate the system EE problem with all time intervals in all BS areas with the optimization problem. Yet while taking all of the components into consideration, the problem becomes a concave optimization problem. In this case, directly solving the problem is intractable. In the following study, to solve it, we further prove that the problem can be addressed based on an convex optimization problem of each time interval in each BS area plus an off-line selection mechanism. Finally the EE performance is addressed with numerical results of the integrated system.

The contributions of this study can be summarized as follows: a) More components are taken into consideration in the system EE optimization problem in this study. By optimizing the more engaged components with EE definition, the problem is described with an convex optimization problem. b) The concave optimization problem is intractable to solve directly. In this case, the solution is addressed while converting it into a convex optimization problem plus an off-line selection mechanism with our study. c) Simulation demonstrates that the transmit antenna is the dominate factor of the energy consumption and system EE performance. It is found that given a constant sum rate of each BS area and the whole system, an optimal Component Carrier (CC) bandwidth exists with the off-line selection method.

The structure of this chapter was organized as follows: the proposed integrated system is discussed by Section III. Here in this section, the system model is investigated in detail by uniformly scheduling multiple BS resources with a unitive Base Band Unit (BBU). After the introduction of the integrated system model, the system sum rate and energy consumption of each component is investigated. Based on the system sum rate and energy consumption analysis, the EE optimization problem is given by

Section IV. In this section, the solution of this optimization problem is also addressed with the proposed off-line selection method and the convex optimization mechanism. Simulation results to compare this proposal and prior studies is addressed by Section V. Finally, the chapter is concluded by Section VI.

**NOTATIONS:** All over this chapter, the uppercase boldface letters are used to denote the matrix, lowercase boldface letters are the vectors, and normal letters are the scalar quantities, respectively. In addition,  $\mathbf{A}^H$  denotes the Hermitian transposition of a matrix  $\mathbf{A}$ ;  $\mathbf{A}^T$  denotes the transpose of a matrix  $\mathbf{A}$ ;  $\mathbf{A}_{ij}$  is the  $(i, j)$  entry of a matrix  $\mathbf{A}$  with  $i$ th row and  $j$ th column;  $\|\mathbf{A}\|_F^2$  is the Frobenius 2-norm of a matrix  $\mathbf{A}$ ;  $\mathbb{E}$  is the expectation operation;  $\xrightarrow{a.s.}$  denotes the almost sure convergence, respectively.

### 4.3 Proposed system model and analysis of the transmission rate, energy consumption

As the definition of EE [111, 112], in order to investigate the EE, achievable sum rate and consumed energy expression should be achieved beforehand. Thus in the following subsections, the optimized system model, the sum rate and its consumed energy investigation based on this model, were addressed beforehand.

#### 4.3.1 The proposed system model

Typically, C-RAN consists of BBU, RRHs and high bandwidth low latency back-haul links that connecting the RRHs and BBU for information delivery [110]. The benefits of C-RAN reside in its joint information processing and resource scheduling, which can be executed via the Virtual Base Station (VBS) that connects with a General Purpose Platform (GPP) server. In contrast, with traditional BS architecture, no uniform information scheduling can be done.

Consequently, an example of the proposed system model can be shown by Fig. 4.1. As shown here, multiple massive MIMO antenna array replaced RRHs are combined together with the same BBU. In addition, while scheduling several BSs' resources, the "BBU" sections are separated into two parts: plant & control center, switcher connected to the core network. The uniformly power plant is used to provide the power for RRHs associating to the same BBU. Unlike several BBUs within one C-RAN cluster, here the system is further modified by connecting all of its connecting BSs to one "BBU" for uniformly resource scheduling purpose. The benefit of this strategy is stated by [103]. Here the latency issue is left for further study while

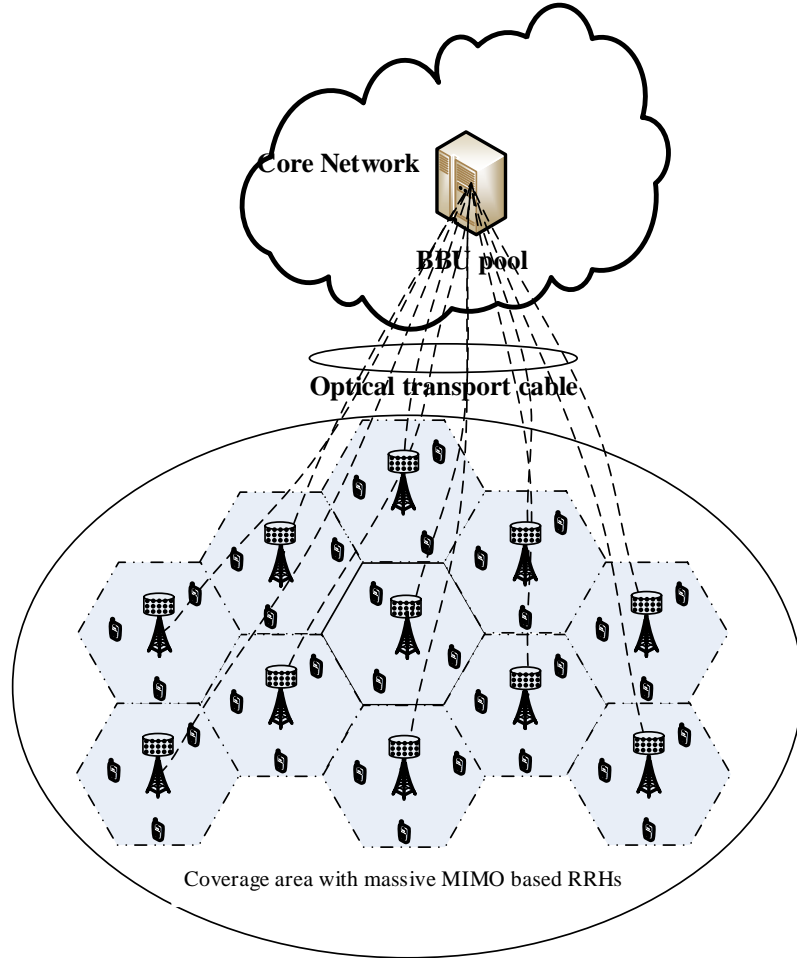


Figure 4.1 Proposed system model with C-RAN architecture.

adopting the CoMP-JP with cooperating cellular in line with the majority work of this, such as [113].

### 4.3.2 The transmission and sum rate analysis

The transmission rate is addressed first by the following analysis. Take the hypothesis that there are  $K$  active UEs that each of them associating with  $b$  active antennas for its transmission. Furthermore, suppose that all of the UEs's requests are routed back to the uniform "BBU" through the backhaul links. Moreover, power of each antenna is equally assumed to be  $P_a$ . By ignoring the inter-cluster interferences from the neighboring BS area (this can be done with frequency reuse and other technologies by orthogonally isolate the neighboring CC bandwidth) [5, 103], further taking  $\mathbf{h}_k$ , a  $1 \times M$  complex-Gaussian vector with zero-mean-complex-Gaussian entries, and

variance  $\frac{1}{2}$  for each dimension, as the channel from BS to UE  $k$  [28], additionally, assuming CC bandwidth assigned to each UE is  $B_{CCs}$  where CC number is sufficient enough for  $K$  UEs. In line with study in [5, 97, 103], with  $K, M$  growing large with a constant ratio  $M/K$ , by an equal power allocation, achievable rate of UE  $k$  can be given by [103]

$$\begin{aligned} R_k &= \mathbb{E} \left\{ B_{CCs} \log_2 \left( 1 + \frac{\rho}{\text{tr}[(\mathbf{H}\mathbf{H}^H)^{-1}]} \right) \right\} \\ &\geq B_{CCs} \log_2 \left( 1 + \frac{\rho}{\mathbb{E}\{\text{tr}[(\mathbf{H}\mathbf{H}^H)^{-1}]\}} \right) \\ &\xrightarrow{a.s.} B_{CCs} \log_2 \left( 1 + \rho \frac{M-K}{K} \right), \end{aligned} \quad (4.1)$$

where

$$\rho = \frac{P_k}{P_{n_k}}, \quad (4.2)$$

with  $P_{n_k}$  the noise power for each user  $k$ . Here the second step of (4.1) is obtained by employing the Jensen's inequality. Moreover, the approximate equation of (4.1) by the third step is obtained in line with prior studies in [103, 108]. This is also called as the ‘‘channel hardening’’ effect in massive MIMO system. It means that with  $K, M$  growing large, the off-diagonal  $\mathbf{H}^H\mathbf{H}$  effects becomes increasing weaker compared with the diagonal matrix of  $\mathbf{H}$  [14, 114].

The sum rate within each C-RAN under this assumption turns out to be the total transmission rate of the overall BS areas. In addition, for the sake of compactness, it is further assumed the UE number is equal among different cellular areas. Thus the sum rate, while denoting  $B$  as the total cellular number of this system, turns out to be

$$R_{sum} = \sum_{i=1}^B \sum_{j=1}^K R_{i,j}^k, \quad (4.3)$$

where  $R_{i,j}^k$  is equal to  $R_k$ . With this sum rate in hand, the left work is the power consumption analysis, which was addressed by the following sections.

### 4.3.3 The energy consumption analysis

Energy consumption of C-RAN can be summarized into the dynamic energy consumption plus the constant energy consumption parts. The dynamic energy consumption mainly comes from the transmission (for instance, antenna, RF Chain, and circuit to serve the transmission) and coverage area maintaining [103]. In contrast, the constant energy consumption mainly results from the machine room and other equipments. As seldom light is casted on in prior studies, will be the focus of our studies as one of the

contributions. Under this circumstance, by summing up the dynamic and constant energy consumptions, total energy consumption of the system will read [115]

$$P_{clu}(t) = \sum_{i=1}^B (p_i^{dyn,BS} + p_i^{fix,BS}), \quad (4.4)$$

where  $p_b^{dyn,BS}$ ,  $p_b^{fix,BS}$  yield the dynamic energy consumption of each BS area (to serve the UEs and maintain the BS coverage area) and constant energy consumption of each BS area. Additionally, the dynamic energy consumption can be further decomposed with

$$p_b^{dyn,BS} = \sum_{j=1}^K \left( \frac{1}{\eta} P_j^k + P_j^c + P_j^{RF} + P_j^{cc} \right). \quad (4.5)$$

Here  $P_j^k$  is the transmission rate energy consumption (equal to  $P_k$ , the allocated antenna energy power of UE  $k$  with rate  $R_{i,j}^k$ ). In addition,  $P_j^{RF}$ ,  $P_j^c$ ,  $P_j^{cc}$  are the RF chain, circuit, and the allocated coverage area maintaining energy consumption, respectively. Furthermore,  $\eta$  denotes the Power Amplifier (PA) efficiency with value  $0 < \eta < 1$ .

As discussed before, the goal of this study is to explore the EE merits of this proposal while taking more components into consideration. In order to describe this comprehensive EE with mathematics model, two lemmas are given beforehand.

**Lemma 1:** (*lemma 3.1* in [116]) only consider the downlink transmission while setting the power of uplink transmission period to be zero<sup>2</sup>, the optimal power allocation for an epoch  $t$  is  $P_j^k > 0$  for power on time period  $\tau^{on} \subseteq (t(i-1), t(i)]$  (downlink), and  $P_j^k = 0$  for the remaining time periods  $\tau^{off} \subseteq (t(i-1), t(i)]$  (uplink). The following identities also hold:  $\tau^{on} \cap \tau^{off} = \emptyset$ ,  $\tau^{on} \cup \tau^{off} = (t(i-1), t(i)]$ .

*Proof:* See *Lemma 3.1* in [116].

**Lemma 2:** by assuming the arrive of UE request obeys a Poisson Point Process (PPP) distribution with mean  $\mu$  variance  $\sigma^2$  of all epoch time, and  $T = \sum_{t=1}^T (t_{i-1}, t_i]$ . Optimal power allocation can be obtained while adding the optimal power allocation in all time intervals, and the performance of UEs obeys a PPP distribution with mean  $\mu$ , variance  $\sigma^2$ . In this case, UEs' performance within the total time intervals obeys a PPP distribution with mean  $T\mu$ , variance  $T\sigma^2$ .

*Proof:* See Appendix A.

---

<sup>2</sup>In this chapter, we try to solve the EE optimization problem in downlink, the uplink EE optimization although not considered here, but can be also obtained while setting the downlink power as zero, as discussed in the following sections.

## 4.4 The energy efficiency model and its solution with off-line selection and convex optimization method

The EE optimization model and its solution of this study are addressed in this section. As discussed before, EE is defined as the achievable sum-rate divided by the consumed energy. Hence, in line with prior study [114], the global EE optimization problem of this modified system (within all time intervals of all BS areas), while integrated taking the antenna, RF Chain, circuit, dynamic and constant power into consideration, can be described as

$$\max_{P_{i,j}^k, P_{i,j}^{RF}} \int_0^T \sum_{i=1}^B \sum_{j=1}^K \frac{R_{i,j}^k}{P_{clu}} dt, \quad (4.6)$$

subject to:

$$C1 : \int_0^T \sum_{i=1}^B \sum_{j=1}^K \left( \frac{1}{\eta} P_{i,j}^k + P_{i,j}^c + P_{i,j}^{RF} \right) dt \leq P_T^{total}, \quad (4.7a)$$

$$C2 : \int_0^T \sum_{i=1}^B P_b^{dyn,BS} dt \leq P_{bs}^{total}, \quad (4.7b)$$

$$C3 : \int_0^T \sum_{i=1}^B \sum_{j=1}^K \left( \left\lceil \frac{R_{i,j}^k}{\log_2(1 + \rho^{\frac{M-K}{K}})} \right\rceil \right) dt \leq N_{CCs}^{total}, \quad (4.7c)$$

$$C4 : \int_0^T \sum_{i=1}^B \sum_{j=1}^K N_{i,j}^a dt \leq N_{bs}^{a,total}, \quad (4.7d)$$

$$C5 : \int_0^T \sum_{i=1}^B \sum_{j=1}^K N_{i,j}^{UE} dt \leq N_{bs}^{rf,total}, \quad (4.7e)$$

$$C6 : P_{i,j}^k, P_{i,j}^c, P_{i,j}^{RF}, P_b^{dyn,BS} \geq 0, \forall k, \quad (4.7f)$$

where  $P_{i,j}^k, P_{i,j}^c, P_{i,j}^{RF}$  are of the same value as  $P_j^k, P_j^c, P_j^{RF}$ . Here  $P_T^{total}, P_{bs}^{total}, N_{CCs}^{total}, N_{bs}^{a,total}, N_{bs}^{rf,total}$  yield the total transmission power, total BS power, and the number of CC, the number of antenna, the number of RF chain, respectively. Further,  $N_{i,j}^a, N_{i,j}^{UE}, N_{bs}^{rf,total}$  denote the number of antenna allocated to each UE, number of UE indicator, and the total number of RF Chain within one cluster, respectively. Note that here C1, C2 specify that in one cluster, the total transmission power should be no greater than the allocated power, and the total cellular power consumption should be no greater than the total BS power, respectively. In addition, C3, C4, C6 denote that in one cluster, the number constraints of CC, antenna, as well as the power

constraints should be satisfied. Whereas C5 yields the UE number can not exceed the RF Chain number. This is because of the assumption that one active RF Chain could only serve one active UE, in line with the prior MIMO structure, for the sake of compactness.

The EE optimization problem, although has been addressed so far and can be solved by the concave optimization method, but it will cost more resources and calculation time due to the constraint C3 comparing with the linear searching method. Thus another purpose of this chapter is to find an alternative method to simplify the processing. Fortunately, in line with prior study [115], it is noted that if  $C_k$  was taken as the used CCs of the previous UEs, a minimum CC selection method can be obtained beforehand, whereas  $I_m(t)$  is defined as

$$I_m(t) = \begin{cases} 1, & C_k \in \Omega_m, C_k = \arg \min_{C_k \in \Omega_m} P_j^k, \\ 0, & \text{otherwise,} \end{cases} \quad (4.8)$$

with  $C_k, \Omega_m$  denote the optimal CC for  $k$ th UE and the set of CCs. For the left optimization problem, we dig more and find the following *Corollary* existing.

**Corollary 1:** according to *Lemma 2*, the binary value of power allocation  $P_{i,j}^k$ , and its time distribution  $\tau^{on}$  both obey the identically Poisson distribution in every time interval  $(t(i-1), t(i)]$ . While linearly adding every individual power allocation within each time interval, it turns out to be the optimal solution of the total time intervals. This can be proved as follows.

*Proof:* in  $\tau^{on}$  time period, whenever there is a transmission request, power allocation is triggered with a constant value of  $P_{i,j}^k$  (proof of *Lemma 1* in [116]). Otherwise, in  $\tau^{off}$  period, no power is allocated. This is because  $\tau^{on}$  and  $P_{i,j}^k$  displaying the same performances like the active UEs' existences with their on-off binary values. Thus it is clear that the binary values of  $\tau, P_{i,j}^k$  are of the same distribution performances just like UEs'.

With the aforementioned *Lemma 1*, *Lemma 2* and *Corollary 1* in hand, the global EE optimization solution can be obtained while summing up the single time interval EE optimization problems other than the aforementioned integration to the total time intervals. In addition, the single time interval EE optimization problem is the same among different time periods on condition that among each of them, the UEs are performing the same distribution. Thus once the optimal solution is obtained in a time interval, the global optimization is achieved. In this case, while removing the

integration to the total time intervals, the problem can be further described as follows

$$\max_{P_{i,j}^k, P_{i,j}^{RF}} \sum_{i=1}^B \sum_{j=1}^K \frac{R_{i,j}^k}{P_{clu}}, \quad (4.9)$$

subject to:

$$C1 : \sum_{i=1}^B \sum_{j=1}^K \left( \frac{1}{\eta} P_{i,j}^k + P_{i,j}^c + P_{i,j}^{RF} \right) \leq P_T^{total}, \quad (4.10a)$$

$$C2 : \sum_{i=1}^B P_b^{dyn,BS} \leq P_{bs}^{total}, \quad (4.10b)$$

$$C3 : \sum_{i=1}^B \sum_{j=1}^K \left( \left\lceil \frac{R_{i,j}^k}{\log_2(1 + \rho^{\frac{M-K}{K}})} \right\rceil \right) \leq N_{CCs}^{total}, \quad (4.10c)$$

$$C4 : \sum_{i=1}^B \sum_{j=1}^K N_{i,j}^a \leq N_{bs}^{a,total}, \quad (4.10d)$$

$$C5 : \sum_{i=1}^B \sum_{j=1}^K N_{i,j}^{UE} \leq N_{bs}^{rf,total}, \quad (4.10e)$$

$$C6 : P_{i,j}^k, P_{i,j}^c, P_{i,j}^{RF}, P_b^{dyn,BS} \geq 0, \forall k. \quad (4.10f)$$

Note that the purpose of C3 is to find the optimal CC solution under CC number constraint, which has less relationship with the power allocation. In this case, it can be solved via an off-line method. That is, whenever request coming, select the least CC number for its transmission under CC constraint in (4.8). The remaining part after this selection, turns out to be a component selection and power allocation problem with respect to the achievable transmission rate. In addition, without loss of generality, it is further assumed that each antenna consuming a same power once activated, as well as the circuit, RF Chain.

In addition, similar to *Lemma 2*, while adding up all users' location performances within every BS areas, it is the UEs' location performances of the whole cluster. Moreover, the PPP distribution of UE within one cluster, with large time range, can be taken as a sum of separate PPP distribution of each BS area. Whereas in each area, the UE displaying the same PPP distribution but with a smaller range. Thus the optimal solution can be obtained by optimizing the EE problem of one BS area within one time interval. Which is, the remaining problem can be decomposed as a

optimization problem with

$$\max_{P_j^k, P_j^{RF}} \sum_{k=1}^K \frac{R_j^k}{P_j^k + P_j^{RF}}, \quad (4.11a)$$

subject to:

$$C1 : \sum_{k=1}^K \left( \frac{1}{\eta} P_j^k + P_j^c + P_j^{RF} \right) \leq P_T, \quad (4.11b)$$

$$C2 : \sum_{k=1}^K N_j^{a,k} \leq N_j^a, \quad (4.11c)$$

$$C3 : \sum_{k=1}^K N_j^k \leq N_j^{RF}, \forall t, \quad (4.11d)$$

$$C4 : P_j^k, P_j^c, P_j^{RF} \geq 0, \forall k, \quad (4.11e)$$

Here the definitions are given as:  $R_j^k$ , transmission rate of  $k$ -th user with  $j$  RRHs;  $P_j^k$  power of  $k$ -th user with  $j$  RRHs;  $P_j^{RF}$  power of RF chain with  $j$  RRHs;  $\eta$ , power amplifier (PA);  $P_j^c$ , power of circuit within  $j$ -th RRHs;  $P_T$  total power constraint within  $j$ -th RRHs;  $N_j^a$ , number of antenna associating with  $k$ -th user;  $N_j^k$ , total antenna number within  $j$ -th RRHs;  $N_j^k$  number of users within  $j$  RRHs;  $N_j^{RF}$ , number of RF chain within  $j$ -th RRHs;  $t$ , each time period.

whereas the global optimization solution is the summarization of each of this single-time-interval-single-BS-area optimization problem. To this optimization problem, it is proved by *Theorem 1* in [26] that, if we define a maximum weighted solution with  $S^* = \max(P_j^k, P_j^{RF}) = \sum_{k=1}^K R_j^{k*} / (P_j^k + P_j^{RF})^*$ , and further suppose the problem has an optimal solution  $S^*$ . Optimal solution of the EE problem in (4.11a) if any, should satisfy the following constraint

$$\begin{aligned} \max(P_j^k, P_j^{RF}) - S^*(P_j^k + P_j^{RF})^* &= \sum_{k=1}^K R_j^{k*} - S^*(P_j^k + P_j^{RF})^* \\ &= 0, \end{aligned} \quad (4.12)$$

and its optimal solution with  $\max(P_j^k, P_j^{RF})$  must be equal to  $S^*$  if any. Note that RF chain power consumption has nothing to do with the achievable sum rate although it is needed for the transmission. Under this circumstance, while searching for the optimal solution, it will converge to zero. To avoid this, in line with [117], we assume that in each search step, the number of RF Chain is equal to the number of antenna in order to satisfy the transmission requirement.

$$\begin{aligned} \frac{\partial \max(P_j^k, P_j^{RF})}{\partial P_j^k} &= \frac{\partial \sum_{j=1}^K \frac{R_j}{P_j^k + P_j^{RF}}}{\partial P_j^k} \\ &= \sum_{j=1}^K \frac{B_{CCs} \left( \frac{M-K}{\ln 2 [KN_0 + P_j^k (M-K)]} - \log_2 \frac{KN_0 + P_j^k (M-K)}{KN_0} \right)}{(P_j^k + P_j^{RF})^2}, \end{aligned} \quad (4.13)$$

$$\begin{aligned} \frac{\partial^2 \max(P_j^k, P_j^{RF})}{\partial (P_j^k)^2} &= \frac{\partial^2 \sum_{j=1}^K \frac{R_j}{P_j^k + P_j^{RF}}}{\partial (P_j^k)^2} \\ &= - \sum_{j=1}^K \frac{B_{CCs} \left( \frac{(M-K)^2}{\ln 2 [KN_0 + P_j^k (M-K)]^2} + \frac{M-K}{\ln 2 [KN_0 + P_j^k (M-K)]} \right)}{(P_j^k + P_j^{RF})^2} \\ &\quad - \sum_{j=1}^K \frac{2B_{CCs} \left( \frac{M-K}{\ln 2 [KN_0 + P_j^k (M-K)]} - \log_2 \frac{KN_0 + P_j^k (M-K)}{KN_0} \right)}{(P_j^k + P_j^{RF})^3}. \end{aligned} \quad (4.14)$$

---

After this, the extreme point existence is verified by the lagrange method as shown in (4.13) and (4.14). As we can see, it always has an extreme point on condition that (4.13) is equal to zero, and (4.14) lower than zero. Thus at least one optimal solution of our EE optimization problem exists. In addition, this optimal solution can be straightforward obtained while comparing all of those extreme points and keeping the one with best EE performance. As all constraints are in linear functions now. One can use the linear searching method to obtain the optimal solution of (4.11a) with constraints (4.11) plus an off-line searching method of CC. That is, in each step, search the optimal solution with every possible combination of the constraints, compare them, and only keep the best one. As the linear constraints, one can obtain the optimal solution within a much shorter time. Whereas the searching can be achieved by IBM Cplex (Refer IBM ILOG CPLEX Optimization Studio V12.60 documents) or Matlab based Linear Programming (LP) [118].

## 4.5 Numerical analysis and results

Here in this paper, in line with prior studies, while studying the EE performance in cellular network, we set up the simulation environment as in Table 4.1 [25, 26, 119]. As talked aforementioned, the user terminals' (user equipments' (UEs')) distributions obey PPP distribution in each cellular. We further assume that in each cellular, the largest number of active UE is 20 of each time interval. Thus the achievable capacity of each cellular will be the sum rate of all active UEs' transmission rate. The location

Table 4.1 Simulation components.

| Parameters                               | Value   |
|--|---------|
| Antenna number per RRH                   | 100     |
| RRH number                               | 10      |
| Machine room                             | 480 W   |
| Number of UE per BS area                 | 20      |
| Mean transmission rate per UE            | 200 MHz |
| Circuit power of per RF chain $P_j^{RF}$ | 160 mW  |
| Constant circuit power $P_j^c$           | 160.8 W |
| PA efficiency $\eta$                     | 35 %    |
| Power of antenna $P_j^k$                 | 37 dBm  |

distribution of UEs is randomly generated with the number of active UE growing with the PPP distribution.

In addition, we serve the UE's transmission rate by different CC with equal value, where the value is given ahead. This is the off-line selection mechanism. Whenever the optimal value arrives (by further increase the CC bandwidth value has little effect to the system performance), it is the selected CC bandwidth value for the simulation. In order to be more closer to the reality, we randomly generate the transmission rate value of each user by a random distribution.

We first evaluate the performance of elements selection and EE performance in one cellular area. The simulation results are Fig. 4.2 and Fig. 4.3. Here Fig. 4.2 yields the number of selected elements by different number of access UE while Fig. 4.3 is its EE performance within a specific RRHs. Note that as the PPP distribution of UE location and Poisson distribution of requirement of transmission rate of each UE, the curves of EE performance in Fig. 4.2 and Fig. 4.3 go up and down. That lies in the fact that in each step, with transmission rate is generated randomly, the total transmission rate goes up sharply or slowly, and also the total energy consumption value. Thus while calculating the EE, its value also goes up and down.

From Fig. 4.2 we can see that the number of selected antennas decreases with CC increasing. The CC has less effect to the elements selection while arrived at the best one,  $C_k$ . On condition that each pair of elements possesses equal power consumption,  $C_k$  is the one that achieves the least number of elements for the first time, which is 35 MHz in this simulation. It can be further convinced from Fig. 4.3, where  $B_{CC_s}$  takes the value of 35 MHz and 40 MHz displaying almost the same EE performance

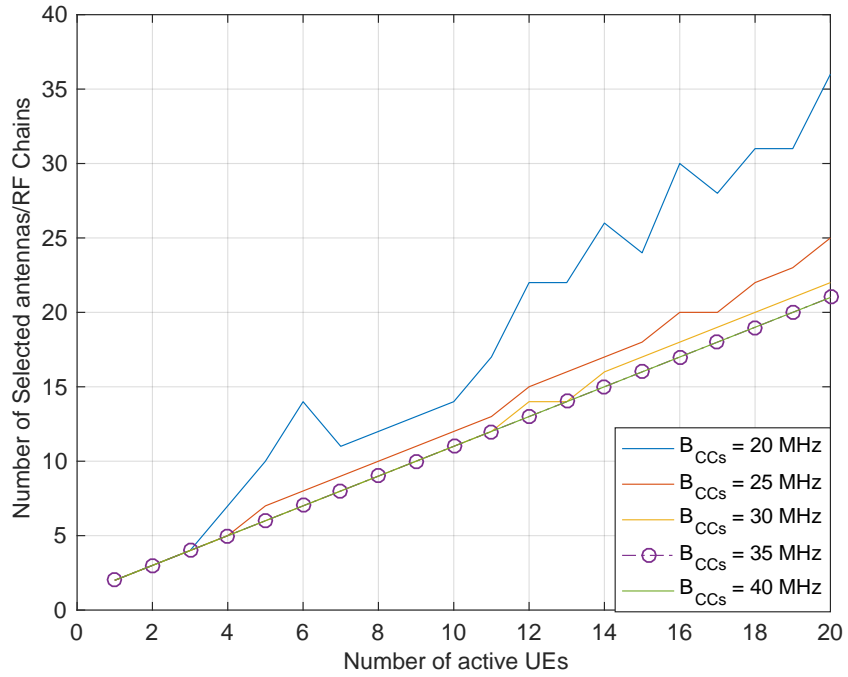


Figure 4.2 Component Selection Performance of our scheme, one cellular area.

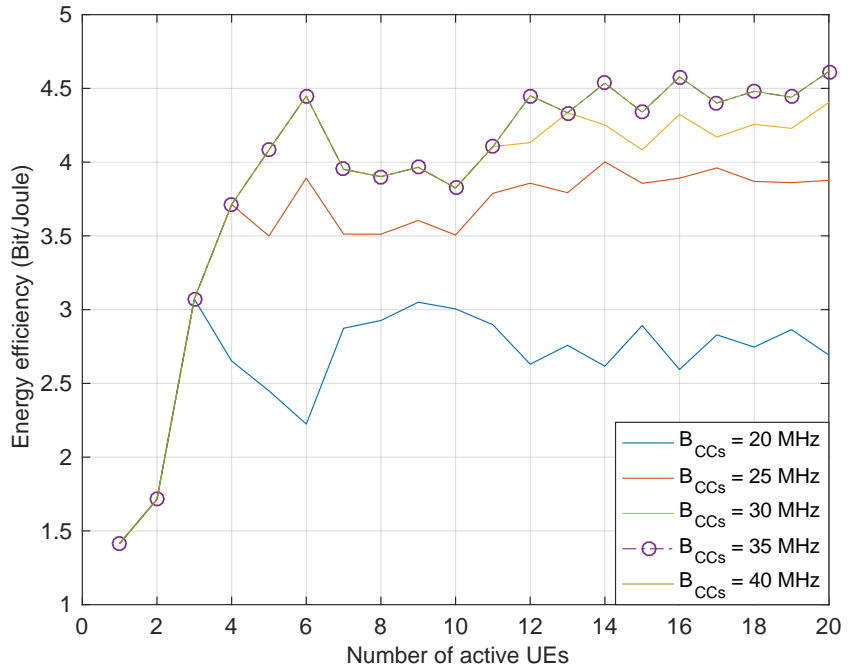


Figure 4.3 Energy efficiency performance of our scheme, one cellular area.

(although further increase the CC bandwidth can increase the EE, but the effect is almost invisible). Thus we can say that before  $C_k$ , the number of selected elements

decreases and EE performance increases with  $B_{CC_s}$  increasing. While  $B_{CC_s}$  arrives at  $C_k$ , simply increase CC bandwidth value has few effect to the EE performance. The best  $B_{CC_s}$  should be  $C_k$  and the best elements selection mechanism can be obtained by  $C_k$ , which is the Fig. 4.3.

We further verified our findings with simulation of the whole system with 10 RRHs. In line with prior simulations of the one cellular area, the user location and transmission rate value are randomly generated as well. Where the results with the elements selection performance is given by Fig. 4.4. In addition, the EE performance of the whole integrated system based on the C-RAN architecture is given by Fig. 4.5. Here we suppose one cluster consists of 10 massive MIMO RRHs while each of them serving 20 UEs and the transmission rate requests obey Poisson distribution as talked aforementioned. As shown here, similar to one cellular area scenario, because of the randomly generated transmission rates, the elements selection performance as well as the EE curves go up and down both in Fig. 4.4 and Fig. 4.5. We can further confirm this by the two figures that the optimal  $B_{CC_s}$  is 35 MHz. Because after this value, simply increase the  $B_{CC_s}$  has much less effect to the system EE performance enhancement. Although some increments can be achieved by increasing the CC bandwidth value, but this is mostly a dis-economic choice. This is due to the fact that the CC frequency is valuable un-renewable resources, we will say that the optimal CC bandwidth value is 35 MHz with the randomly generated transmission rate values as well as the distance.

One can further observe from the Fig. 4.2 and Fig. 4.4 that, only about 20 antennas are selected in one cellular area scenario and about 200 antennas are selected in one cluster scenario while adopting the CoMP-JP to serve the mean 300 Mbit/s users, whereas we deploy 100 antennas in each cellular area as the massive MIMO is, which is larger than the selected ones. Thus we can conclude that all of the 20 UEs' transmission requirements in one cellular area scenario and 200 UEs' transmission requirements in one cluster scenario are fulfilled in our simulation.

## 4.6 Conclusion

In this chapter, an optimized system model is proposed for economical deployment in outdoor environment and better adoption of the selecting/sleeping mechanism. Afterwards, the system EE performance is modeled into a global optimization problem. Solution of this problem is obtained while summing up the solution of each BS coverage area within a single-time-interval-single-BS-area optimization problem.

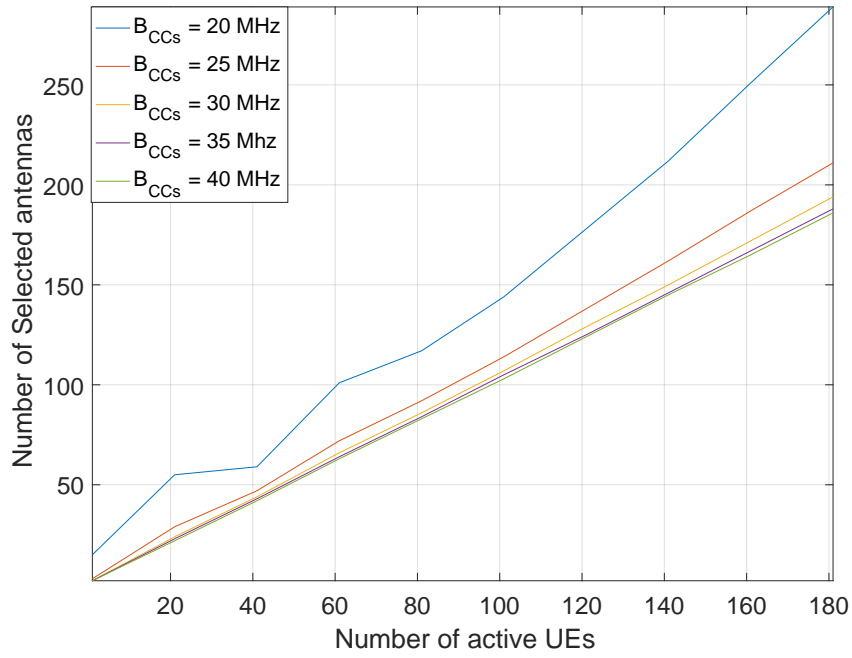


Figure 4.4 Component Selection Performance in the whole system.

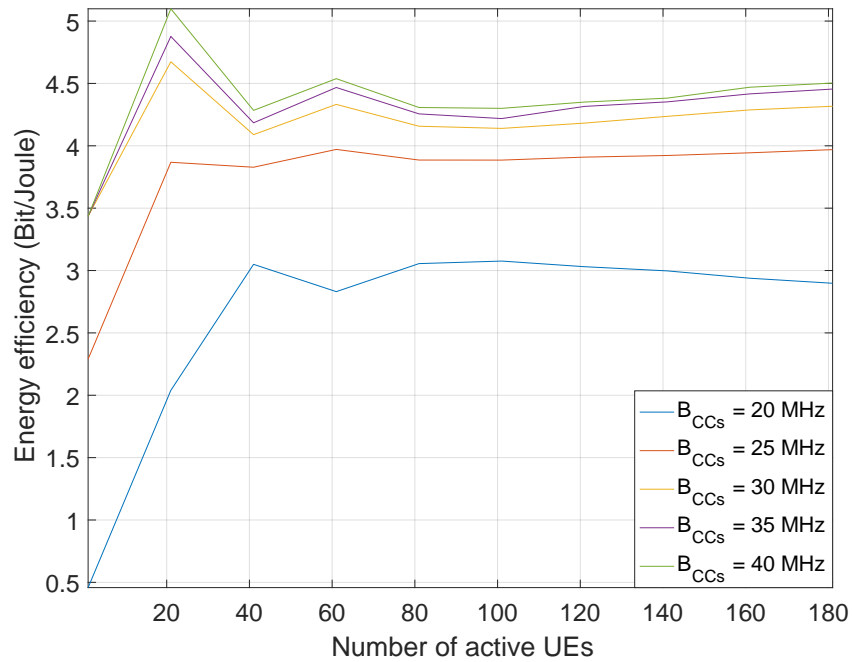


Figure 4.5 Energy efficiency performance of the whole system.

In addition, the single-time-interval-single-BS-area optimization problem is solved by a linear convex optimization problem plus an off-line selection method. Numerical results manifest that the proposal here displaying better EE performance comparing

with the previous proposal, by further reducing the reminder component power consumptions other than the antenna, RF Chain or other component alone. In addition, CC has great effect to the performance before reaching the optimal one and little influence after this. The numerical results further indicate that among the component power consumptions, antenna power consumption is the dominant one.

## Appendix A

That is difficult to proof the lemma directly, but the prove could be done by some division and summarization methods, i.e., to prove that the sum distribution  $\sum_{t=1}^T UE_t$  of independent identically distributed Poisson distribution of each time period  $UE_t$  was a Poisson distribution. Whereas this can be confirmed by some linear operations. Which is, according to the basic property of expectation value and variance in statistics, expectation calculation of the independent identically Poisson distribution is a linear operation, and the variance is independent. Thus it has

$$E(UE) = \sum_{t=1}^T E(UE_t) = T\mu, \quad (4.30)$$

$$\text{var}(UE) = \sum_{t=1}^T \text{var}(UE_t) = T\sigma^2. \quad (4.31)$$

In addition, according to the deduction of *Lemma 1*, in each time period, the optimal power, if any, should be allocated with a constant value. Suppose this constant value is  $P_k$ , where  $P_k > 0, t \in (t(i-1), t(i)]$ . By assuming “ $EE$ ” as the optimal solution operator, according to Jensen’s inequality, it follows

$$EE \left[ \int_0^T \left( \frac{P_k}{l_t} \right) dt \right] \leq \int_0^T EE \left[ \left( \frac{P_k}{l_t} \right) \right] dt, \quad (4.32)$$

where  $l_t$  denotes a time interval length. Furthermore, assume a suboptimal solution with value  $\hat{P}_t$  existing, which of course, a constant value with  $\hat{P}_t > 0, t \in (t(i-1), t(i)]$  existing. We have

$$EE \int_0^T \left[ \left( \frac{P_k - \hat{P}_k}{l_t} \right) \right] dt \geq \int_0^T \left\{ \left[ EE \left( \frac{P_k}{l_t} \right) - EE \left( \frac{\hat{P}_k}{l_t} \right) \right] \right\} dt. \quad (4.33)$$

However, according to the optimization results, there should be

$$EE \int_0^T \left[ \left( \frac{P_k - \hat{P}_k}{l_t} \right) \right] dt \leq \int_0^T \left[ EE \left( \frac{P_k}{l_t} \right) - EE \left( \frac{\hat{P}_k}{l_t} \right) \right] dt. \quad (4.34)$$

As we can see, this resulted in a paradox. Thus  $\hat{P}_k$  must be equal to  $P_k$  in order to get one and only one integral optimal result. In this case, the global optimal result of EE can be obtained by the sum optimal power in each independent time period. This completes the proof.

# Chapter 5

## Conclusion

### 5.1 Summary and discussion

Fifth Generation (5G) wireless communications have attracted various attentions both from academia and industry. Of all 5G's technologies, they can be summarized to tumble down the Spectrum Efficiency (SE) and Energy Efficiency (EE) requirement toughies. Recently, other than the SE and EE issues, the low latency, mobility, frequency sharing and multiplexing, and the back-hauling/ front-hauling links issues are investigated a lot. Yet here in this dissertation, it is only focused on the SE and EE issue. In literature, apart from the prior studies with Multi-Input-Multi-Output (MIMO), Orthogonal Frequency Division Multiple Accessing (OFDMA) in Long Term Evolution (LTE) and other generations, the millimeter Wave (mmWave), massive MIMO, Non-Orthogonal Multiple Access (NOMA), are addressed a lot on the SE and EE issues. In this dissertation, chapter 2 is focused on the SE issue, whereas chapter 3 and chapter 4 are investigating the EE issue of 5G.

The general evolution of wireless communications was reviewed in the chapter 1 of the introduction as the preliminary knowledge. In which, the wireless communication channel and the wave transmission characteristics were focused. Afterwards, the Rayleigh and Rice channel models were safely arrived as well as some experimental models, such as the Okumura-Hata model. The evolution of base station (BS) was introduced as well, where the driving force behind the Single-Input-Single-Output (SISO) to MIMO system was elaborated as well as the technology evolutions. As prior studies, the massive MIMO can enhance the SE and EE performance of 5G with associated antenna growing large. In addition, the NOMA was brought up to further improve the SE performance. Yet still, it is not sufficient to achieve the 5G's claiming goal with 1000 folds transmission rate compared with prior LTE system. In this case, mmWave was discussed a lot in literature and industry. The benefit

of mmWave lies in its even wider bandwidth once adopted in 5G as the Component Carrier (CC) frequency. Some other technologies such as the Devices to Devices (D2D) communications, full duplex communications, were mentioned as well.

With the prior investigation in hand, in the chapter 2, the NOMA was combined with the massive MIMO and mmWave for the capacity analysis. From an intuitive point of view, by combining the NOMA with massive MIMO, better capacity can be achieved. In addition, with even wider bandwidth mmWave brings in, even faster transmit rate can be achieved. Yet less studies have been done before on combining all of those three. Thus in our study with chapter 2, the capacity performances both in low Signal to Noise Ratio (SNR) and high-SNR regimes were addressed with the analysis. The division into high and low-SNR regimes is because of the way complex analysis while taking all of those three. On the other hand, as high-SNR regime can be used to denote the cellular center area where low-SNR regime denoting the cellular edge area, the majority conditions can be covered. In the analysis, the deterministic equivalent method was adopted as the tool to solve the low SNR regime capacity problem. In contrast, as the condition was changed in the high SNR regime, the statistics and probability mathematics tools were invoked to deal with the interference dominated high SNR capacity analysis. By comparing with prior LTE system, it was found that the combination of NOMA-mmWave-massive-MIMO can greatly enhance the system capacity performance.

After the discussion on SE issue with chapter 2, we further stepped forward to study the EE issue of 5G. The study was summarized by chapter 3 and chapter 4. The integrated system model was proposed for 5G with our studies. Additionally, based on this integral system model, some EE optimization problems were addressed by while taking more engaged components into consideration. The numerical results demonstrate that the proposed integrated system model with CPZ, and the proposed EE optimization method with more engaged components can further enhance the system EE performance compared with prior studies. The detailed review of chapter 3 and 4 will be addressed by the following paragraph.

In chapter 3, the integrated system model was introduced by uniformly scheduling the resources with a centralized Base Band Unit (BBU). In addition, the massive MIMO antenna array was utilized to replace the Remote Radio Head's (RRH's) single antenna for faster transmission rate. The coverage area can be maintained while investment can be reduced compared to deploying the single antenna RRHs largely to cover a wide outdoor area. The information within all BS was collected and transmitted to the centralized BBU for engaging resource scheduling. Another, with

the uniform machine room that providing power for all RRHs within the Cloud Radio Access Network (C-RAN), the energy consumption is further reduced. Thus according to the definition of EE, the EE performance is improved while consuming less energy with this amended system model. Other than this, the Cellular Partition Zooming (CPZ) scheme was further proposed to divide the cellular area with regard to the distance as well as the angle. Simulation results demonstrated that this CPZ scheme can further enhance the system EE performance.

Based on the proposed integrated system model, in chapter 4, the EE optimization problem was further investigated while taking more elements (circuit, Radio Frequency chain (RF chain), machine room, etc.) into consideration. As more considered components, the problem becomes intractable to tackle down. To solve this optimization problem, we converted it into the convex optimization problem plus an off-line selection mechanism. It was proved by the computer based simulation that the comprehensive optimization method displayed better EE performance compared with prior studies. This is because of the integrated optimizing with more engaged components. Via this, the consumed energy is further reduced by turning off the unwanted components with the select-and-sleep mechanism.

## 5.2 Future work

Although the latest technologies to satisfy 5G's requirement with SE and EE were addressed and discussed with various methods in this dissertation, yet still, the full scope of this can not be totally covered. Some of the potential work in future can be listed as follows.

The mmWave is discussed a lot in literature as well as here by our study. it is noticed that the specific frequency that used for carrier bandwidth is still in the air. In addition, with the vulnerable propagation characteristics of mmWave and shorter distance that massive MIMO can support, how to effectively combine those two together for commercial use is still a big challenge. Moreover, with mmWave engaged in, how to effectively make use of the macro wave and mmWave for various application scenarios need to pay more attention as well. In this regard, some study groups has already on the way of frequency sharing and coexisting research. It is worth note that prior Unlicense/ License Assisted Access (U/LAA) mechanisms and Soft Frequency Reusing (SFR) mechanism, etc., although effective but not enough in 5G.

Some alternative technologies to achieve the SE requirement with low complexity and better latency merit are still needed while paving the way of 5G. As known, although the massive MIMO, small cell and NOMA can improve the system SE performance, but they all have limitations. For instance, the inevitable denser deployment of massive MIMO with small cell will cost the vender a great deal of investments while compared with LTE system. On the other hand, for NOMA, the Successful Interference Cancellation (SIC) is too complex to accomplish especially at the receiver side. Because normally cell-phone has limited space and battery, which too complex decoding devices may be even impossible to install.

# References

- [1] Z. Niu, Y. Wu, J. Gong, and Z. Yang, “Cell zooming for cost-efficient green cellular networks,” *IEEE Commun. Mag.*, vol. 48, no. 11, pp. 74–79, Nov. 2010.
- [2] D. Tse and P. Viswanath, *Fundamentals of Wireless Communication*. Cambridge University Press, 2004.
- [3] H. Q. Ngo, E. G. Larsson, and T. L. Marzetta, “Energy and spectral efficiency of very large multiuser mimo systems,” *IEEE Trans. Commun.*, vol. 61, no. 4, pp. 1436–1449, Apr. 2013.
- [4] P. Begovic, N. Behlilovic, and E. Avdic, “Applicability evaluation of okumura, ericsson 9999 and winner propagation models for coverage planning in 3.5 ghz wimax systems,” in *IWSSIP*, Apr. 2012, pp. 256–260.
- [5] D. Zhang, K. Yu, Z. Zhou, and T. Sato, “Energy efficiency scheme with cellular partition zooming for massive mimo systems,” in *IEEE ISADS*, Mar. 2015, pp. 266–271.
- [6] A. Goldsmith, *Wireless Communications*. Cambridge University Press, 2005.
- [7] P. Keawbunsong, P. Supanakoon, and S. Promwong, “Hata’s path loss model calibration for prediction dttv propagation in urban area of southern thailand,” *IOP Conference Series: Materials Science and Engineering*, vol. 83, no. 1, p. 012013, 2015.
- [8] M. Prasad, K. Ratnamala, M. Chaitanya, and P. Dalela, “Terrestrial communication experiments over various regions of indian subcontinent and tuning of hatas model,” *Annals of Telecommunications*, vol. 63, no. 3-4, pp. 223–235, 2008.
- [9] T. Bai and R. Heath, “Coverage and rate analysis for millimeter-wave cellular networks,” *IEEE Trans. Wireless Commun.*, vol. 14, no. 2, pp. 1100–1114, Feb. 2015.

- [10] A. Thornburg, T. Bai, and R. W. Heath, "Mmwave ad hoc network coverage and capacity," in *IEEE ICC*, Jun. 2015, pp. 1310–1315.
- [11] F. J. Lopez-Martinez and J. M. Romero-Jerez, "Asymptotically exact approximations for the symmetric difference of generalized marcum q -functions," *IEEE Trans. Vehi. Technol.*, vol. 64, no. 5, pp. 2154–2159, May 2015.
- [12] Y. Liu, Y. Yu, W.-J. Lu, and H. bo Zhu, "Stochastic multiple-input multiple-output channel model based on singular value decomposition," *IET Commun.*, vol. 9, no. 15, pp. 1852–1856, Oct. 2015.
- [13] G. Lebrun, J. Gao, and M. Faulkner, "Mimo transmission over a time-varying channel using svd," *IEEE Trans. Wireless Commun.*, vol. 4, no. 2, pp. 757–764, Mar. 2005.
- [14] F. Rusek, D. Persson, B. K. Lau, E. Larsson, T. Marzetta, O. Edfors, and F. Tufvesson, "Scaling up mimo: Opportunities and challenges with very large arrays," *IEEE Signal Process. Mag.*, vol. 30, no. 1, pp. 40–60, Jan. 2013.
- [15] J. Hoydis, S. ten Brink, and M. Debbah, "Massive mimo in the ul/dl of cellular networks: How many antennas do we need?" *IEEE J. Sel. Areas Commun.*, vol. 31, no. 2, pp. 160–171, Feb. 2013.
- [16] T. Marzetta, "Noncooperative cellular wireless with unlimited numbers of base station antennas," *IEEE Trans. Wireless Commun.*, vol. 9, no. 11, pp. 3590–3600, Nov. 2010.
- [17] J. Andrews, "Will densification be the death of 5g?, available: <http://www.comsoc.org/ctn/will-densification-be-death-5g>," IEEE Com-Soc CTN, Tech. Rep., 2015.
- [18] C. Fang, F. Yu, T. Huang, J. Liu, and Y. Liu, "A survey of green information-centric networking: Research issues and challenges," *IEEE Commun. Surveys Tuts.*, vol. 17, no. 3, pp. 1455–1472, Aug. 2015.
- [19] A. Luiz Garcia Reis, A. Barros, K. Gusso Lenzi, L. Pedroso Meloni, and S. Barbin, "Introduction to the software-defined radio approach," *IEEE Trans. Latin America*, vol. 10, no. 1, pp. 1156–1161, Jan. 2012.

- [20] A. Asadi, Q. Wang, and V. Mancuso, “A survey on device-to-device communication in cellular networks,” *IEEE Commun. Surveys Tuts.*, vol. 16, no. 4, pp. 1801–1819, 2014.
- [21] Y. Liao, T. Wang, L. Song, and Z. Han, “Listen-and-talk: Protocol design and analysis for full-duplex cognitive radio networks,” *IEEE Trans. Veh. Technol.*, vol. 66, no. 1, pp. 656–667, Jan. 2017.
- [22] Y. Liao, L. Song, Z. Han, and Y. Li, “Full duplex cognitive radio: a new design paradigm for enhancing spectrum usage,” *IEEE Commun. Mag.*, vol. 53, no. 5, pp. 138–145, May 2015.
- [23] M. Matthaiou, M. McKay, P. Smith, and J. Nosssek, “On the condition number distribution of complex wishart matrices,” *IEEE Trans. Commun.*, vol. 58, no. 6, pp. 1705–1717, Jun. 2010.
- [24] S. Jin and X. Zhang, “Optimal energy efficient scheme for mimo-based cognitive radio networks with antenna selection,” in *CISS*, Mar. 2015, pp. 1–6.
- [25] X. Zhang, S. Zhou, Z. Niu, and X. Lin, “An energy-efficient user scheduling scheme for multiuser mimo systems with rf chain sleeping,” in *IEEE WCNC*, Apr. 2013, pp. 169–174.
- [26] Z. Zhou, S. Zhou, J. Gong, and Z. Niu, “Energy-efficient antenna selection and power allocation for large-scale multiple antenna systems with hybrid energy supply,” in *IEEE GLOBECOM*, Dec. 2014, pp. 2574–2579.
- [27] J. Choi and D. To, “Energy efficiency of harq-ir for two-way relay systems with network coding,” in *Eu Wireless*, Apr. 2012, pp. 1–5.
- [28] M. Zhao, Z. Zhang, W. Zhou, and J. Zhu, “Maximizing energy efficiency in analog network coding based two-way relay-assisted system,” in *WCSP*, Oct. 2014, pp. 1–6.
- [29] M. Zhao and Y. Yang, “Packet scheduling with joint design of mimo and network coding,” in *IEEE MASS*, Oct. 2009, pp. 227–236.
- [30] L. Chen, H. Jin, H. Li, J.-B. Seo, Q. Guo, and V. Leung, “An energy efficient implementation of c-ran in hetnet,” in *IEEE VTC*, Sep. 2014, pp. 1–5.

- [31] M. Khan, R. Alhumaima, and H. Al-Raweshidy, “Reducing energy consumption by dynamic resource allocation in c-ran,” in *EuCNC*, Jun. 2015, pp. 169–174.
- [32] Y. Niu, Y. Li, D. Jin, L. Su, and A. V. Vasilakos, “A survey of millimeter wave communications (mmwave) for 5g: opportunities and challenges,” *Wireless Networks*, vol. 21, no. 8, pp. 2657–2676, 2015.
- [33] S. Sun, T. Rappaport, R. Heath, A. Nix, and S. Rangan, “Mimo for millimeter-wave wireless communications: beamforming, spatial multiplexing, or both?” *IEEE Commun. Mag.*, vol. 52, no. 12, pp. 110–121, Dec. 2014.
- [34] A. Alkhateeb, O. El Ayach, G. Leus, and R. Heath, “Channel estimation and hybrid precoding for millimeter wave cellular systems,” *IEEE J. Sel. Topics Signal Process.*, vol. 8, no. 5, pp. 831–846, Oct. 2014.
- [35] L. Dai, B. Wang, Y. Yuan, S. Han, C.-L. I, and Z. Wang, “Non-orthogonal multiple access for 5g: solutions, challenges, opportunities, and future research trends,” *IEEE Commun. Mag.*, vol. 53, no. 9, pp. 74–81, Sep. 2015.
- [36] Y. Saito, Y. Kishiyama, A. Benjebbour, T. Nakamura, A. Li, and K. Higuchi, “Non-orthogonal multiple access (noma) for cellular future radio access,” in *IEEE VTC*, Jun. 2013, pp. 1–5.
- [37] T. Rappaport, S. Sun, R. Mayzus, H. Zhao, Y. Azar, K. Wang, G. Wong, J. Schulz, M. Samimi, and F. Gutierrez, “Millimeter wave mobile communications for 5g cellular: It will work!” *IEEE Access*, vol. 1, pp. 335–349, May 2013.
- [38] T. Riihonen, S. Werner, and R. Wichman, “Hybrid full-fuplex/half-duplex relaying with transmit power adaptation,” *IEEE Trans. Wireless Commun.*, vol. 10, no. 9, pp. 3074–3085, Sep. 2011.
- [39] Cisco, “Cisco visual networking index: Global mobile data traffic forecast update, 2015-2020,” *White paper*, Feb. 2016.
- [40] F. Boccardi, H. Shokri-Ghadikolaei, G. Fodor, E. Erkip, C. Fischione, M. Kountouris, P. Popovski, and M. Zorzi, “Spectrum pooling in mmwave networks: Opportunities, challenges, and enablers,” *IEEE Commun. Mag.*, vol. 54, no. 11, pp. 33–39, Nov. 2016.

- [41] R. G. Gallager, *An Inequality on the Capacity Region of Multiaccess Multipath Channels*. Springer, 1994, pp. 129–139.
- [42] Z. Gao, L. Dai, and Z. Wang, “Channel estimation for mmwave massive mimo based access and backhaul in ultra-dense network,” in *IEEE ICC*, May 2016, pp. 1–6.
- [43] M. N. Kulkarni, A. Ghosh, and J. G. Andrews, “A comparison of MIMO techniques in downlink millimeter wave cellular networks with hybrid beamforming,” *IEEE Trans. Commun.*, vol. 64, no. 5, pp. 1952–1967, May 2016.
- [44] G. Lee, Y. Sung, and J. Seo, “Randomly-directional beamforming in millimeter-wave multiuser MISO downlink,” *IEEE Trans. Commun.*, vol. 15, no. 2, pp. 1086–1100, Feb. 2016.
- [45] J. Choi, “Minimum power multicast beamforming with superposition coding for multiresolution broadcast and application to noma systems,” *IEEE Trans. Commun.*, vol. 63, no. 3, pp. 791–800, Mar. 2015.
- [46] Z. Ding, P. Fan, and H. V. Poor, “Impact of user pairing on 5g nonorthogonal multiple-access downlink transmissions,” *IEEE Trans. Veh. Technol.*, vol. 65, no. 8, pp. 6010–6023, Aug. 2016.
- [47] Z. Yang, Z. Ding, P. Fan, and Z. Ma, “Outage performance for dynamic power allocation in hybrid non-orthogonal multiple access systems,” *IEEE Commun. Lett.*, vol. 20, no. 8, pp. 1695–1698, Aug. 2016.
- [48] H. Zhang, S. Jin, M. R. McKay, X. Zhang, and D. Yang, “High-snr performance of mimo multi-channel beamforming in double-scattering channels,” *IEEE Trans. Commun.*, vol. 59, no. 6, pp. 1621–1631, Jun. 2011.
- [49] R. Yu, J. Ding, X. Huang, M. T. Zhou, S. Gjessing, and Y. Zhang, “Optimal resource sharing in 5g-enabled vehicular networks: A matrix game approach,” *IEEE Trans. Veh. Technol.*, vol. 65, no. 10, pp. 7844–7856, Oct. 2016.
- [50] M. R. Akdeniz, Y. Liu, M. K. Samimi, S. Sun, S. Rangan, T. S. Rappaport, and E. Erkip, “Millimeter wave channel modeling and cellular capacity evaluation,” *IEEE J. Sel. Areas Commun.*, vol. 32, no. 6, pp. 1164–1179, Jun. 2014.

- [51] A. Alkhateeb, O. E. Ayach, G. Leus, and R. W. Heath, “Channel estimation and hybrid precoding for millimeter wave cellular systems,” *IEEE J. Sel. Areas Commun.*, vol. 8, no. 5, pp. 831–846, Oct. 2014.
- [52] X. Liu and X. Wang, “Efficient antenna selection and user scheduling in 5g massive mimo-noma system,” in *IEEE VTC*, May 2016, pp. 1–5.
- [53] Z. Ding and H. V. Poor, “Design of massive-mimo-noma with limited feedback,” *IEEE Signal Process. Lett.*, vol. 23, no. 5, pp. 629–633, May 2016.
- [54] D. Zhang, K. Yu, Z. Wen, and T. Sato, “Outage probability analysis of noma within massive mimo systems,” in *IEEE VTC*, May 2016, pp. 1–5.
- [55] H. Yang and T. L. Marzetta, “Performance of conjugate and zero-forcing beamforming in large-scale antenna systems,” *IEEE J. Sel. Areas Commun.*, vol. 31, no. 2, pp. 172–179, Feb. 2013.
- [56] H. Ji, B. Lee, B. Shim, Y. H. Nam, Y. Kwak, H. Noh, and C. Shin, “3d beamforming for capacity boosting in lte-advanced system,” in *IEEE PIMRC*, Aug. 2015, pp. 2344–2348.
- [57] Y. Liu, G. Pan, H. Zhang, and M. Song, “On the capacity comparison between mimo-noma and mimo-oma,” *IEEE Access*, vol. 4, pp. 2123–2129, May 2016.
- [58] M. Debbah and R. R. Muller, “Mimo channel modeling and the principle of maximum entropy,” *IEEE Trans. on Inf. Theory*, vol. 51, no. 5, pp. 1667–1690, May 2005.
- [59] R. Couillet, M. Debbah, and J. W. Silverstein, “A deterministic equivalent for the analysis of correlated mimo multiple access channels,” *IEEE Trans. on Inf. Theory*, vol. 57, no. 6, pp. 3493–3514, Jun. 2011.
- [60] A. a. Lu, X. Gao, and C. Xiao, “A free deterministic equivalent for the capacity of mimo mac with distributed antenna sets,” in *IEEE ICC*, Jun. 2015, pp. 1751–1756.
- [61] J. Zhang, C. K. Wen, S. Jin, X. Gao, and K. K. Wong, “On capacity of large-scale mimo multiple access channels with distributed sets of correlated antennas,” *IEEE J. Sel. Areas Commun.*, vol. 31, no. 2, pp. 133–148, Feb. 2013.

- [62] A. Firag, P. J. Smith, and M. R. McKay, “Capacity analysis of mimo three product channels,” in *AusCTW*, Feb. 2010, pp. 13–18.
- [63] E. Bjornson, L. Sanguinetti, J. Hoydis, and M. Debbah, “Optimal design of energy-efficient multi-user mimo systems: Is massive mimo the answer?” *IEEE Trans. Wireless Commun.*, vol. 14, no. 6, pp. 3059–3075, Jun. 2015.
- [64] Y. Liu, Z. Ding, M. ElKashlan, and H. V. Poor, “Cooperative non-orthogonal multiple access with simultaneous wireless information and power transfer,” *IEEE J. Sel. Areas Commun.*, vol. 34, no. 4, pp. 938–953, Apr. 2016.
- [65] M. N. Kulkarni, A. Ghosh, and J. G. Andrews, “A comparison of mimo techniques in downlink millimeter wave cellular networks with hybrid beamforming,” *IEEE Trans. Commun.*, vol. 64, no. 5, pp. 1952–1967, May 2016.
- [66] C. K. Wen, G. Pan, K. K. Wong, M. Guo, and J. C. Chen, “A deterministic equivalent for the analysis of non-gaussian correlated mimo multiple access channels,” *IEEE Trans. on Inf. Theory*, vol. 59, no. 1, pp. 329–352, Jan. 2013.
- [67] J. Dehardt, “Generalizations of the glivenko-cantelli theorem,” *Ann. Math. Statist.*, vol. 42, no. 6, pp. 2050–2055, Dec. 1971.
- [68] J. W. Silverstein and A. M. Tulino, “Theory of large dimensional random matrices for engineers,” in *IEEE Ninth International Symposium on Spread Spectrum Techniques and Applications*, Aug. 2006, pp. 458–464.
- [69] N. Letzepis and A. Grant, “Shannon transform of certain matrix products,” in *IEEE ISIT*, Jun. 2007, pp. 1646–1650.
- [70] C. K. Wen, S. Jin, and K. K. Wong, “On the sum-rate of multiuser mimo uplink channels with jointly-correlated rician fading,” *IEEE Trans. Commun.*, vol. 59, no. 10, pp. 2883–2895, Oct. 2011.
- [71] J. Choi, “H-arq based non-orthogonal multiple access with successive interference cancellation,” in *IEEE GLOBECOM*, Nov. 2008, pp. 1–5.
- [72] J. Hoydis, S. ten Brink, and M. Debbah, “Massive mimo in the ul/dl of cellular networks: How many antennas do we need?” *IEEE J. Sel. Areas Commun.*, vol. 31, no. 2, pp. 160–171, Feb. 2013.

- [73] R. R. Muller, “On the asymptotic eigenvalue distribution of concatenated vector-valued fading channels,” *IEEE Trans. Inf. Theory*, vol. 48, no. 7, pp. 2086–2091, Jul. 2002.
- [74] H. Holma and A. Toskala, *LTE for UMTS: Evolution to LTE-Advanced, 2nd Edition*. Wiley, 2011.
- [75] T. L. Narasimhan and A. Chockalingam, “Channel hardening-exploiting message passing (chemp) receiver in large-scale mimo systems,” *IEEE J. Sel. in Signal Process.*, vol. 8, no. 5, pp. 847–860, Oct 2014.
- [76] A. M. Tulino and S. Verdú, “Random Matrix Theory and Wireless Communications,” *Foundations and Trends in Communications and Information Theory*, vol. 1, no. 1, pp. 1–182, 2004.
- [77] R. Couillet and M. Debbah, *Random Matrix Methods for Wireless Communications*. Cambridge, UK: Cambridge University Press, 2011.
- [78] F. P. F. n and P. M. Espineira, *Modeling the Wireless Propagation Channel A Simulation Approach with MATLAB*. Wiley, 2008.
- [79] S. Jin, M. R. McKay, K. K. Wong, and X. Gao, “Transmit beamforming in rayleigh product mimo channels: Capacity and performance analysis,” *IEEE Trans. Signal Process.*, vol. 56, no. 10, pp. 5204–5221, Oct. 2008.
- [80] M. Kang and M. S. Alouini, “Impact of correlation on the capacity of mimo channels,” in *IEEE ICC*, vol. 4, May 2003, pp. 2623–2627.
- [81] D. Zwillinger and V. Moll, *Table of Integrals, Series, and Products 8th ed.* Academic Press, 2015.
- [82] K. Skouby and P. Lynggaard, “Smart home and smart city solutions enabled by 5g, iot, aai and cot services,” in *IC3I*, Nov. 2014, pp. 874–878.
- [83] H. Wang, Z. Pan, and L. Chih, “Perspectives on high frequency small cell with ultra dense deployment,” in *IEEE ICC*, Oct. 2014, pp. 502–506.
- [84] A. Bousia, E. Kartsakli, A. Antonopoulos, L. Alonso, and C. Verikoukis, “Sharing the small cells for energy efficient networking: How much does it cost?” in *IEEE Globecom*, Dec. 2014, pp. 2649–2654.

- [85] S. Mumtaz, K. M. S. Huq, J. Rodriguez, and V. Frascolla, “Energy-efficient interference management in lte-d2d communication,” *IET Signal Processing*, vol. 10, no. 3, pp. 197–202, Apr. 2016.
- [86] A. Bousia, E. Kartsakli, A. Antonopoulos, L. Alonso, and C. Verikoukis, “Multiobjective auction-based switching off scheme in heterogeneous networks to bid or not to bid?” *IEEE Trans. Veh. Technol.*, vol. PP, no. 99, pp. 1–1, Jan. 2016.
- [87] S. Mumtaz, A. Al-Dulaimi, K. M. S. Huq, F. B. Saghezchi, and J. Rodriguez, “Wifi in licensed band (wifi-lic),” *IEEE Commun. Lett.*, vol. PP, no. 99, pp. 1–1, Jun. 2016.
- [88] B. Di, S. Bayat, L. Song, Y. Li, and Z. Han, “Joint user pairing, subchannel, and power allocation in full-duplex multi-user ofdma networks,” *IEEE Trans. Wireless Commun.*, vol. 15, no. 12, pp. 8260–8272, Dec 2016.
- [89] M. Jang, H. Park, Y. Kwon, and T. Hwang, “Energy-efficient adaptation of pilot power, data power, and transmission rate for downlink multiuser mimo systems,” *IEEE Trans. Veh. Technol.*, vol. 64, no. 6, pp. 2692–2698, June 2015.
- [90] R. Bolla, R. Bruschi, F. Davoli, and F. Cucchietti, “Energy efficiency in the future internet: A survey of existing approaches and trends in energy-aware fixed network infrastructures,” *IEEE Commun. Surveys Tuts.*, vol. 13, no. 2, pp. 223–244, Second 2011.
- [91] P. Vetter, D. Suvakovic, H. Chow, P. Anthapadmanabhan, K. Kanonakis, K.-L. Lee, F. Saliou, X. Yin, and B. Lannoo, “Energy-efficiency improvements for optical access,” *IEEE Commun. Mag.*, vol. 52, no. 4, pp. 136–144, Apr. 2014.
- [92] H. Li, L. Song, and M. Debbah, “Energy efficiency of large-scale multiple antenna systems with transmit antenna selection,” *IEEE Trans. Commun.*, vol. 62, no. 2, pp. 638–647, Feb. 2014.
- [93] C. M. R. Institute, “C-ran, the road towards green ran, white paper,” China Mobile, Tech. Rep. 2.5, Oct. 2011.
- [94] D. W. K. Ng, E. S. Lo, and R. Schober, “Energy-efficient resource allocation in multi-cell ofdma systems with limited backhaul capacity,” *IEEE Trans. Wireless Commun.*, vol. 11, no. 10, pp. 3618–3631, Oct. 2012.

- [95] M. Popov, D. Peinado, M. Nilson, A. Vastberg, and T. Sjolund, “Green distributed antenna systems: Optimized design and upper bound for energy efficiency,” in *IEEE SoftCOM*, Sep. 2013, pp. 1–5.
- [96] Y. Zeng, R. Zhang, and Z. N. Chen, “Electromagnetic lens-focusing antenna enabled massive mimo: Performance improvement and cost reduction,” *IEEE J. Sel. Areas Commun.*, vol. 32, no. 6, pp. 1194–1206, Jun. 2014.
- [97] M. Jung, T. Kim, K. Min, Y. Kim, J. Lee, and S. Choi, “Asymptotic distribution of system capacity in multiuser mimo systems with large number of antennas,” in *IEEE VTC*, Jun. 2013, pp. 1–5.
- [98] E. Mino, E. Torrecilla, L. del Apio, and I. Berberana, “Son use case study energy saving for lte enbs,” *IEEE Trans. Latin America*, vol. 8, no. 2, pp. 184–189, Apr. 2010.
- [99] D. Astely, E. Dahlman, A. Furuskar, Y. Jading, M. Lindstrom, and S. Parkvall, “Lte: the evolution of mobile broadband,” *IEEE Commun. Mag.*, vol. 47, no. 4, pp. 44–51, Apr. 2009.
- [100] R. De Francisco and D. Slock, “An optimized unitary beamforming technique for mimo broadcast channels,” *IEEE Trans. Wireless Commun.*, vol. 9, no. 3, pp. 990–1000, March 2010.
- [101] H. Cheng, D. Persson, E. Bjornson, and E. Larsson, “Massive mimo at night: On the operation of massive mimo in low traffic scenarios,” in *IEEE ICC*, Jun. 2015, pp. 1697–1702.
- [102] M. Katsigiannis and H. Hammainen, “Energy consumption of radio access networks in finland,” *Telecommun. Syst.*, vol. 55, no. 2, pp. 241–251, 2014.
- [103] D. Zhang, S. Mumtaz, Z. Zhou, and T. Sato, “Integrating energy efficiency mechanism with components selection for massive mimo based c-ran,” in *IEEE ICC*, May 2016, pp. 74–79.
- [104] D. Zhang, Z. Chen, M. K. Awad, N. Zhang, H. Zhou, and X. S. Shen, “Utility-optimal resource management and allocation algorithm for energy harvesting cognitive radio sensor networks,” *IEEE J. Se. Areas Commun.*, vol. 34, no. 12, pp. 3552–3565, Dec. 2016.

- [105] J. wu, I. Akingeneye, and J. Yang, “Energy efficient optimum sensing with energy harvesting power sources,” *IEEE Access*, vol. 3, pp. 989–997, July. 2015.
- [106] Q. Zhang, C. Yang, H. Haas, and J. Thompson, “Energy efficient downlink cooperative transmission with bs and antenna switching off,” *IEEE Trans. Wireless Commun.*, vol. PP, no. 99, pp. 1–14, May 2014.
- [107] S. ZHANG, Y. WU, S. Zhou, and Z. Niu, “Traffic-aware network planning and green operation with bs sleeping and cell zooming,” *IEICE Trans. Commun.*, vol. E97-B, no. 11, pp. 2118–2126, Nov. 2014.
- [108] M. Ju, H. K. Song, and I. M. Kim, “Joint relay-and-antenna selection in multi-antenna relay networks,” *IEEE Trans. Commun.*, vol. 58, no. 12, pp. 3417–3422, Dec. 2010.
- [109] E. Bjornson, L. Sanguinetti, J. Hoydis, and M. Debbah, “Optimal design of energy-efficient multi-user mimo systems: Is massive mimo the answer?” *IEEE Trans. Wireless Commun.*, vol. 14, no. 6, pp. 3059–3075, Jun. 2015.
- [110] C. Lab, *Cloud Radio Network White Paper (3rd edition)*, 3rd ed., CMCC, May 2014.
- [111] K. Saidul Huq, S. Mumtaz, J. Bachmatiuk, J. Rodriguez, X. Wang, and R. Aguiar, “Green hetnet comp: Energy efficiency analysis and optimization,” *IEEE Trans. Veh. Technol.*, vol. 64, no. 10, pp. 4670–4683, Oct. 2015.
- [112] K. Mohammed Saidul Huq, S. Mumtaz, and J. Rodriguez, “Qos aware energy-efficient resource scheduling for hetnet comp,” in *IEEE ICC*, Jun. 2015, pp. 5954–5960.
- [113] J. Xu, L. Duan, and R. Zhang, “Cost-aware green cellular networks with energy and communication cooperation,” *IEEE Commun. Mag.*, vol. 53, no. 5, pp. 257–263, May 2015.
- [114] T. L. Narasimhan and A. Chockalingam, “Channel hardening-exploiting message passing (chemp) receiver in large-scale mimo systems,” *IEEE J. Sel. Topics Signal Process.*, vol. 8, no. 5, pp. 847–860, Oct. 2014.
- [115] H. Chen, Y. Jiang, J. Xu, and H. Hu, “Energy-efficient coordinated scheduling mechanism for cellular communication systems with multiple component carriers,” *IEEE J. Sel. Areas Commun.*, vol. 31, no. 5, pp. 959–968, May 2013.

- [116] J. Xu and R. Zhang, “Throughput optimal policies for energy harvesting wireless transmitters with non-ideal circuit power,” *IEEE J. Sel. Areas Commun.*, vol. 32, no. 2, pp. 322–332, Feb. 2014.
- [117] X. Chen, X. Wang, and X. Chen, “Energy-efficient optimization for wireless information and power transfer in large-scale mimo systems employing energy beamforming,” *IEEE Wireless Commun. Lett.*, vol. 2, no. 6, pp. 667–670, Dec. 2013.
- [118] O. L. M. Michael C. Ferris and S. J. Wright, *Linear Programming with MATLAB*. SIAM, 2008.
- [119] D. Zhu and M. Lei, “Traffic adaptation and energy saving potential of centralized radio access networks with coordinated resource allocation and consolidation,” in *CHINACOM*, Aug. 2013, pp. 587–593.

## List of academic achievements

| Category   |  |   |
|--|--|---|
| Articles in refereed journals                                    | <p>○ <b>D. Zhang</b>, T. Muhammad, S. Mumtaz, J. Rodriguez, and T. Sato, "Integrating energy efficiency analysis of massive MIMO based C-RAN", <i>EURASIP Journal of Wireless Communications and Networking</i>, vol. 2016, no. 1, pp. 277-285, Nov. 2016.</p> <p>○ <b>D. Zhang</b>, Z. Zhou, S. Mumtaz, J. Rodriguez, and T. Sato, "One integrated energy efficiency proposal for 5G IoT communications", <i>IEEE Internet of Things Journal</i>, vol. 3, no. 6, pp. 1346-1354, Dec. 2016.</p>  | Chapter 4<br><br>Chapter 3                  |
| Presentations at International conferences                       | <p>○ <b>D. Zhang</b>, S. Mumtaz, Z. Zhou, and T. Sato, "Integrating energy efficiency mechanism with components selection for massive MIMO based C-RAN," in <i>IEEE ICC</i>, pp. 74-79, Kuala Lumpur, Malaysia, May 2016.</p> <p>○ <b>D. Zhang</b>, K. Yu, Z. Wen, and T. Sato, "Outage probability analysis of NOMA within massive MIMO systems," in <i>IEEE VTC 16' Spring</i>, pp. 1-5, Nanjing, China, May 2016.</p> <p>○ <b>D. Zhang</b>, K. Yu, Z. Zhou, and T. Sato, "Energy efficiency scheme with cellular partition zooming for massive MIMO systems", in <i>IEEE ISADS</i>, pp. 266-271, Taichung, Taiwan, Mar. 2015.</p> | Chapter 4<br><br>Chapter 2<br><br>Chapter 3 |
| Published Books  | <p><b>D. Zhang</b>, and Shahid Mumtaz "MmWave-Massive MIMO: A paradigm for 5G", Chapter 2, Elsevier, London, UK, 2017.</p>   | Chapter 1                                   |
| Presentations at domestic academic meetings held by study groups | <p><b>D. Zhang</b>, and T. Sato, "Performance analysis of NOMA within massive MIMO systems", in <i>IEICE RCS</i>, vol. 115, no. 113, RCS2015-57, pp. 67-70, Jun. 2015.</p>   |   |
| Presentations at domestic conferences                            | <p><b>D. Zhang</b>, K. Yu, Y. Su, and T. Sato, "Towards SE and EE in 5G with NOMA and Massive MIMO Technologies", in <i>IEICE General Conference</i>, pp. 95-96, Otsu, JP, Mar. 2015.</p>  |   |
| Presentations at Workshops                                       | <p><b>D. Zhang</b> and T. Sato, "5G tutorial- research topics in 5G", Exchange Seminar between Waseda University and Hanyang University, Nov. 2014.</p> <p><b>D. Zhang</b> and T. Sato, "Outage probability analysis of NOMA within massive MIMO systems", Exchange Seminar between Waseda University and Hanyang University, Nov. 2016.</p> <p><b>D. Zhang</b>, Y. Su, F. Bai and T. Sato, "Wireless communications research activities in Sato lab, Waseda University", Exchange Seminar between Waseda University and National Taiwan University, Aug. 2016.</p>  |   |

|        |   |  |
|--------|---|--|
| Others | <p>Z. Wen, <b>D. Zhang</b>, K. Yu, and T. Sato, " Node name routing in information-centric Ad-Hoc network", <i>IEICE Transactions on Fundamentals of Electronics, Communications and Computer Sciences</i>, vol. E100-A, no. 2, pp. 680-687, Feb. 2017.</p> <p>Z. Zhu, Z. Chu, Z. Wang, and <b>D. Zhang</b>, "Beamforming optimization via max-min SINR in MU-MISO SWIPT systems under bounded channel uncertainty", <i>IEICE Transactions on Fundamentals of Electronics, Communications and Computer Sciences</i>, vol. E99-A, no. 12, pp. 2576-2580, Dec. 2016.</p> <p>Z. Wen, <b>D. Zhang</b>, K. YU, and T. Sato, "Information centric networking for disaster information sharing services," <i>IEICE Transactions on Fundamentals of Electronics, Communications and Computer Sciences</i>, vol. E98-A, no. 8, pp. 1610-1617, Aug. 2015.</p> <p>K. Yu, A. Mohammad, Z. Wen, <b>D. Zhang</b>, and T. Sato "A key management scheme for secure communications of information centric advanced metering infrastructure in smart grid," <i>IEEE Transactions on Instrumentation and Measurement</i>, vol. 64. no. 8, pp. 2072-2085, Jul. 2015.</p> <p>Z. Zhou, G. Ma, <b>D. Zhang</b>, and C. Xu, "Energy-efficiency context-aware resource allocation in D2D communications: An iterative matching approach" in <i>IEEE ICTC</i>, pp. 90-96, Jeju, Korea, Oct. 2016.</p> <p>K. Yu, <b>D. Zhang</b>, A. Mohammad, Q. Nguyen, "A key management scheme for secure communications of information centric advanced metering infrastructure in smart grid," in <i>IEEE PowerCom</i>, pp. 2019-2024, Chengdu, China, Oct. 2014.</p> |  |
|--------|---|--|